DEVELOPMENT OF SOLAR INTEGRATED EVACUATED GLASS – THERMAL ABSORBER TUBE COLLECTOR (EGATC) IN AIR HEATING APPLICATION

BY

ZAIRUL AZRUL ZAKARIA

A thesis submitted in fulfilment of the requirement for the degree of Doctor of Philosophy (Engineering)

Kulliyyah of Engineering
International Islamic University Malaysia

MARCH 2023

ABSTRACT

An efficient solar collector design that effectively absorbs solar energy and converts it into heat is required during intermittent solar radiation. Existing Flat Plate Collector (FPC) and Heat-Pipe Evacuated Tube Collector (HP ETC) are designed for water heating required storage tanks, while an additional heat exchanger is required for air heating application which leads to extra spacing and cost. The installation also needs to be tilted at the correct angle and positioned to south/north facing to optimize the system performance. These could lead to design limitations. Therefore, this study aims to design, develop and investigate the thermal performance of an Evacuated Glass-Thermal Absorber Tube Collector (EGATC) for air heating applications. EGATC was designed from a conventional HP ETC, and the performance was compared through parameter and performance experimental setup. The three days performance experiments showed EGATC performed better with daily outlet temperature increased by 9.0%, 7.2%, and 4.9%, respectively, with an average of 7.0% compared with HP ETC. EGATC also had greater efficiency compared to HP ETC, with the average efficiency for EGATC being 51.3% compared with HP ETC's 41.8%. EGATC's inner absorber was designed to create a double pass flow with the ventilated chamber. The parameter experiment shows the design could increase the outlet temperature by a difference of 6.3% (for stainless-steel inner absorber compared with insulation material inner absorber). Regarding energy storage, the stainless-steel inner absorber also had an advantage compared to the insulation material inner absorber, with a 1.3% difference. On the effect of other parameters such as inner absorber surface area air contact (perforated fin), outer absorber selective coating surface, outer absorber wall thickness, double layer non-vacuum glass tube, single layer transparent outer glass tube, and single-layer thin film inner glass tube was investigated by parameter experimental setup on energy storage. It was proven that the outlet temperature, energy store, and energy buffer could be enhanced with the combination of wind speed 0.9 m/s, zero (0) perforated fin, non-coating outer absorber, and 1mm outer absorber wall thickness. It was also reported that double-layer vacuum glass tubes promise better thermal performance enhancement compared with double-layer non-vacuum glass tubes, single-layer transparent outer glass tubes, and single-layer thin film inner glass tubes. The mathematical equation of each EGATC component was formulated based on the first law of thermodynamics. The total acceptable error of 5% shows that the model at each node was valid. The performance curves for those 0 fins (equation), 0 fin (experimental), and 3 fins (experimental) were obtained. The results showed that the efficiency (collector + storage) was affected by the number of fins. The efficiency (collector + storage) was 68.7%, 71.2%, and 71.0%, respectively. In conclusion, the application of EGATC in air heating applications proved beneficial to the application of solar drying processes, especially in equatorial climate countries such as Malaysia.

خلاصة البحث

ما يزال البحث عن تصميم فعال لألواح الطاقة الشمسية مستمراً، خاصة امتصاص الطاقة أثناء انقطاع الشعاع الشمسي كحجب السحب لها. اللوح الشمسي الحالي المتاح (FPC) وكذلك الأنبوب الحراري (HP ETC) صممت لتسخين المياه، بينما يلزم استخدام مُغيّر حراري إضافي لتسخين الهواء؛ وهذا يؤدي في مجمله إلى زيادة المساحة والتكلفة. يحتاج تثبيت الألواح أيضاً إلى إمالتها بزاوية صحيحة ووضعه في اتجاه الجنوب/الشمال لتحسين أداء اللوحات وهذا يمكن أن يؤدي إلى قيود في التصميم. لذلك، تهدف الدراسة الحالية إلى تصميم وتطوير وفحص الأداء الحراري لمجمع أنبوب امتصاص الزجاج الحراري المفرغ (EGATC) لتطبيقات تسخين الهواء. تم تصميم EGATC من HP ETC التقليدي، وتمت مقارنة الأداء من خلال الإعداد التجريبي. أظهرت تجارب الأداء التي استمرت ثلاثة أيام أداء EGATC بشكل أفضل مع زيادة درجة حرارة المخرج اليومية بنسبة 9.0٪ و 7.2٪ و 4.9٪ بمتوسط 7.0٪ مقارنة بـ HP ETC. كما كان لدى EGATC كفاءة أكبر مقارنة بـ HP ETC، حيث بلغ متوسط الكفاءة لـ EGATC 51.3٪ مقارنة بـ HP ETC 41.8٪. تم تصميم جهاز الامتصاص الداخلي من EGATC لخلق تدفق مزدوج مع غرفة تهوية. توضح التجربة أن التصميم يمكن أن يزيد درجة حرارة المخرج بفارق 6.3٪ (للممتص الداخلي من الفولاذ المقاوم للصدأ مقارنة بالممتص الداخلي لمواد العزل). فيما يتعلق بتخزين الطاقة، فإن الممتص الداخلي من الفولاذ المقاوم للصدأ يتمتع أيضاً بميزة مقارنة بالممتص الداخلي لمواد العزل بفارق 1.3٪. حول تأثير المتغيرات الأخرى مثل ملامسة الهواء لمساحة سطح الامتصاص الداخلي (الزعنفة المثقبة)، سطح الطلاء الانتقائي للامتصاص الخارجي، سمك جدار الممتص الخارجي، أنبوب زجاجي غير مفرغ بطبقة مزدوجة، أنبوب زجاجي خارجي شفاف بطبقة واحدة، وطبقة واحدة رقيقة تم فحص الأنبوب الزجاجي الداخلي للفيلم من خلال الإعداد التجريبي على تخزين الطاقة. لقد ثبت أن درجة حرارة المخرج، ومخزن الطاقة، ومحكم الطاقة يمكن تحسينها من خلال الجمع بين سرعة الرياح 0.9 م/ث ، صفر (0) زعنفة مثقبة، ماص خارجي غير مغطى، وسماكة جدار ممتص خارجي 1 مم. وجد أن الأنابيب الزجاجية المفرغة ذات الطبقة المزدوجة تعد بتحسين أداء حراري أفضل مقارنة بالأنابيب الزجاجية غير المفرغة من الطبقة المزدوجة، والأنابيب الزجاجية الخارجية الشفافة أحادية الطبقة، والأنابيب الزجاجية الداخلية ذات الطبقة الرقيقة أحادية الطبقة. تمت صياغة المعادلة الرياضية لكل مكون من مكونات الـEGATC بناءً على القانون الأول للديناميكا الحرارية. يوضح إجمالي الخطأ المقبول البالغ 5٪ أن النموذج في كل عقدة كان صالحاً. تم الحصول على منحنيات الأداء لتلك الزعانف 0 (معادلة)، 0 زعنفة (تجريبية)، و 3 زعانف (تجريبية). أظهرت النتائج أن كفاءة (المجمع+التخزين) تأثرت بعدد الزعانف حيث بلغت الكفاءة 68.7٪، 71.2٪، 71.0٪. في الختام، أثبت EGATC في تطبيقات تسخين الهواء أنه مفيد لتطبيق عمليات التجفيف الشمسي، خاصة في البلدان الاستوائية مثل ماليزيا.

APPROVAL PAGE

The thesis of Zairul Azrul Zakaria has been approved by the following:

Zafri Azran Abdul Majid
Supervisor

Sany Izan Ihsan
Co-Supervisor

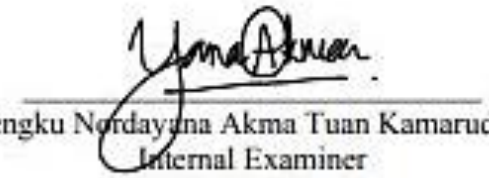

Tengku Nordayana Akma Tuan Kamaruddin
Internal Examiner

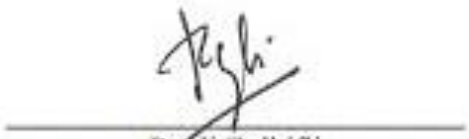

Rozli Zulkifli
External Examiner

Ahmad Faris Ismail
Chairman

DECLARATION

I hereby declare that this dissertation is the result of my own investigations, except where otherwise stated. I also declare that it has not been previously or concurrently submitted as a whole for any other degrees at IIUM or other institutions.

Zairul Azrul Zakaria

Signature 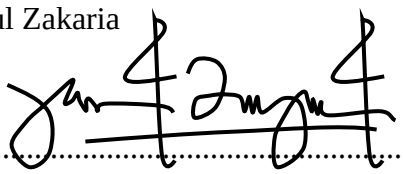 Date 25 MARCH 2023

INTERNATIONAL ISLAMIC UNIVERSITY MALAYSIA

DECLARATION OF COPYRIGHT AND AFFIRMATION OF FAIR USE OF UNPUBLISHED RESEARCH

DEVELOPMENT OF SOLAR INTEGRATED EVACUATED GLASS-THERMAL ABSORBER TUBE COLLECTOR (EGATC) IN AIR HEATING APPLICATION

I declare that the copyright holders of this dissertation are jointly owned by the student and IIUM.

By signing this form, I acknowledged that I have read and understand the IIUM Intellectual Property Right and Commercialization policy.

Affirmed by Zairul Azrul Zakaria

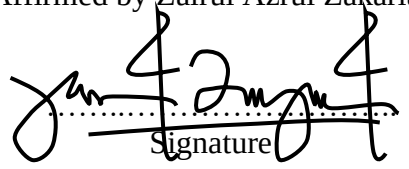

……. Signature

25 MARCH 2023 ……..
Date

DEDICATION

This thesis is dedicated to my late father and my mother for laying the foundation of what I turned out to be in life.

ACKNOWLEDGEMENTS

All glory is due to Allah, the Almighty, whose Grace and Mercies have been with me throughout the duration of my programme. Although it has been tasking, His Mercies and Blessings on me eased the herculean task of completing this thesis.

Firstly, it is my utmost pleasure to dedicate this work to my dear mother; Habsah @ Imah Sulong, my wife; Norazida Muda and my children; Ariff Fakhri Ghanimi, Azim Fahmi Hakimi, Nur Auni Faiqihah and Akid Faidh Baihaqi who granted me the gift of their unwavering belief in my ability to accomplish this goal: thank you for your support and patience.

I wish to express my appreciation and thanks to those who contributed their time, effort, support, and cooperation to the outcome of this work. To the members of my dissertation committee, Prof. Ahmad Faris Ismail, Associate Prof. Dr. Sany Izan Ihsan, and Prof. Dato' Dr. Kamaruzzaman Sopian, thank you for sticking with me. Not to forget, Dr. Iqbal Jamaludin, Dr. Ahmad Fadzil Sharol, Dr. Amir Abdul Razak, Dr. Muhammad Amin Harun and my fellow research group members who always gave words of encouragement.

Finally, a special thanks to Assistant Prof. Dr. Zafri Azran Abdul Majid, for his continuous support, encouragement, and leadership. I am most indebted to my supervisor, whose enduring disposition, kindness, promptitude, thoroughness, and friendship have facilitated the successful completion of my work. I put on record and appreciate his detailed comments, useful suggestions, and inspiring queries, which have considerably improved this thesis. His brilliant grasp of the aim and contents of this work led to his insightful comments, suggestions, and queries, which helped me a great deal. Despite his commitments, he took the time to listen and attend to me whenever requested. The moral support he extended to me is undoubtedly a boost that helped build and write the draft of this research work, and for that, I will be forever grateful.

Once again, we glorify Allah for His endless mercy on us, which enabled me to successfully round off the efforts of writing this thesis. Alhamdulillah.

TABLE OF CONTENTS

LIST OF TABLES

LIST OF FIGURES

LIST OF SYMBOLS

A	Cross-sectional area (m^2)
A_c	Surface area of collector (m^2)
A_s	Surface area (m^2)
C_p	Specific heat capacity (kJ/kg.K)
$\dot{E}_{in}$	Rate of energy, inlet (W)
$\dot{E}_{out}$	Rate of energy, outlet (W)
$\dot{E}_{system}$	Change of rate of energy in the system (W)
G_T	Global solar radiation, total (kW/m², W/m²)
H	Convective heat transfer coefficient ($W/m^2.K$)
H	Height (m, mm)
K	Thermal conductivity (W/m.K)
L	Length (m, mm)
S_R	Solar radiation (kW/m², W/m²)
T	Temperature (K, °C)
T_f	Temperature of fluid (K, °C)
$T_{f,i}$	Temperature of fluid, inlet (K, °C)
$T_{f,o}$	Temperature of fluid, outlet (K, °C)
T_{f1}	Temperature of fluid at point 1 (K, °C)
T_{f2}	Temperature of fluid at point 2 (K, °C)
T_i	Temperature, inlet (K, °C)
T_o	Temperature, outlet (K, °C)
T	Thickness (m, mm)
T	Time (s)
$\dot{Q}_u$	Rate of useful energy gain (W)
V	Air velocity (m/s)
W	Width (m, mm)
$\dot{m}$	Air mass flow rate (kg/s)
$\dot{m}_{in}$	Air mass flow rate, inlet (kg/s)
$\dot{m}_{out}$	Air mass flow rate, outlet (kg/s)

A	Thermal diffusivity (m^2/s)
E	Emissivity
H	Thermal efficiency
P	Air density (kg/m^3)
Tα	Transmittance-absorptance product

LIST OF ABBREVIATIONS

BOM	Bills of Materials
CFD	Computational Fluid Dynamic
DAQ	Data acquisition
e.g.	*(exempli gratia)*: for example
EGATC	Evacuated Glass-Thermal Absorber Tube Collector
et al.	*(et alia)*: and others
etc	*(et cetera)*: and so forth
fig./ figs.	*figure/ figures*
FPC	Flat Plate Collector
GMP	Good Manufacturing Practice
HP ETC	Heat Pipe Evacuated Tube Collector
i.e.	*(id est)*: that is
ID	Inner diameter
NA	Not applicable
OD	Outer diameter
PV	Photo-voltaic
PVC	Polyvinyl Chloride
SAHP	Solar Assisted Heat Pump
SS	Stainless steel
Vol./ Vols.	Volume/ Volumes

CHAPTER ONE

INTRODUCTION

1.1 BACKGROUND OF THE STUDY

Generally, the application of solar technology, either water or air heating, is limited due to weather conditions and system design. In Malaysia, the solar heating system is widely used for water heating and other applications, such as air heating, which was actively developed but is still in research. Solar heating system, either water or air operations, is more efficient using a solar thermal collector compared to a photo-voltaic (PV) system (Matuska & Sourek, 2017). Numerous types of solar thermal collectors, namely flat plate collectors (FPC) and heat-pipe evacuated tube collectors (HP ETC), have been developed in various countries and have become increasingly important for integrated solar heating systems (Sabiha et al. 2015). However, conventional FPC had low thermal efficiency, and its energy efficiency decreased during the off-sunshine hours (Ahmad Fudholi & Sopian, 2019).

Several researchers (G. L. Morrison et al., 2004)(Zubriski & Dick, 2012) agreed that ETC has much better efficiency than FPC. Solar thermal collector efficiencies were found to be 46.1% and 60.7% for FPC and HP ETC, respectively whilst the system efficiencies were found to be 37.9% and 50.3% (Ayompe et al., 2011). This experiment between FPC and HP ETC was conducted simultaneously with similar environmental conditions. Regarding performance, HP ETC had better performance in producing high outlet temperatures than FPC, especially in cold climates (Mahdjuri, 1979). The performance levels of solar thermal collectors have been enhanced through several techniques, such as using extended surfaces i.e. fins, corrugated thermal absorbers, packed bed materials, and artificial roughness (Abhishek Saxena et al., 2015). A large range of temperatures had been obtained by different solar thermal collector configurations; for example, 20ºC - 80ºC was the operating temperature of FPC (N.

Sharma & Diaz, 2011), and 50ºC - 200ºC was for HP ETC (Soteris A. Kalogirou, 2014) (Tyagi, Kaushik, et al., 2012). Although FPC produced low and moderate hot air temperatures, it was appropriate for drying agricultural products (Ahmad Fudholi & Sopian, 2019). To be in line with technological advancements, the technical directions in the development of solar-assisted drying systems for agricultural products should be of compact collector design, having high efficiency, integrated storage, and long-life drying system (A. Fudholi et al., 2010).

1.1.1 Climate Condition in Malaysia

The solar energy received by the earth differs for each location depending on climate conditions and various other factors, which required the solar radiation studied for different world regions (Chuah & Lee, 1981). The Peninsular of Malaysia is at the equatorial climate located from a latitude 1°20'N to 6°40'N, and a longitude of 99°35'E to 103°20'E. It was rare to have a cloudless clear sky even during severe drought (Jabatan Meteorologi Malaysia, 2021). Generally, Malaysia had a constant temperature throughout the year with a moderate temperature of 25.6°C to 27.8°C with high humidity, heavy rainfall, and low wind speed (Othman & Sopian, 2002). It has mostly two Monsoons, south-west and north-east, in which both phases bring heavy rain and clouds to the west and east coast, respectively. During the sunny season, the weather is hot and sunny, with scattered cloud formation and rainfall (Chuah & Lee, 1981).

Malaysia received an average global solar radiation per annum of 4.63 kWh/m² (Tamer Khatib et al., 2012), with an average diffused solar radiation within 2.65 kWh/m² to 2.977 kWh/m² in a year (Azhari et al., 2012). In contrast, direct solar radiation was 1.98 kWh/m², which was less dominant than diffused solar radiation. Recently, according to International Energy Agency et al. (2021), Malaysia received about 5.0 kWh/m² of average solar radiation throughout the year. Diffused solar radiation condition was more frequent with cloudy skies than clear sky condition since Malaysia was located in the equatorial region (Oliver, 2005).

1.2 STATEMENT OF THE PROBLEM

Nowadays, the solar thermal collector technology for drying applications has become more significant. This is due to food preservation after considering unpredictable weather changes as well as the increasing of the earth's temperature and greenhouse gases in the world's atmosphere. The situation is worsening with the food demand of the world population and the advancement of agricultural technology (Elferink & Schierhorn, 2016). This study identified several problems related to a stationary solar thermal collector drying systems that can serve as a guide for the development of an appropriate system. There are:

1.2.1 Diffuse Solar Radiation

A flat plate collector (FPC) was used to convert solar radiation into heat during day time, and the performance was decreased at night or in poor weather conditions such as cloudy or rain (Z. Wang et al., 2018)(Abuşka et al., 2020). For countries with four seasons, the system efficiency using solar thermal collectors, namely FPC was limited during winter and autumn. This demonstrated that FPC was very dependent on solar radiation (Majid et al., 2009)(Rassamakin et al., 2013)(Motahayyer et al., 2019). Although Malaysia was located close to the equatorial line, the duration of day and night throughout the year was almost identical. However, the gained intensity was inconsistent due to weather factors such as rainy and cloudy conditions (Oliver, 2005). This has affected the low and outlet temperature’s instability due to heat storage and heat conversion time issues.

1.2.2 Solar Thermal Collector Position

FPC requires a sun tracker to obtain maximum yearly solar energy collection. FPC needs to be positioned either to South facing for Northern Hemisphere or North facing for Southern Hemisphere (Shafieian et al., 2019). As in the Northern Hemisphere, the sun's path during the daytime was crossed from East to West. A South facing position

could ensure that the solar thermal collector absorbs more solar radiation, especially in the period when solar radiation reaches its maximum level (Mao et al., 2019). The use of sun-tracking concentrating collectors has increased either in the preliminary setup or maintenance cost for both residential users and solar plants (Ullah et al., 2019) and also limited the structure design. Carballo et al. (2019) presented a new approach to the sun tracking system, which could improve the control strategies of the system and, therefore, the system performance. This system required large and higher altitude site placement to maximize the power output, which leads to design limitations of a solar thermal collector.

1.2.3 Limitation on Orientation

The tilted angle of the solar thermal collector robustly contributes to the amount of solar radiation absorbed by the solar thermal collector (Hafez et al., 2017). Both FPC (passive system) and HP ETC (as its working condition), which are inherently exposed to continuously variable weather conditions, may produce significant capacitance effects (Klein et al., 1974) and need to be tilted at the correct angle to maximize the performance of the system (Shariah et al., 2002)(Karmakar et al., 2019)(Q. Li et al., 2020). This orientation may limit the arrangement layout. For areas located in the equatorial, the solar thermal collectors need to be flat to obtain maximum energy from solar radiation throughout the year (Soteris Kalogirou, 2003)(Abdul Majid, 2011)(Arvind Kumar et al., 2020). The approach used in this investigation was similar to other researchers on solar photovoltaic (PV). The maximum output of the PV cell requires a perpendicular light on its surface where radiation can be captured (T. Khatib et al., 2015)(Fazlizan et al., 2019).

1.2.4 Thermal Losses

In order to increase the heat transfer rate between hot air and the thermal absorber, the surface contact area of the thermal absorber with the working liquid had to be higher (Razak et al., 2019). However, certain energy absorbed by the flat plate collector (FPC)

was lost to the atmosphere due to the higher temperature of the plate (Sekhar et al., 2009). The effects of thermal losses on FPC were similar to those of heat-pipe evacuated tube collector (HP ETC). As an existing air dryer design, the hot air for drying agricultural products can be forced to flow in the water to the air heat exchanger. According to A. Fudholi et al. (2010), the small surface contact area between the heat pipe and water via the thermosyphon effect and the usage of a hot water tank as heat storage of the solar drying system leads to further thermal losses and efficiency. Normally, FPC uses non-vacuum flat glass, and ETC uses double layer vacuum glass, in which the vacuum provides better sun energy absorption and simultaneously reduces the heat transfer mechanism lost by radiation.

1.2.5 Split Design of Thermal Energy Storage

The technical directions in developing solar-assisted drying systems for an agricultural product were compact collector design, high efficiency, integrated storage, and long-life drying system (A. Fudholi et al., 2010). For flat plate collector (FPC) and heat-pipe evacuated tube collector (HP ETC), which integrates energy storage in its system, the energy storage compartment was generally constructed separately from the solar thermal collector unit (Luo et al., 2017). The main disadvantage of solar thermal collectors that operated at low to medium temperatures was their lower thermal performance due to imperfections in their structural design and manufacturing, as well as the type of materials that were utilized in the construction of different parts, including the thermal absorbers (Gorjian et al., 2020). This condition led to a bulky solar thermal collector system. It also affects the performance in terms of energy losses from convection.

1.2.6 Design Flexibility

The existing design of FPC and HP ETC solar drying or space heating, water heater, and Solar Assisted Heat Pump (SAHP) available in the market required additional space for a heat exchanger module and working liquid reservoir to be attached to the

system, which leads to the load increment. The working liquid acts as the medium of heat storage, which requires large space, low heat storage per mass ratio, and needs a special compartment to store the latent heat (Lane GA., 1983)(A. Sharma et al., 2009). The effects of the research on space allocation were similar to the SAHP study by Baradey et al. (2015). They discovered that the main differences between available commercial heat pumps in the market nowadays were the type and size of the heat source, heat storage system, and solar thermal collector type. Ahmad Fudholi et al. (2015) developed a greenhouse solar drying system with a heat exchanger. This forced convection design consists of the HP ETC, electric heater, blower, water pumps, storage tank, and drying chamber, which required extra space on the design, resulting in load increment. This design was inappropriate due to its location and placement on the rooftop. Infact, Mohd Chachuli et al. (2021) also had discussed similar factors that limit renewable energy research and development activities in Malaysia.

Based on the listed problems, it can be summarized that the problems related to a stationary solar thermal collector drying systems were diffused solar radiation conditions and the system's design.

1.3 RESEARCH OBJECTIVES

The main aim of this research is to fabricate the solar integrated evacuated glass-thermal absorber tube collector (EGATC) that can be used in air heating applications with better thermal collector performance during diffuse solar radiation conditions. Meanwhile, the specific objectives of this research are as follows:

i. To design and develop the evacuated glass-thermal absorber tube collector (EGATC) by improving performance and efficiency.

ii. To improve the thermal absorber with double pass flow arrangement for EGATC.

iii. To systematically investigate the effect of parameters (such as inner absorber surface area air contact (perforated fin), outer absorber selective coating surface, outer absorber wall thickness, double layer non-vacuum glass tube, single layer transparent outer glass tube and single layer thin film inner glass tube) on the performance of the EGATC.

iv. To formulate the mathematical equation for each EGATC's main component and validate with the experimental results with performance analysis.

1.4 SIGNIFICANCE OF THE STUDY

The research significantly influences the performance of evacuated glass-thermal absorber tube collector (EGATC) in terms of heat storage capability by a heat transfer mechanism (i.e., radiation, conduction, and convection), thermal absorber temperature uniformity and thermal inertia/ thermal reliability, which are beneficial during diffuse solar radiation conditions. This new technology applied direct heat induction to replace conventional heat-pipe evacuated tube collector (HP ETC), which focused on a water heating system.

EGATC was developed purposely for an air heating system that is assembled together with the ventilated chamber. The thermal absorber collects the heat energy from the sun and converts it into the air. The absorber wall thickness itself acted as heat storage material. EGATC was designed to meet the requirement of Good Manufacturing Practice (GMP) for food drying, whereby selective coating was coated on the outer surface of the thermal absorber to avoid direct air contact with drying material. The design also provided double pass flow arrangement to increase the heat gained efficiency. The results obtained from this study will serve as fundamental knowledge of the EGATC, which is utilized towards the commercialization of the Solar Integrated EGATC Air Heater.

1.5 RESEARCH METHODOLOGY

The methodology starts with the process of studying the current design of solar thermal collectors and dryers. The existing solar thermal collectors, specifically heat-pipe evacuated tube collector (HP ETC), was studied, and the gap existing between them was defined. Besides, the existing research on the HP ETC air dryers also was reviewed and investigated due to several affected parameters in order to increase the performance. The literature on the specific topic, methodology, and theoretical approach is also discussed here in detail as well.

Then, it was followed by the design and development of a preliminary system. At this stage, the experimental research setup and data collection procedure were stated clearly. The preliminary experiments were directed to ensure the design was on the right path by monitoring the theoretical statements that were similar to the experimental results. It was conducted under real ambient conditions. If the result is aligned theoretically, it will only then proceed to the next process. Otherwise, the earlier process has to be restarted again.

Next, the Bills of Materials were prepared (BOM), and the items were purchased. The BOM was prepared according to the technical drawing and components needed. Then only the purchasing process was started. The detailed itemized cost and specification also was stated here based on the recent market search and availability for future reference.

After that, was the fabrication of the experimental test rig, determination, and installation setup of Data Acquisition (DAQ) system for parameter experiment. Several parameter experiments were conducted as indoor experiments under artificial solar radiation to obtain the best design that was able to enhance the performance. The parameter involved were inner absorber surface area air contact (perforated fin), outer absorber selective coating surface, outer absorber wall thickness, inner absorber double pass flow arrangement, double layer non-vacuum glass tube, single layer transparent

outer glass tube and single layer thin film inner glass tube. The fabrication work of the experimental performance rig was started after the ideal design was defined.

Later, the testing and evaluation of the experimental performance rig were done. The designed solar thermal collector was tested, and the reading was evaluated. Consequently, data analysis was done based on the results to determine the solar thermal collector performance and efficiency. The results also were analyzed on the heat transfer process, and by developing a mathematical model that was used to determine the heat gain that occurred in the system

Lastly, the results obtained from the experiment was compared with the results obtained from the mathematical model. The mathematical model was the equation derived from the heat transfer equation involved inside the solar thermal collector. If the comparison results were satisfied, then only the process proceeded to the next step. If not, the testing and evaluation of the test rig were conducted again. After that, the documentation and report writing are started.

1.6 RESEARCH SCOPE

This research comprises of several main scopes as follows:

i. The Evacuated Glass-Thermal Absorber Tube Collector (EGATC) prototype was fabricated with an overall size OD 38mm × L590mm inside double layer evacuated glass tube with dimension OD 58mm × L500mm ended with the ventilated chamber with dimensions 50.8mm × 50.8mm × 63.5mm.
ii. EGATC inner absorber with dimension OD 12mm × L497mm × t1mm was placed inside EGATC outer absorber with dimension OD 38mm × L467mm × t1mm to create a double pass flow design arrangement.
iii. EGATC experimental test rig was set up in an array arrangement with a Heat Pipe Evacuated Tube Collector (HP ETC) by heat pipe dimension, L400mm × header diameter 14mm × pipe diameter 8mm inside similar

dimension of double layer evacuated glass tube and drying chamber with dimension OD 110mm × L300mm × t1mm. Each solar thermal collector was assembled as a portable with an overall size L850mm × W450mm × H900mm.

iv. The material used for EGATC was stainless steel pipe for both inner and outer absorbers. While the material used for HP ETC was copper for the heat pipe attached with an aluminium mounting per available in the market. The drying chamber for each solar thermal collector was in the form of a PVC (Polyvinyl Chloride) pipe.

v. The maximum temperature inside the drying chamber experienced a temperature range of 50°C to 60°C to ensure the perfect drying.

vi. The outdoor experiment was conducted during the non-raining condition and was exposed to ambient conditions, i.e., dust, clouds, and wind.

vii. A mathematical model for each EGATC's main components will be developed, considering that the thermal system was in a steady-state condition. The computation of the model will be developed using Microsoft Excel.

1.7 REPORT STRUCTURE

As the introduction, Chapter 1 gave a clear background of what this research was all about. The problem statements, research objectives, significance of the study, research methodology, research scope, and report structure are explained clearly in this chapter. Chapter 2, on the other hand, covers a wide range of literature reviews from past research done by researchers in the field of solar thermal from all over the world. Detailed literature was discussed in terms of global solar energy needs, food drying needs, the definition of solar thermal, type of solar panels and collector, their categories, technologies and applications, thermal absorber technology, double pass flow design arrangement and the influence of mass flow rate in a solar collector. It also discussed heat transfer analysis of evacuated glass-thermal absorber tube collector (EGATC).

Chapter 3 talks about the research methodology used for this research. The path was properly arranged through the design process's flow chart to ensure the research's success. The methods were divided into three sections, preliminary experimental design, experimental parameter design, and performance experimental design. In the preliminary experimental design, the first step was done by studying the current design of the solar thermal collector and solar air dryer. The preliminary design was built and set up as a preliminary experiment. This pilot test was done to ensure that the results obtained from the preliminary experiment were aligned theoretically. In the second section, which was experimental rig design, it starts with list of bills of materials (BOM) and fabrication of the portable test rig for parameter experiment and performance experiment. The parameter experiment was done to investigate several parameters that affect the performance, whereas the performance experiment was conducted to obtain the EGATC performance. Both preliminary and performance experiments were conducted as outdoor experiments by exposure to real solar radiation, while parameter experiment was conducted as indoor experiments under artificial solar radiation. Based on the collected data, the analysing was done to determine the performance and efficiency of the EGATC. The theoretical analysis method consists of a mathematical modelling role, thermodynamics energy balance, collector performance, heat transfer analysis, and analytical solution for mathematical modelling is also presented.

In chapter 4, the results and discussion are placed here. The results of the preliminary and test rig experiment were determined. Regarding the preliminary experiment, the data was recorded, followed by the plot of the graph Temperature, T (°C) versus Time, t (s). For the parameter experiment, the parameters involved taken into consideration were thermal absorber surface area air contact (perforated fin), outer absorber selective coating surface, outer absorber wall thickness, inner absorber double pass flow arrangement, double layer non-vacuum glass tube, single layer transparent outer glass tube and single layer thin film inner glass tube. The data on the performance experimental also was recorded. The graph Temperature, T (°C) versus Time, t (s) was

plotted in order to evaluate the performance of the thermal absorber. In fact, the effect of the heat transfer process and airflow are described here.

Finally, Chapter 5 concluded whether the research objectives were achieved or not based on the experimental runs, testing, and evaluation performed in this research. In addition, the recommendations for future work are stated here as well.

1.8 CHAPTER SUMMARY

This chapter has presented and discussed the background of the study. It explained why solar thermal collectors which were FPC and HP ETC, are crucial in various countries, the drawback of FPC, the advantages of HP ETC, and the climate condition in Malaysia. Additionally, the problem statements were discussed, as this study is set to enhance the existing HP ETC technology that is available in the market. These are followed by research objectives, the significance of the study, and the research methodology. This chapter also presented the research scopes and, finally, the research structure.

CHAPTER TWO

LITERATURE REVIEW

2.1 INTRODUCTION

Since the study aimed to develop a new design of thermal absorber, namely an Evacuated Glass-Thermal Absorber Tube Collector (EGATC) in air heating applications, it is important to explore the thermal absorbers technology and Evacuated Tube Collectors (ETC). Furthermore, the literature review emphasized on the types of solar thermal collectors, the influence of wind speed, mass flow rate, and insulation material on the solar thermal collector. What should also be covered is the existing technology of solar thermal dryers on HP ETC (Heat-Pipe Evacuated Tube Collector). Ultimately, mathematical modelling and EGATC's configuration in air heating applications are discussed.

2.2 NATIONAL AGRICULTURAL POLICY

The demand for food and the advances in agricultural technology had challenged the technologists to produce a more sophisticated drying system. This was seen through the National Agriculture Policy, which tried to reduce the dependency on imported food. To implement this policy, agricultural industry operators must introduce more efficient ways of food processing, which also involves the existing drying technologies.

Some existing drying technologies needed to be enhanced to process food more efficiently. Therefore, numerous studies have been carried out on the development of advanced solar-assisted drying systems in Malaysia (Desa et al., 2020)(Mat Desa et al., 2019)(Sopian et al., 2012)(A. Fudholi et al., 2010)(Othman et al., 2006). Drying of agricultural products is carried out in a variety of ways, from

directed exposure to solar radiation to a system that operates automatically. These methods depended on how easy and efficient the sources of drying energy were to be obtained.

2.3 DRYING IN THE AGRICULTURAL SECTOR

According to Baradey et al. (2018), in the next fifty years, the total global population will reach about 9 billion people. Following that global trend, the Malaysian population will continue to increase concurrently. Data from the Department of Statistics Malaysia (2022) shows that the Malaysian population was at 32.4 million people in 2018 compared to 32.0 million in 2017, with an annual growth rate of 1.1 percent. Based on the situation, Malaysia's population increased to 32.7 million in 2019, and recently it was at 32,920,286 in 2022.

Generally, Malaysia's population was projected to increase from 28.6 million in 2010 to 41.5 million in 2040. Nevertheless, the population increased, with the annual population growth forecast rate decreasing from 1.8 percent in 2010 to 0.8 percent in 2040. The average population growth rate decreases by 0.05 percent per year. This growth significantly affected the amount of food consumption. Large-scale agricultural products should be kept in stock to ensure the food supply is sufficient and persistent in the long term. Therefore, the food should be preserved and stored for future use or the market.

Drying has become one of the options for food preservation in the agricultural industry. In maintaining the available stock, the agricultural products should be dried so that the water content reaches the standard value. The value of the standard water content is the amount of water contained in an appropriate agricultural product to keep it within a long period of time before the product is processed into food or for other uses. According to Tamrin et al. (2017), moisture content and relative humidity during delayed rough rice drying affected the physical quality of milled rice. The study was conducted in Indonesia and found that most of the rough rice was not dried immediately

due to a lack of sunlight in the rainy season. The best delayed rough rice drying duration in such conditions should not exceed 3 days.

2.4 DRYING PROCESS

Drying is one of the concise preservation methods, i.e., extracting the water content in the substance to be dried. According to M.Y.H. et al. (2000), there are three processes involved in the process of drying, namely the physical, chemical, and biological processes. The physical process is extracting water from the substance, which depends on the type of substance to be dried. Chemical processes affected changes in the dried substance's flavour, colour, and structure. Meanwhile, Biological processes are like yeast and fungal growth caused by microorganisms such as bacteria. The water content of an agricultural product is not the only factor that should be considered in marketing. The other factors include the content of foreign substances, such as the percentage of broken seeds, dust, wood twigs, and dry pith. However, water content becomes one of the most important factors because high water content causes the grain to fail to withstand being stored for long periods because the seeds will be germinated or turn into mold (El-Sebaii & Shalaby, 2012)(Inyang et al., 2018). The less water it consumes, the longer the seeds can be stored.

Nevertheless, the seeds may break or crush if the grain is dried up beyond its dry limit. This would reduce the quality of agricultural products and simultaneously reduce the income of the entrepreneurs as well. The effect of the quality is similar to the other researchers' findings. According to Musembi et al. (2016), agricultural products were dried to increase shelf-life, reduce packaging cost, increase shipping capacity and enhance appearance while maintaining flavor and nutritional value. Therefore, whether the drying process is realized or not, should be controlled. Factors affecting drying in drying chambers were discussed by Abdul Majid (2011). Six parameters were identified that affected drying, i.e., temperature, relative humidity, pressure, air velocity, air circulation, and the surface area of the substance to be dried.

These factors are very important to ensure the optimum quality of the product and energy consumption.

2.4.1 Drying Kinetics

Drying kinetics is represented as the drying rate against drying time. It indicates the reduction of the moisture content from the material. Drying kinetics is important for predicting drying time and conditions in the drying process. The understandings of drying kinetics influence the drying method and controls the drying process (Maisnam et al., 2016). The drying rate with controlled temperature affects the drying times. At the constant air humidity, the increasing drying air temperature may enhance the drying process.

There are several studies on drying kinetics for food products, such as the drying kinetics of apples (Bi et al., 2015), black carrots (Garba et al., 2015), strawberries (Bórquez et al., 2015), carrots (C. Xu et al., 2014), garlic (Calín-Sánchez et al., 2014), guava (P. S. Kumar & Sagar, 2014), green beans (Tekin et al., 2017), jackfruit (Alok Saxena et al., 2012), sweet potato (Doymaz, 2012), banana (Borges et al., 2011) mushroom (Giri & Prasad, 2007), lemon slices(J. Wang et al., 2018) and Mediterranean mussels (*mytilus galloprovincilis*) (Kouhila et al., 2020).

Experiments also had been carried out in Malaysia to study the effect of drying air temperature and humidity on the drying characteristics of lemon grass by Ibrahim et al. (2009). They found that the major element that affected the drying kinetics was the drying air temperature. Hence, a higher drying air temperature influences a higher drying rate and decreases the moisture ratio.

2.5 GLOBAL ENERGY CRISIS

The world is now facing an energy crisis (Global Energy Review 2020, 2020). The energy crisis is a phenomenon where energy resources are constantly declining, and it is seen as an important factor in sustaining the world economy. It is often associated with the main energy sources people have used at a certain place at a given time, for example, countries that provide electricity grids or use them as fuel in vehicles. According to Goswami (2015), the amount of fossil fuels will decline in the next 50 years due to fast-growing energy demand in the Asia Pacific, specifically in China and India. This will create a world energy crisis as the energy demand exceeds the available energy reserves.

Formerly, fossil fuels, especially diesel and kerosene were the drying system's most commonly used energy sources. During this time, petroleum-based technology was more advanced compared to other technologies. The price was lower and easy to access, which became an important factor in why petroleum was widely used (M.Y.H. et al., 2000). Since the world is facing an energy crisis, the need for an alternative energy source, such as renewable energy, to replace the over-reliance energy production from fossil fuels is crucial (Hordeski, 2020). It has become more important as the cost of petroleum increases.

2.6 NATIONAL GREEN TECHNOLOGY POLICY

In Malaysia, the awareness of the petroleum energy crisis has increased, and the government, through the Ministry of Energy, Science, Technology, Environment, and Climate Change, has stated the strategies for not relying on existing energy resources (Oh et al., 2010). Hence an initiative was carried out by reviewing the old policy of Net Energy Metering (NEM). NEM adopted the practice where the energy produced from the solar Photovoltaic (PV) system installed would be consumed first, and any excess to be exported to the official distribution licensee, Tenaga Nasional Berhad (TNB).

Effective 1 January 2019, the new mechanism of NEM allowed electricity users who had installed solar panels at their homes or premises to reduce electricity bills to create savings (Razali et al., 2019). This initiative was aligned with the National Green Technology Policy (Ministry of Energy Green Technology and Water, 2017) (Water, 2010), which emphasized the increase in the energy supply sector through green technology applications in energy generation and supply management, including co-generation in the industrial and commercial sectors. The existence of this policy in the nation's agenda saw the government's support and willingness to give a very high commitment to ensure sustainable development and conserve the environment for future generations and subsequently to become the catalyst for the development of solar energy in Malaysia (Mustapa et al., 2010).

2.7 TYPES OF SOLAR PANELS AND COLLECTOR

The use of solar energy in human activity has reached unexpected usage. This is due to the ongoing research conducted to find alternative sources to replace the usage of fossil fuels. According to Mekhilef et al. (2011), solar energy conversion was widely used to generate heat and produce electricity. A comparative study on world energy consumption released by International Energy Agency (2015) shows that in 2050, low-carbon energy technologies will be the world's main supplier of energy demand. Energy revolutions such as energy efficiency, carbon capture and storage, nuclear power, new transport technologies, renewable energy, and solar energy must be gradually imposed to reduce greenhouse gas (GHG) emissions.

Solar energy could be harvested from solar panels. There are four (4) types of solar panels and collectors, namely Photovoltaic (PV) panels, solar thermal (ST) collectors, Photovoltaic-Thermal (PV-T) panels, and Concentrating solar panels (Ahmad et al., 2020). Mainly, PV panels are used to gain electricity from solar energy directly, whereas ST collectors use solar energy to generate heat. The combination of both PV and ST creates PV-T. The PV-T panels use solar energy to produce electricity and heat (Ramos et al., 2017). On the other hand, solar panels use mirrors or lenses to

focus on solar energy by reflecting solar irradiation to a receiver to generate heat (Hairat & Ghosh, 2017).

2.8 SOLAR THERMAL COLLECTORS' CATEGORIES

Solar thermal was the leading renewable energy in terms of cumulated installed heat capacity for many years until 2016, when the wind energy system took the lead (Weiss & Spörk-Dür, 2018). Solar thermal collectors heat a working liquid such as water by absorbing directed heat from the sun. The paybacks offered by the system comprised of free supply of sustainable heat throughout the year, reduced carbon dioxide emissions and lower energy bills (Energy Saving Trust, 2010).

The performance levels of solar thermal collectors could be enhanced through several techniques, such as using extended surfaces i.e., fins, corrugated absorbers, packed bed materials, and artificial roughness (Abhishek Saxena et al., 2015). **Figure 2.1** shows the categories of solar thermal collectors adapted from Soteris A. Kalogirou (2004) and Sarbu et al. (2017). As far as the stationary collectors are concerned, there are mainly three (3) of them, namely flat plate collector (FPC), evacuated tube collector (ETC), and compound parabolic collector (CPC).

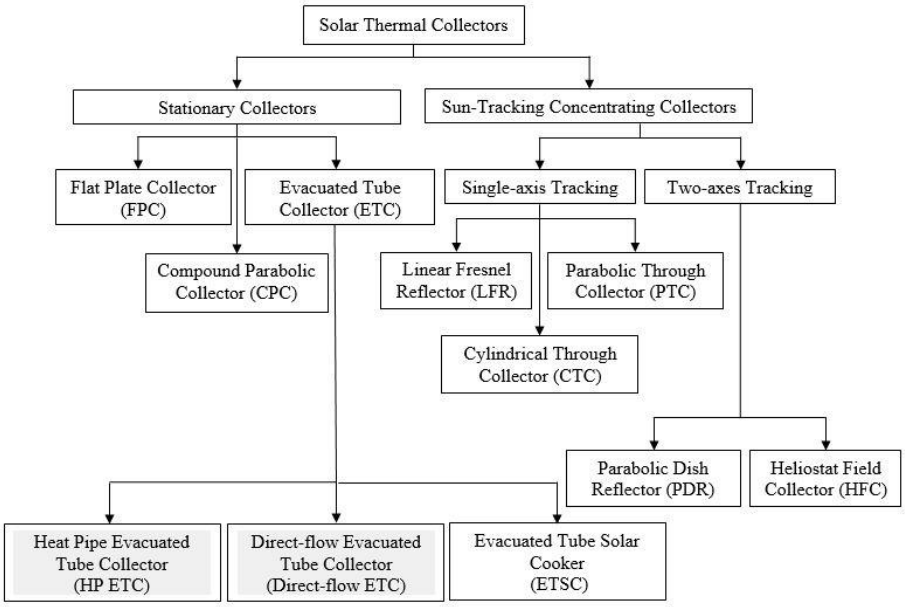

Figure 2.1: Types of existing solar thermal collectors (Soteris A. Kalogirou (2004) and Sarbu et al. (2017))

Although solar thermal was predominated by small-scale individual systems for residential water heating (Freeman et al., 2015), it has been expanding to large-scale solar thermal plants connected to district heating networks or large buildings (Tian et al., 2019). The interest in using solar thermal in industrial applications also grew as well (L. Kumar et al., 2019). The most attractive solar thermal technology studied by several researchers includes flat plate collector (FPC) (Drosou et al., 2014)(Sridharan & Shenbagaraj, 2021), evacuated tube collector (ETC) (Freeman et al., 2015b)(I. Singh & Vardhan, 2021), parabolic trough collector (PTC) (Calise, 2012)(Zaaoumi et al., 2021), and compound parabolic collector (CPC) (Eicker et al., 2014)(Xia et al., 2021).

2.9 ETC TYPES AND TECHNOLOGY

Evacuated tube collector (ETC) comprised of a glass tube from which the air had been evacuated. The evacuated glass tube contained a metallic absorber, at which the solar radiation was absorbed and through which water is pumped (Sabiha et al., 2015) in the study of ETC water heaters. The absorber tube is evacuated to minimize heat loss from

the metallic absorber to the environment. According to Arvind Kumar et al. (2020), the efficiency of ETC depends mainly on three factors, i.e., the collector's design, the absorber tube's optical properties, and the working fluid inside the tube. By using reflectors, the total solar input was increased.

The first evacuated tubular collector was built and tested by Speyer (1965). Speyer constructed a U- tube joining the two conduits attached with a spiral spring (conduits support) as a thermal absorber which was mounted inside the evacuated glass tube. Teles et al. (2019) investigated the thermal performance of low-concentration ETC and discovered that thermal efficiency could be achieved by more than 60% of the system annually. Recently, there were various studies on the specific types of ETC, namely Heat-Pipe Evacuated Tube Collector (HP ETC) (Huang et al., 2019)(Abo-Elfadl et al., 2020), Direct-flow Evacuated Tube Collector (Direct-flow ETC) (X. Zhang et al., 2014)(Abokersh et al., 2017)(Essa et al., 2021) and Evacuated Tube Solar Cooker (ETSC) (Herez et al., 2018)(Hosseinzadeh et al., 2020).

In regards to installation guidelines, the evacuated tubes should be aligned in a parallel arrangement. Sadeghi et al. (2020) demonstrated that the change in longitude did not influence the amount of solar radiation, whereas the change of latitude could affect such an amount. The regions with higher latitudes (northern orientation) should receive more radiation during the daytime. In a North South orientation, the tubes could passively track heat from the sun all day. While in an East West orientation, they could track the sun all year round. Alghoul et al. (2005) studied materials and heat transfer properties of materials and the manufacturing challenges of a flat plate, evacuated tubes, and heat pipe tube. On the other hand, I. Budihardjo & Morrison (2009) mentioned that HP ETC was the most used collector among other evacuated collectors in solar water heaters due to its simple construction and low manufacturing costs. **Table 2.1** shows the characteristics of a typical ETC adapted from Soteris A. Kalogirou (2004).

Table 2.1: Characteristics of a typical ETC system

Parameter	Value
Glass tube diameter	65mm
Glass thickness	1.6mm
Collector length	1965mm
Absorber plate	Copper
Coating	Selective
Collector slope angle	Latitude +5° to 10°

Essentially, HP ETC consists of single- or double-layer glass tubes containing a copper heat pipe and mounted with an aluminium bracket. Inside the copper heat pipe, the working liquid (usually methanol or ethanol) experiences an evaporating-condensing cycle as long as the sunlight heats the collector (Kocer, A. et al., 2015)(S. A. Kalogirou, 2016). The high vacuum formed in the gap between double-layer tubes in ETC eliminates convection heat loss and provides effective thermal insulation; therefore, higher temperature levels occur compared to FPC (Papadimitratos et al., 2016).

HP ETC used working liquid as a phase change material (PCM) to transfer heat at high efficiency from the liquid to the vapour phase (Siva Kumar et al., 2017). This type of solar thermal collector features a sealed copper heat pipe placed inside a vacuum-sealed tube. The pipe is attached to an aluminium fin as a mounting. The heat pipe was separated into two (2) sections, namely, header and pipe. The header was placed on the top and attached to the sealed pipe. Inside the heatpipe, the pipe contained a small amount of working liquid that undergoes an evaporating-condensing cycle. In this cycle, heat gained from solar radiation evaporates the working liquid inside the pipe, and the vapour travels to the header, where it condenses and releases its latent heat. The condensed fluid returned to the pipe, and the process was repeated. **Figure 2.2** shows the specification of the heat pipe available in the market manufactured by MISOLIE TECHNOLOGY in China.

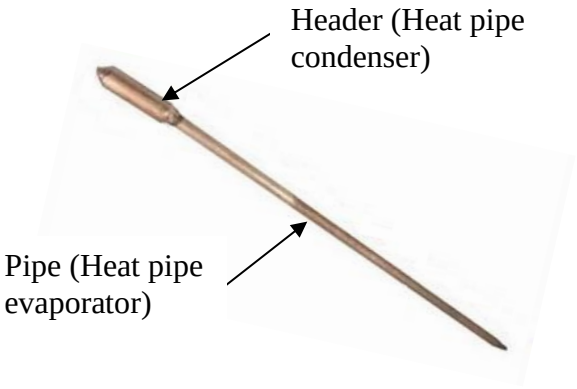

(a)

Parameter	Value
Material	Copper
Header diameter × length	Ø14mm × 55mm
Pipe diameter × length	Ø8mm × 345mm
Total length	400mm
Fit for ETC	500mm

(b)

Figure 2.2: (a) HP ETC and (b) Specification of the heat pipe available in the market

2.9.1 Glazing Materials

Glass has been widely used to cover solar collectors since it transmits as much of the incoming shortwave solar radiation while none of the longwave radiation emitted outward by the thermal absorber (Mandalaki & Tsoutsos, 2020). Glass with low iron content has a relatively high transmittance for solar radiation (approximately 0.85–0.90 at normal incidence), but its transmittance was essentially zero for the longwave thermal radiation (5.0–50 mm) emitted by sun-heated surfaces (Soteris A. Kalogirou, 2004).

For direct radiation, the transmittance varies considerably with the angle of incidence (ASHRAE, 2019). Daily PV power losses and monthly efficiency reduction occurs due to dust in some locations being more than 1% and 80%, respectively, which was relatively high (Kazem et al., 2020). The glazing should admit as much solar irradiation as possible and reduce the upward heat loss as much as possible. Radwan et al. (2020) reported experimental and theoretical studies on various thermal and electrical performances of glazing systems. The results showed that the semi-transparent Photo-Voltaic with Vacuum Glass (VGPV) system achieved a lower transient temperature variation of the inner and outer surfaces of the glazing systems.

The effect of glazing also was studied by Messaouda, Hamdi, et al. (2020), Memon et al. (2020), Raza et al. (2020), Memon & Eames (2020), and Dabra (2020). Although glass was virtually opaque to the longwave radiation emitted by the thermal collector, absorption of radiation caused a rise in the glass temperature and a loss of heat to the surrounding atmosphere by radiation and convection.

ETC was manufactured from high borosilicate evacuated glass tubing as a glazing material that provides a medium of heat transfer from solar radiation directly or indirectly with minimum heat losses through radiation and convection (G. Saxena & Gaur, 2018). It received over 90% of solar ultraviolet radiation, while another spectral composition of solar radiation was completely blocked by the oxygen contained in the upper layers of the atmosphere and by the ozone layer (Who, 2002)(Grandi & D'ovidio, 2020). The inner glass tube transmitted the short-wavelength solar radiation to the thermal absorber inside but blocked the reflection of the longer-wavelength irradiation to the vacuum pocket due to the opaque surface. Hence, it absorbs approximately all the solar radiation in it. **Figure 2.3** shows the evacuated tube collector (ETC) available in the market manufactured by MISOLIE TECHNOLOGY.

Figure 2.3: Conventional evacuated tube collector (ETC) design

2.9.2 Vacuum Tube

ETC basically consists of a heat pipe inside a vacuum-sealed tube. A large number of solar thermal collector variations and shapes of ETC are available in the market (Arvind Kumar et al., 2020). Another variation of this collector is called the Dewar tube. Two (2) concentric glass tubes were used, and the space in between the tubes was evacuated and known as a vacuum jacket. Due to turbulent conditions in the straight-through all-glass tube, a higher heat transfer rate could be achieved than in a Dewar-tube ETC, by increasing heat extraction and decreasing heat losses (Gong et al., 2020). The advantage of this design is that it is made entirely of glass, and it is not required to infiltrate the glass envelope to extract heat from the tube; thus, leakage losses do not exist, and it is also less expensive than the single envelope system (Graham L. Morrison, 2013). George et al. (2020), after approximately 40 years in storage condition, also verified the vacuum's stability as the aged tube still functions to a high standard in terms of maintaining a low emissivity and good vacuum level.

Table 2.2 shown the specification of the evacuated tube manufactured by MISOLIE TECHNOLOGY. The tube was similar to the conventional Dewar flask and consisted of two (2) borosilicate glass tubes with high chemical and thermal shock resistance. The outer side of the inner glass was coated with a sputtered solar selective surface (thin film). This coated inner glass was closed at one end and sealed at the other end to the outer glass. The annular space between the outer glass and inner glass was evacuated to avoid heat loss in conduction and convection (Arora et al., 2011). The effect of vacuum on ETC was studied by Bamasag et al. (2019), Nokhosteen & Sobhansarbandi (2020), Xia & Chen (2020), Yurddaş (2020), and Messaouda, Hazami, et al. (2020).

Table 2.2: The specification of conventional evacuated tube

Structure	**All-Glass Double-tube co-axial structure**
Glass Material	High borosilicate 3.3 glass
External pipe diameter and thickness	58mm, +/-0.6mm; T=1.6mm
Internal pipe diameter and thickness	48mm, +/-0.6mm; T=1.6mm

Pipe Length		500mm
Absorptive coating property	Structure	ALN – SS/Cu
	Sediment method	3 Target magnetron sputtering plating
Vacuum Tightness		P<=5.0×10^{-3}Pa

2.9.3 Inner Glass Tube Thin Film- Selective Surface Coating

ETC outer surface at the inner glass tube was coated with a secondary dielectric material that reduced overall reflectivity with a considerably high absorptive ability (Kumar Singh & Samsher, 2020). The thin film-selective surface-coated material was able to absorb direct and diffuse radiations around the vacuum jacket of ETC and drastically improve the overall performance (Chow et al., 1984). **Figure 2.4** shows the as-built ETC design with three tiers layer available in the market.

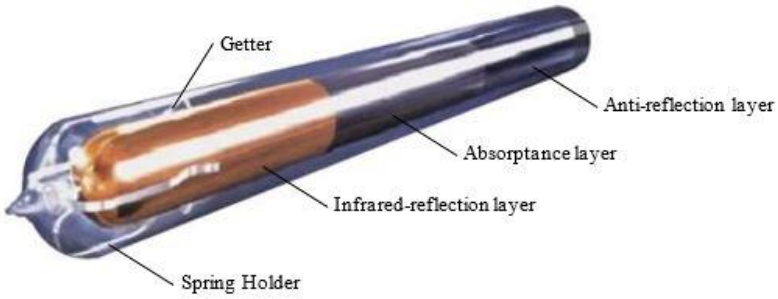

Figure 2.4: The as-built ETC design available in the market (Source: https://www.hydro1.com.my/solarwave-solar-water-heater-2/)

In the photovoltaic (PV) study, some researchers called the selective surface coating a thin film. Jarimi, Lv, et al. (2020) focused on a novel design of vacuum-insulated semi-transparent thin-film for photovoltaic (PV) glazing, while Han et al. (2019) discussed thermal regulation of PV façade integrated with thin-film solar cells through a naturally ventilated open air channel. Other researchers who have studied on thin film were Jarimi, Qu, et al. (2020), Tao & Zhang (2020), Park & Kim (2021), Ramanujam et al. (2020), Dey (2020), and Sarkın et al. (2020). Regarding the term, either a selective surface coating or a thin film was used, and the studies aimed to improve the thermal performance of glazing material.

The last tier at the thin film's end is called the infrared reflective layer. It blocks the heat reflection from penetrating the vacuum pocket of ETC, simultaneously accumulating the heat gained inside. Shanmugam et al. (2020) briefly reviewed antireflective coating from a PV perspective, including its underlying principle theory. Numerous types of research have been studied and developed in several classes of antireflective coating materials such as Si-based; (Y. Xu et al., 2020) (Silicon), (Chi et al., 2020) (Silica), (van de Loo et al. 2020) (SiNx), metal-based; (Y. Y. Zhang et al., 2021) (Au), (Chen et al., 2020) (Ag), metal oxide; (Du et al., 2011) (Nauryzbekova et al., 2021) (TiO_2), (Zhong et al., 2019) (ZnO,) (W. Yang et al., 2020) (ITO), metal fluorides and sulphides; (Ning et al., 2020) (MgF_2), (Jung et al., 2020) (ZnS), polymer-based; (Balbay & Acıkgoz, 2020) (Polystyrene), (PMMA), (Chaudhary et al., 2020) (PET), (Gao et al., 2020) (PDMS), and advanced materials including carbon nanotubes (Mitin et al., 2020) and graphite (Song et al., 2021). Antireflective coatings and surface texture also improved the efficiency of a solar collector and the thermal performance of solar heating systems (Furbo & Jivan Shah, 2003).

Generally, K. Xu et al. (2020) reviewed high-temperature selective absorbing coatings for solar thermal applications. Specifically, in the ETC study, Ma et al. (2020) studied the development of a novel CPC (compound parabolic collector) evacuated tube solar collector using a medium-temperature selective coating. The medium-temperature selective coating was obtained by co-sputtering titanium and aluminum targets. The experimental rig was developed on the steam system application. The results showed the novel CPC solar collector produced steam from water with temperatures at about 108°C –145°C during sunny days. It was also shown that the thermal performance of the solar collector did not degrade significantly. Other researchers who studied on specifically ETC selective coating were Zhao et al. (2020), Bello & Shanmugan (2020), Wannagosit et al. (2018), Sobhansarbandi et al. (2017), Martinez et al. (2017) and Selvakumar & Barshilia (2012).

In conclusion, the thin film-selective surface coating was studied by those researchers purposely to recognize the best coatings and textures that absorb direct and

diffuse solar radiation in order to improve the performance and efficiency of the inner glass vacuum tube.

2.10 FPC AND HP ETC

Solar water or air heating system operations were more efficient using solar thermal collectors compared to photo-voltaic (PV) systems (Matuska & Sourek, 2017). Numerous types of solar thermal collector, namely flat plate collector (FPC) and heat-pipe evacuated tube collector (HP ETC), have been developed in various countries and has become increasingly important for integrated solar heating system in the past years (Sabiha et al. 2015). However, conventional FPC has low thermal efficiency, and its exergy efficiency decreases during the off-sunshine hour (Ahmad Fudholi & Sopian, 2019). Several researchers (G. L. Morrison et al., 2004)(Zubriski & Dick, 2012) agreed that ETC has much better efficiency than FPC. Solar thermal collector efficiencies were found to be 46.1% and 60.7% for FPC and HP ETC, respectively whilst the system efficiencies were found to be 37.9% and 50.3% (Ayompe et al., 2011). This experiment between FPC and HP ETC was conducted simultaneously with similar environmental conditions. Regarding performance, HP ETC has better performance in producing high outlet temperatures than FPC, especially in cold climates (Mahdjuri, 1979).

A large range of temperatures can be obtained by different solar thermal collector configurations; for example, 20ºC - 80ºC was the operating temperature of FPC (N. Sharma & Diaz, 2011), and 50ºC - 200ºC was for HP ETC (Soteris A. Kalogirou, 2014)(Tyagi, Kaushik, et al., 2012). However, FPC produces low and moderate temperatures of hot air, and it was found to be appropriate for drying agricultural products (Ahmad Fudholi & Sopian, 2019). To be in line with technological advancements, the technical directions in the development of solar-assisted drying systems for agricultural products should be of compact collector design, high efficiency, integrated storage, and a long-life drying system (A. Fudholi et al., 2010).

Both FPC and HP ETC need to be positioned either south facing for Northern Hemisphere or north facing for Southern Hemisphere (Shafieian et al., 2019). The use of a sun tracker may increase the preliminary setup and maintenance costs for both residential users and solar plants (Ullah et al., 2019). Furthermore, both need to be tilted at the correct angle during installation to maximize the system's performance, which can limit its orientation (Shariah et al., 2002)(Karmakar et al., 2019). For areas located in the equatorial, the solar collector needs to be flat in order to obtain maximum energy from solar radiation throughout the year (Abdul Majid, 2011).

Regarding the panel orientation, the maximum output of the solar PV cell also requires a perpendicular light on its surface where radiation can be captured (Fazlizan et al., 2019). Among the entire categories of stationary collectors, HP ETC was widely used over FPC due to their better performance, especially in cold weather and on cloudy days with regards to hot water generation (Perers, 1988)(Pluta, 2011)(Greco et al., 2020). Arvind Kumar et al. (2020) investigated evacuated solar tube collectors with heat pipes and direct flow in detail. They concluded that evacuated tube collectors (ETC) perform better than flat plate collectors (FPC) under similar working conditions. The performance of HP ETC was higher as compared to direct flow ETC (Chopra et al., 2018).

2.11 HP ETC APPLICATION

Soteris A. Kalogirou (2004) was among the favorite researchers who studied the efficiency of HP ETC for both the water heater and air heating, which use water as heat storage material. Due to the commercial water heater application, these tubes were mounted by directing the heat pipe header in an upward position into a heat exchanger (manifold). The water flowed through the manifold and picked up the heat from the tubes. The heated water circulated through another heat exchanger and gave off its heat to the water that was stored in a solar storage tank. Since no evaporation or condensation above the phase-change temperature occurred, the heat pipe offers inherent protection from freezing and overheating. This self-limiting temperature

control was a unique feature of the HP ETC. Several researchers studied HP ETC, specifically in water heating applications. They were Ghoneim et al. (2016), Chopra, Tyagi, et al. (2020), and Olfian et al. (2020). The existing design of solar drying for space or air heating systems utilized the working liquid as the medium of heat storage, which requires a large space and needs a special compartment to store the latent heat (Lane GA., 1983)(A. Sharma et al., 2009). This design led to additional space and load increment (Furbo, 2015). Other researchers had studied HP ETC in air heating applications were Venkatesan & Arjunan (2015), Amit Kumar & Yadav (2017), and Malakar et al. (2021).

In Malaysia, Ahmad Fudholi et al. (2015) developed a greenhouse solar drying system with a heat exchanger. This forced convection design consists of the HP ETC, electric heater, blower, water pumps, storage tank, and drying chamber that require extra space on the design, resulting in load increment. In fact, by focusing on the topic, Abdulmalek et al. (2018) discussed the effect of HP ETC in solar drying applications. As a country depends on plantation and agricultural sectors as one of the sources of economic growth (Yusof & Kalirajan, 2020) and is located in the equatorial climate (Kwong, 2020), the rate of sunlight acceptance clearly showed great potential in raising the useful daylight levels in all day time hours (Bahdad et al., 2020); The combination between these two factors were considered to be appropriate for Malaysia. Therefore, the solar thermal air heater enhancements were timely to reduce the over-reliance on petroleum sources.

2.12 THERMAL ABSORBER TECHNOLOGY

There are several factors that must be taken into account when designing thermal absorbers, especially on thermal performance, durability, cost, maintenance, and easy installation as well as their lifetime (Tchinda, 2009). These were the factors that could contribute to the decision-making process of whether the thermal absorber was applicable for commercial application. The thermal absorber could be integrated with

heat storage material to increase efficiency. **Table 2.3** shows the mapping of various types of thermal absorbers considering thermal performances design.

Table 2.3: Various types of thermal absorbers with consideration of thermal performance in design

No.	Type	Characteristics		
		Temperature	Sensible Heat Storage	Energy Storage
1	Thermal Absorber	√		
2	Sensible Heat Thermal Absorber	√	√	
3	Thermal Absorber + Heat Storage Material (Integrated or non-integrated)	√		√
4	Sensible Heat Thermal Absorber + Heat Storage Material (Integrated or non-integrated)	√	√	√

In ETC application, the integrated design between the thermal absorber and evacuated glass eliminates conduction and convection losses between the absorbing surface and outside ambient temperature (Elsheniti et al., 2019). The thermal absorber's wall thickness and an extended surface using fins (Abhishek Saxena et al., 2015) acted as thermal energy storage material during diffuse radiation conditions.

The thermal absorber surface area received solar energy by radiation, absorbed the energy, and simultaneously increased the internal energy of the molecules. The phenomena led to the excitation of the molecules, increasing the potential and kinetic energy inside. Thus, the temperature of the thermal absorber was also increased. In accordance with the First Law of Thermodynamics, elevated energy content inside the thermal absorber, by means of conduction, convection, and radiation, was transferred from the surrounding region to the lower temperature region without any energy being destroyed along the process (Cengel & Boles, 2015). The thermal absorber was the main component in determining the performance of the solar thermal collector since its function is to convert the energy from solar radiation to thermal energy. The heat

transfer fluid was used to extract the energy from the thermal absorber by natural or forced convection to increase the fluid temperature level.

2.12.1 Extended Surface Area's Air Contact (Perforated Fin)

The usage of fins as the extended surface has been an interesting topic by many researchers as the fins have a significant effect on heat transfer enhancement (R. Kumar & Chand, 2017)(Priyam & Chand, 2018)(Daliran & Ajabshirchi, 2018)(Kannan et al., 2021). Optimizing the heat transfer rates increased efficiency and saved power supplied in many manufacturing industries, such as computer chips and automobile engines. Due to the demand for compact, lightweight, and economical fins, optimizing the fin size is important. There are various types of fins, but commonly used is the rectangular plate type due to easiness of manufacturing.

The performance levels of solar thermal collectors could be enhanced through several techniques, such as the usage of extended surfaces, i.e., fins, corrugated absorbers, packed bed materials, and artificial roughness (Abhishek Saxena et al., 2015). Heat transfer via convection could be enhanced by using perforated fins instead of the solid fin with the optimum angle of inclination. Several studies have been conducted on shape modifications through the fin body, such as cavities, holes, grooves, slots, or channels, to increase the heat transfer rate.

Bassam and Abu (Abu-Hijleh, 2003a)(Abu-Hijleh, 2003b) conducted the numerical analysis and found that the heat transfer through permeable fins showed significant results over solid fins. They stated that increasing the number of permeable fins resulted in increasing the Nusselt number in solid fins. They used certain assumptions that the fins were made up of highly conducting material to make the analysis simple. However, they did not validate their results with experimental work. Ahn et al. (2007), in their experimental work, compared the heat transfer rates with rounded and elongated holes in the rectangular plate. They showed that elongated holes enhance heat transfer rate more than rounded holes but at the cost of pressure drop.

In another study, Ridouane & Campo (2008) in their research discussed the enhancement in heat transfer using grooved channels. They found that the grooves enhance the local heat transfer relative to flat passage. Mahdi et al. (2019) investigated the simultaneous charging and discharging processes in a triplex-tube heat exchanger. The comparison between the fin system and the one that contained nanoparticles showed that inserting fins with the recommended structure was more promising for attaining higher thermal performance. Several studies have already demonstrated that the use of perforated fins could enhance the heat transfer coefficient (Abu-Hijleh, 2003b)(Suryawanshi & Sane, 2009)(AlEssa & Al-Widyan, 2008).

Ben-Nakhi et al. (2008) investigated the natural convection in an open cavity. They found that the number of thin fins attached to the hot surface increases with the heat transfer rate. Zhnegguo et al. (2004) used petal-shaped finned tubes to improve heat transfer. Awasarmol et al. (Pise & Awasarmol, 2010) (Awasarmol & Pise, 2015) studied the effect of permeability fins on natural and forced convection heat transfer. Based on the temperature profile, they experimentally and numerically concluded that the permeable fins perform better than the solid fins. Several researchers reported a similar trend for perforated surfaces with circular perforations (Pise & Awasarmol, 2010)(Awasarmol & Pise, 2015)(Yakar & Karabacak, 2010).

Awasarmol & Pise (2015) experimentally studied the natural convection heat transfer enhancement from perforated rectangular fin arrays using air. They concluded that perforated fins could increase the heat transfer coefficient up to 32% while decreasing the fin mass by 30%. Kundu et al. (2012) recommended implementing the porous fin of any geometry as it transfers a high heat rate in comparison to the solid fin. The problem of natural convection heat transfer from fin arrays has been studied both experimentally and theoretically by several researchers.

2.12.2 Thermal Absorber Selective Coating Surface

The thermal absorber was selectively coated to absorb solar radiation. Selective coatings have the highest value of absorptivity (>0.95) and negligible emissivity (<0.1) (Barriga et al., 2014). The thermal absorber plates absorbed the heat from solar radiation as much as possible through the glazing and simultaneously transferred the energy to the working liquid.

The absorptance of the absorber surface for shortwave solar radiation depended on the incident angle as well as the nature and colour of the coating. Usually black in colour were used (McDonald, 1980)(S. Kalogirou et al., 2005)(Khamlich et al., 2012)(Babu et al., 2017)(Isac et al., 2018) (Fiuk & Dutkowski, 2019). However, various colour coatings have been proposed mainly for aesthetic reasons (Tripanagnostopoulos et al., 2000)(Wazwaz et al., 2002)(Orel et al., 2005)(C. Li et al., 2020).

2.12.3 Material and Wall Thickness

Common materials used in thermal energy storage are copper, aluminium, and stainless steel. Amongst these, cooper was better in rapid temperature increase due to high conductivity (Rehman & Ali, 2020), but the price was quite expensive and limited due to the material profile as well as being non-commercially used for the food industry in Malaysia. Aluminium offers a low price but is lower in density (Mills, 2017) and is thus limited due to commercial specifications and the fittings for design assembly. Furthermore, low density (Mills, 2017) also affected low energy storage compared to stainless steel. The Current Malaysia market price of Copper as of March 2021 for 4'× 8' metal sheets with 1 mm thickness was RM514.04 (Source: Pumpline (KL) Sdn. Bhd.), Aluminium RM126.60 and Stainless-Steel RM360.00 (Source: Sam’s Metal Trading (Kuantan) Sdn. Bhd.) based on the global reference non-ferrous metal (HKEX, 2021) and Stainless-steel (Outokumpu, 2021) at market price.

Stainless steel represents a good possibility in solar energy applications (Boydağ, 1986). Stainless steel has better specific heat capacity (Mills, 2017) compared to copper, which effected in high energy storage. This non-corrosive material was suitable and widely used for usage in the food industry and established as food-grade material. Even though stainless steel had low thermal conductivity (Mills, 2017) compared with aluminium and copper, this factor is seen as irrelevant due to the closed system and shortened design of EGATC. These selections of materials and wall thickness indirectly affected the heat conductivity, increased density, and mass, thus contributing to the enhancement of thermal energy storage (X. Yang et al., 2020). Several researchers have studied on materials and wall thickness of thermal absorbers. Andemeskel et al. (2017) studied the effects of an aluminum fin thickness coated with solar paint on the thermal performance of ETC. Dutta & Kundu (2020) studied thermal analysis of variable thickness absorber plate fin in flat-plate solar collectors using the differential transform method.

Sakhaei & Valipour (2019) discussed the effect of design parameters such as the thickness and coating of the glass cover, the thickness and material of the absorber plate, the air gap between the absorber plate and the glass cover, and the distance between risers and the insulation materials on the thermal performance of FPCs. Moss et al. (2018) studied on design and fabrication of a hydroformed absorber for an evacuated flat plate solar collector. They ran the heat exchangers experimentally and proved they were highly effective absorbers forming 0.7 mm stainless steel sheets. Abhishek Kumar & Shreeram Barkhane (2019) studied the selection of material for improving the heat transfer rate for fins using CFD.

2.12.4 Thermal Energy Storage

The solar thermal collector performance is normally very sensitive to weather variation because the variation will affect the solar radiation received by the solar thermal collector (Yahya M. 2016). During cloudy weather, the performance of the existing solar thermal dryer is decreased because of the insufficient heat flux received by the

solar thermal collector. The solar radiation was sheltered by the cloud's shadow resulting in the low heat flux rate received by the solar thermal collector. This will cause the minimum heat gain at the same time, reducing the system's efficiency.

According to Majid Z. A. (2011), energy storage was useful in maintaining a constant heat supply to the drying chamber. The solar drying system, combined with heat storage, impacts the stability of the air temperature in the drying chamber during the absence of solar radiation. Several researches were conducted on energy storage to overcome the problem. Latent heat storage systems have gained significant attention from researchers and academicians due to their higher storage density and smaller temperature difference between storing and releasing heat as compared to sensible heat storage.

A. F. Sharol et al. (2019) discussed the performance of a cross-matrix thermal absorber (CMA) utilizing paraffin as the thermal energy storage material. The experiments were carried out by exposing the CMA to different artificial solar radiation for 30 minutes, followed by 30 minutes of the discharging process. This technology indicates that the heat can be stored during the charging or discharging process by melting and freezing the thermal energy storage material for future use. Luisa F. Cabeza et al. (2012), reviewed and discussed the main characteristics of sensible heat storage solid and liquid material work by former researchers since 2010. He concluded that PCM was the better alternative due to its higher energy density compared with other solid and liquid sensible heat materials. Chopra, Pathak, et al. (2020) conducted an experiment on the thermal performance of a phase change material (PCM) integrated heat pipe evacuated tube collector (HP ETC) system and discovered that by utilizing a phase change material integrated manifold with the collector, more than 70% thermal efficiency value could be obtained. With regards to sensible heat thermal energy storage (SHTES), the usage of fins as extended surfaces is seen as an interesting topic by many researchers as the fins have a significant effect on heat transfer enhancement, as per discussed in **Para 2.12.1**.

2.13 DOUBLE PASS FLOW ARRANGEMENT

According to Chamoli et al. (2012), among the several ways to enhance the heat transfer rate at the thermal absorber were by eliminating the interruption of the unchanged fluid velocity, eliminating the existing laminar sub-layer at the turbulent boundary layer, and implementing a secondary heat transfer surface. The concept of implementation of a secondary heat transfer surface means doubling up the surface area contact (to maximize heat extraction from the absorber) in a similar drying chamber (to minimize heat losses), which creates double pass flow without an increase in the system cost (Mohamad, 1997). This design arrangement results in higher thermal efficiency for double-pass solar air heaters (Satyender Singh et al., 2019). Salih et al. (2019) agreed double pass flow solar air heater (DPSAH) produced higher efficiency when the system was operated under natural convection compared to the forced convection case.

There were various studies on double pass flow concerning solar air heaters by Omojaro & Aldabbagh (2010), El-Sebaii et al. (2011), Ho et al. (2012), Krishnananth & Kalidasa Murugavel (2013), Nowzari et al. (2014), Nowzari et al. (2015), Satyender Singh & Dhiman (2016), Alam & Kim (2017), Heydari & Mesgarpour (2018), Sajawal et al. (2019), Satyender Singh (2020) and Sharol et al. (2020). These studies discussed the same findings that double passes achieve better performance than single-pass solar air heaters. This is due to a higher heat transfer coefficient by the increased surface area contact between air and thermal absorber, which increases the heat transport from the thermal absorber to heat transfer fluid and reduces the losses from the collector surface as well (Satcunanathan & Deonarine, 1973). However, further enhancement can be expanded by the flow redirection method, where air in-flow at the thermal absorber was diversified through the diversion of the airflow path.

2.14 MASS FLOW RATE OF WORKING LIQUID

In the system with natural circulation, the highest flow rates resulted in the direct flow through the horizontal manifold without passing through the evacuated tubes. Therefore, collectors having tubes of the shortest length and lesser flow rate provided maximum average temperature and thus maximizing efficiency (Shah & Furbo, 2007). Dabra & Yadav (2018) also found that increasing the air mass flow rate from 0.0053 to 0.0118 kg/s leads to a decrease in forced heat transfer coefficient and exit air temperature.

2.15 MATHEMATICAL MODELING AND CONFIGURATION OF EGATC

The solar thermal collector used in this study is known as an Evacuated Glass–Thermal Absorber Tube Collector (EGATC). The thermal absorber was separated into two (2), particularly the inner absorber and outer absorber. The inner absorber comprises of small diameter pipe attached with zero (0) perforated fins, while the outer absorber is built from a slightly larger pipe diameter closed by one side end cap. Both absorbers were unified together inside the evacuated glass. Although the parameter experiment showed no significance on the number of fins towards the design of shortened evacuated tube collector (ETC), for commercial purposes, the inner absorber was fitted with several fin-like Polyvinyl Chloride (PVC) saddles to uphold the inner absorber to its place. Instead, Razak et al. (2016) reported in their study that higher heat loss occurred at the longitudinal fins attached to the upper and lower channels in the double-pass solar air collector.

EGATC functions changed accordingly due to weather and environmental changes. The concept of its development considers all the heat transfer mechanisms on thermal absorbers, namely conduction, convection, and radiation. While its initial design considers the surface area of the thermal absorber, the maximum nature of radiation reflection and air convection is to obtain maximum efficiency. The mathematical model was developed based on the energy conservation principle from

the 1st Law of Thermodynamics for each EGATC main component, as shown in **Figure 2.5**. The set of equations was derived based on the energy balance principle conducted by each of the main components of the EGATC. These main components are evacuated glass, outer absorber, inner absorber, and working fluid. All of the main components correspond to the nodes of the model.

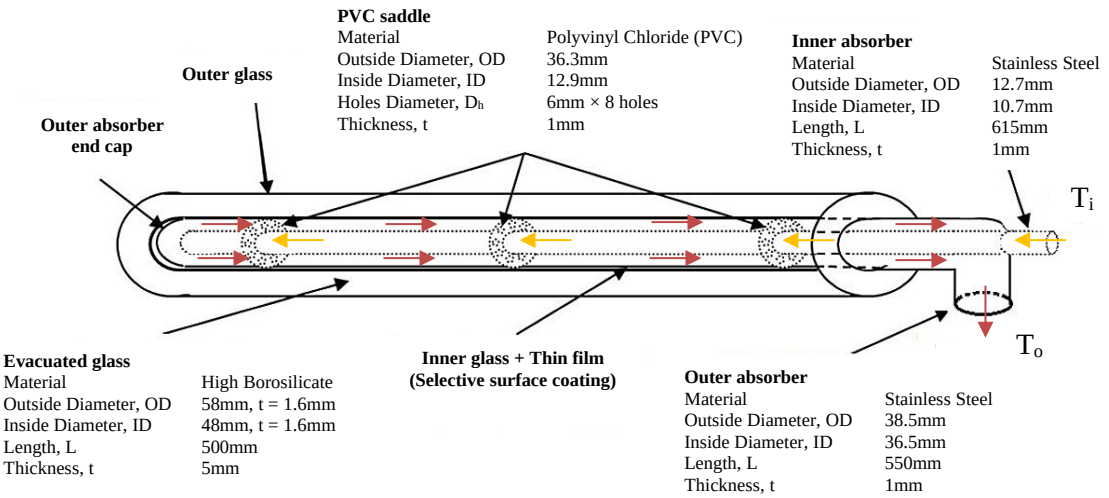

Figure 2.5: The Evacuated Glass – Thermal Absorber Tube Collector (EGATC) main components

2.15.1 EGATC in Air Heating Application

Generally, two common types of solar thermal collectors were applied in the low-medium temperature heating range. They are the Flat plate collector (FPC) and the Evacuated tube collector (ETC). The FPC was uncomplicated in manufacturing and design, and its purchasing costs were lower. However, considering the delivery cost, the FPC was more expensive due to the sizing of the packaging. For the operational cost, ETC systems can attain a payback period of less than the FPC systems (Nájera-Trejo et al., 2016). ETC has lower thermal losses than the FPC. This refers to the vacuum pocket between the outer and inner transparent glass tube with the thermal absorber that reduces conduction and convection heat losses.

Energy from the sun to the earth is in the form of radiation. Nevertheless, not all solar radiation reaches the earth's surface directly due to the mass of air in the atmospheric layer. The outer layer of EGATC, i.e., evacuated glass, received solar radiation and converted it into heat. The design of EGATC makes use of the greenhouse effect concept. **Figure 2.6** shows the schematic diagram of the airflow through EGATC.

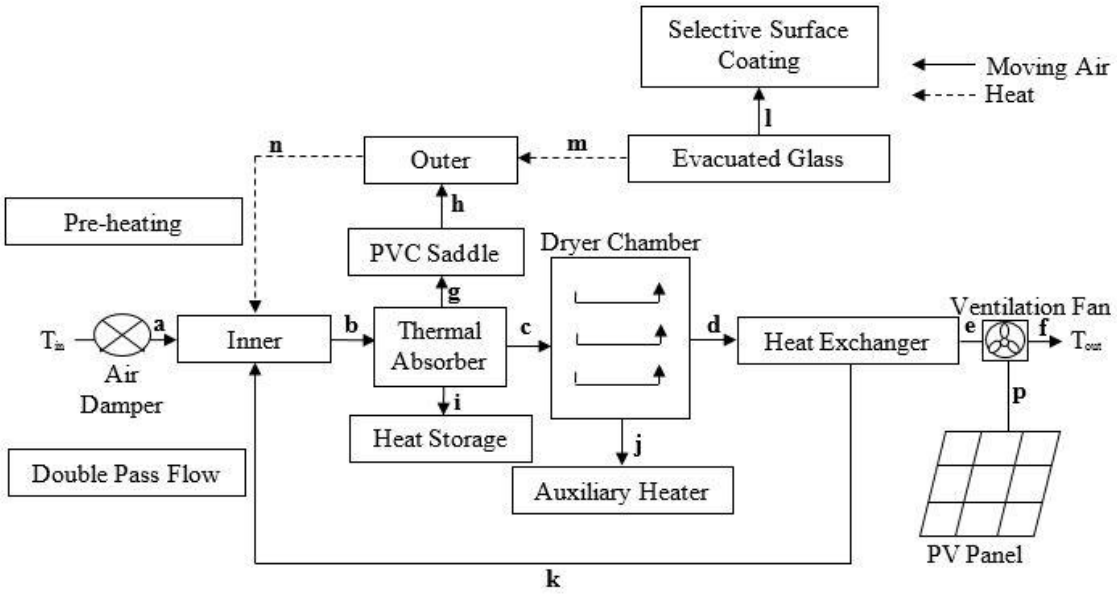

Figure 2.6: The schematic diagram of the airflow through EGATC

Solar radiation consists of long and short waves. EGATC consists of a thermal absorber inside an evacuated tube. The long wavelengths of the solar radiation reflected back to the environment, while the short wavelengths penetrated the evacuated glass directly to the thermal absorber. It turns into a long wave and is trapped inside the EGATC, raising the air temperature inside the respective solar thermal collector, which will be used in the drying process. In order to facilitate the understanding and the implementation of an air heater, **Table 2.4** shows the details process of the airflow inside EGATC in an air heating application.

Table 2.4: The details process of the air flow inside EGATC in an air heating application

Process	Description
P	1. The PV panel absorbs the solar radiation (radiation) 2. The PV panel converts the solar radiation into electricity which is used as a power source for the Ventilation Fan
T_{in}	1. Air damper opens 2. Air damper trapped in surrounding air into the inner absorber
a	1. Inner absorber receives air from the air damper 2. Inner absorber absorbs heat from the dryer chamber through the heat exchanger (convection / conduction) 3. Inner absorber absorbs heat from the outer absorber (convection / conduction)
B	1. Absorber (consists of the inner absorber, PVC fin/ saddle and outer absorber arrangement) receives air from the inner absorber 2. Absorber collects heat then moves it to inner absorber through the absorption of heat between outer absorber and inner absorber (convection) 3. Absorber collects heat and stores it as heat storage (convection / conduction)
C	Dryer chamber receives air from the absorber
d	Heat Exchanger transfers heat from hot air through dryer chamber (convection / conduction)
E	Ventilation fan extracts the air from the environment of T_{in} and then discharges through T_{out}
f/T_{out}	T_{out} discharge the hot air from the dryer chamber
G	PVC saddle, which is located between the inner absorber and outer absorber does not affect the amount of heat flux received by the inner absorber
H	Outer absorber blocked transfer heat to PVC saddle (conduction)
I	Heat storage absorbs heat from the absorber for repository (convection /conduction)
J	Auxiliary heater transfer heat to the dryer chamber (if necessary)
K	Hot air from the dryer chamber transfer heat to the inner absorber through Heat Exchanger (convection /conduction)
L	1. Thin Film assists in the absorption of shortwave solar radiation 2. Evacuated Tube transmit incoming shortwave solar radiation but blocked the longwave radiation emitted outwards by the outer absorber (radiation)
M	Outer absorber collects heat from evacuated tube (convection / conduction)
N	Inner absorber collects heat from the outer absorber (convection / conduction)

The novel thermal absorber EGATC's design created double pass flow at the inner absorber resulting in high cumulative temperature at the outlet temperature. The evacuated glass outer glass tube was purposely design in transparent to directly transmit solar radiation through the vacuum pocket to the inner glass tube. The inner glass tube was coated by a one-sided refraction/reflection characteristic (thin film- selective surface coating), which allowed the heat transfer via radiation and convection to the gap between the inner glass tube and solar thermal absorber (Kumar Singh & Samsher, 2020). The inner glass tube transmitted the short-wavelength solar radiation but blocked the reflection of the longer-wavelength irradiation to the vacuum pocket.

This greenhouse-affected phenomenon accumulates the heat energy inside the gap and simultaneously increases the temperature at the outer absorber. Then the heat is transferred through convection to the inner absorber. Indirectly, the wall thickness of the thermal absorber acted as the heat storage material. This heat transfer process developed the cumulative heat gain inside the solar thermal absorber design. Basically, an Evacuated tube collector (ETC) demonstrated that the combination of a selective surface coating and an effective convection suppressor resulted in better performance at high temperatures (ASHRAE, 2011). **Figure 2.7** shows the heat transfer that occurred inside the EGATC.

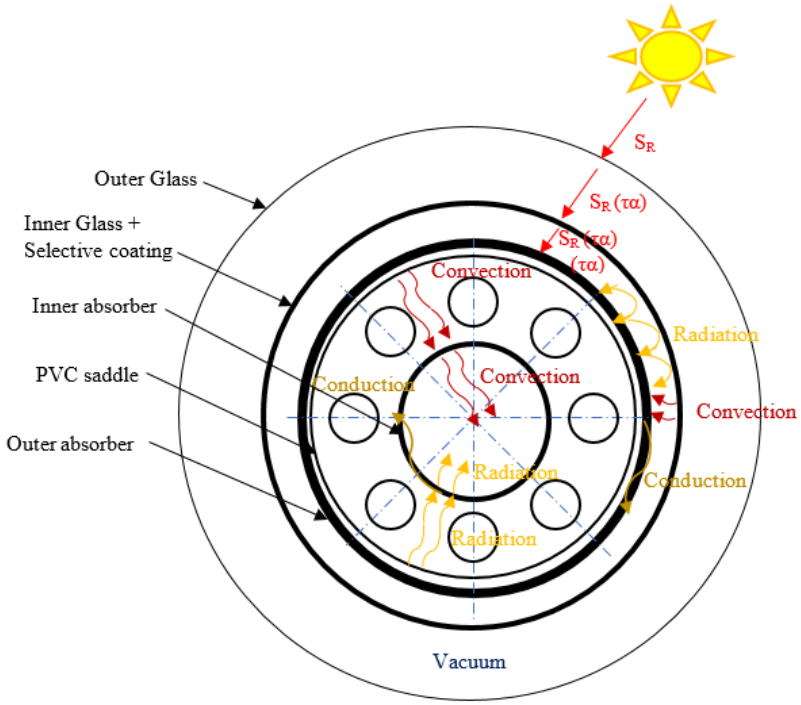

Figure 2.7: The heat transfer mechanism involved at the thermal absorber of EGATC

2.16 CHAPTER SUMMMARY

Throughout this chapter, a specific overview has been presented and discussed in terms of definition, importance, concept, and application in the solar field. There has also been a review of the recent technologies of solar thermal collectors with a brief description of their role, importance, and types. It also has covered the utilization of technologies in Evacuated Tube Collector (ETC) and Solar Thermal Absorbers. Finally, the parameters (i) Glazing materials, (ii) Vacuum, (iii) Glass tube selective surface coating, (iv) Extended surface area contact (perforated fin), (v) Thermal absorber selective coating surface, (vi) Material and wall thickness, (vii) Mass flow rate of working liquid, (viii) Double pass flow influencing the performance and efficiency and (ix) Mathematical modeling and configuration of EGATC in air heating application has been discussed. **Table 2.5** shows the comparison between FPC and HP ETC for research gap identification.

Table 2.5: Comparison between FPC and HP ETC

	Parameter	FPC	HP ETC
1	Diffuse radiation condition	FPC < HP ETC	
2	Working temperature (A.Fudholi & K.Sopian (2019))	30°C-80°C	50°C-200°C
3	Efficiency (Soteris A. Kalogirou (2004))	0.79 (Water heater)	0.82 (Water heater)
4	Application	Water heater, Air heater	Water heater, Air heater
5	Inner vacuum glazing (thin film– selective surface coating)	Yes	Yes
6	Absorber extended surface area / perforated fin	Yes	Yes
7	Absorber selective coating surface	Yes	Yes
8	Varies material selection	Yes	No
9	Varies absorber thickness / Length	Yes	Yes
10	Heat exchanger method (for air heater design)	Direct	Usage of heat exchanger
11	Double pass flow arrangement (for air heater design)	Yes	No
12	Design flexibility	Fix design / required large space	Fix design / required large space

CHAPTER THREE

RESEARCH METHODOLOGY

3.1 INTRODUCTION

This chapter explains each step taken in the design and evaluation, including mathematical modeling, analytical, and validation analysis of the Evacuated Glass-Thermal Absorber Tube Collector (EGATC). To facilitate the understanding and the implementation, the research methodology in the form of a flow chart is shown in **Figure 3.1**.

3.2 STUDY OF THE CURRENT DESIGN OF SOLAR THERMAL COLLECTORS AND DRYERS

Research in the existing solar thermal collectors, specifically heat-pipe evacuated tube collectors (HP ETC), has studied and defined the gap existing between them. The gap should be clear, and the expected solution by EGATC should be significant and strong enough since several researchers had agreed that HP ETC was better than flat plate collectors (FPC) in terms of performance and efficiency during diffused solar conditions. Besides, the existing research on the HP ETC air dryers has been reviewed and investigated with several design parameters that enhanced the performance. **Figure 3.2** shows the design parameters that affected the thermal performance. The study also involved the literature on the topic, methodology, design, and the theoretical and numerical approach.

3.3 DESIGN AND DEVELOPMENT OF PRELIMINARY SYSTEM

The Evacuated Glass-Thermal Absorber Tube Collector (EGATC) was designed in small sizing and portable. It was developed with the special design of a thermal absorber with a double glass evacuated tube collector (ETC). ETC was expected to be the best heat absorption feature to convert solar radiation into heat.

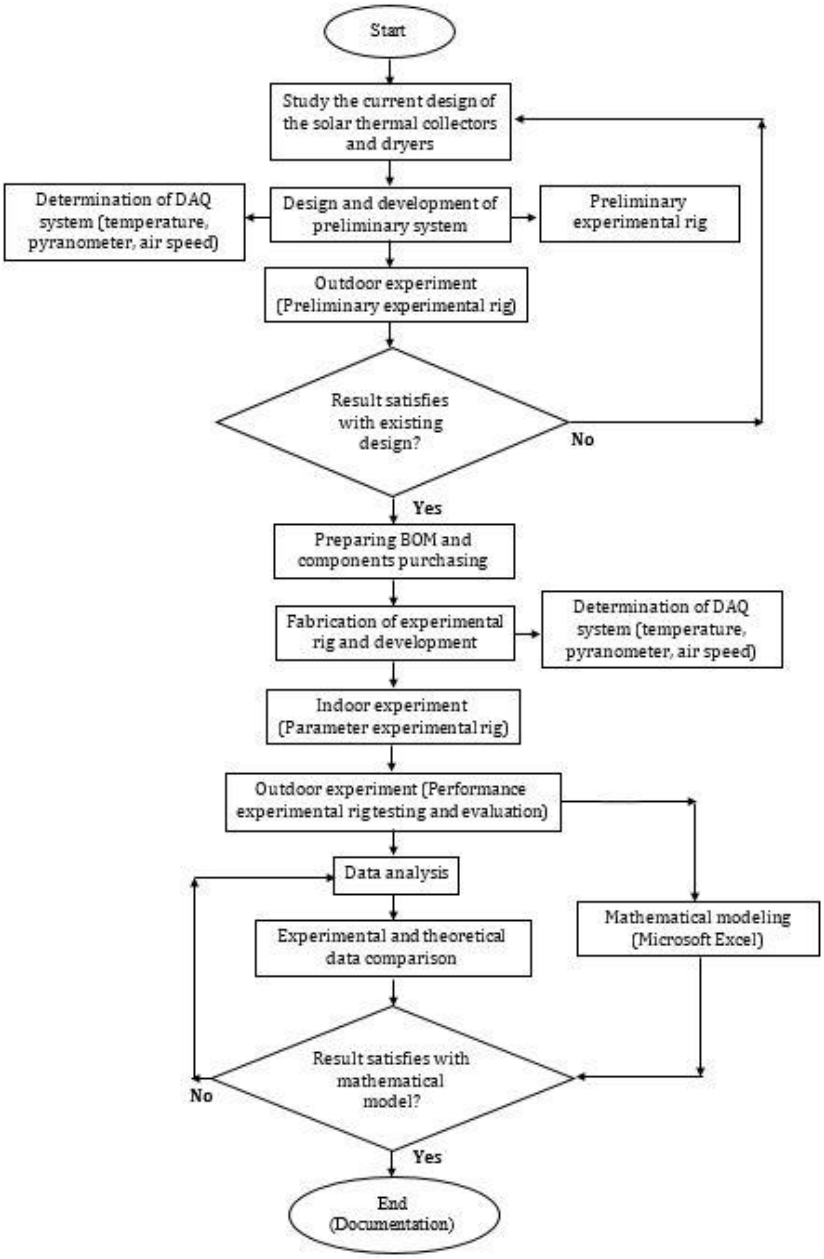

Figure 3.1: The flowchart of the research methodology

According to Soteris A. Kalogirou (2004), ETC works differently than the other thermal collectors available in the market. ETC had demonstrated that the combination of a selective surface and effective convection elimination would obtain a good results and performance at high temperatures. The vacuum pocket of evacuated glass eliminated the heat loss through convection and conduction between the thermal absorber and ambient so that the collectors can operate at higher temperatures (Duffie & Beckman, 2013).

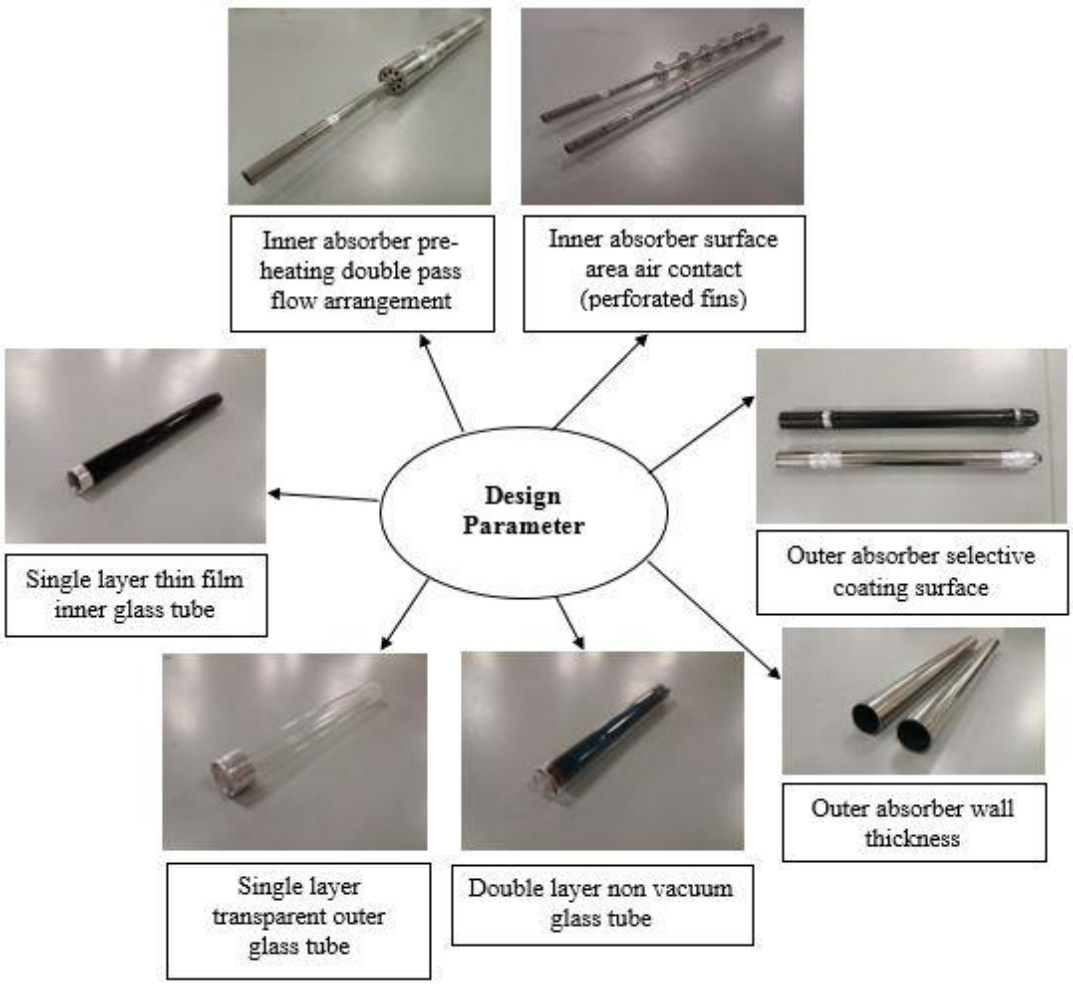

Figure 3.2: The design parameter that affected the thermal performance

From **Figure 3.3**, the outer glass received solar radiation and transferred the heat via radiation through the vacuum to the inner glass. The thin film-selective surface coating attached to the inner glass tube allowed heat transfer via convection to the stainless-steel outer absorber. Simultaneously, the thin film blocked the heat from reflection. Then the heat is transferred via convection to the stainless-steel inner absorber. These heat transfer processes developed cumulative heat gain inside the absorber design. In addition, the pre-heating air flow from the inlet ducting through the dryer chamber also contributed to the increase in the temperature inside the absorber. The ventilation fan channeled the cumulative high-temperature heat gain to the drying chamber.

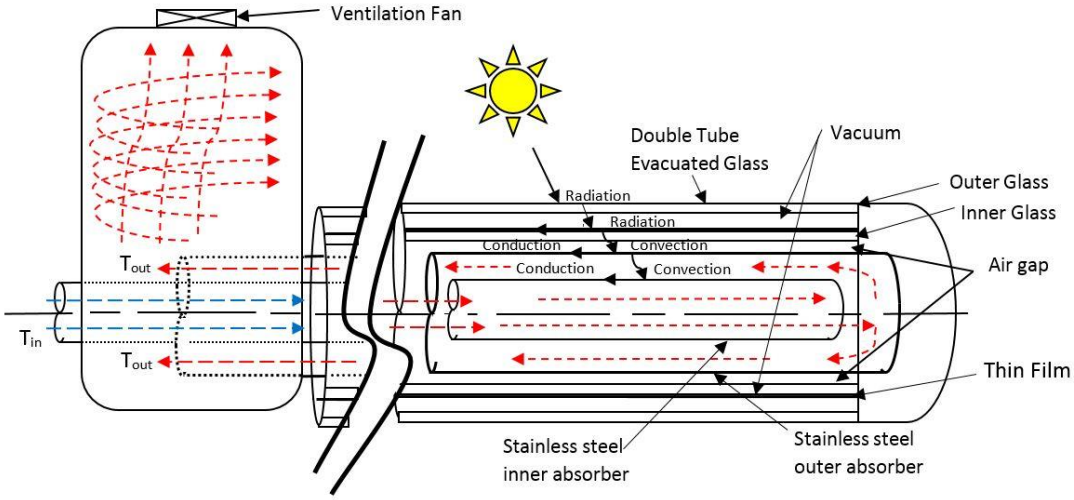

Figure 3.3: EGATC Air Heater preliminary system arrangement

The preliminary system combined the design and fabrication of a preliminary experimental rig with the development of DAQ (Data Acquisition) system installation and setup (see **Figure 3.4**). This design used the same design specification as the experimental performance rig except for fewer DAQ sensor points and a much bigger drying chamber.

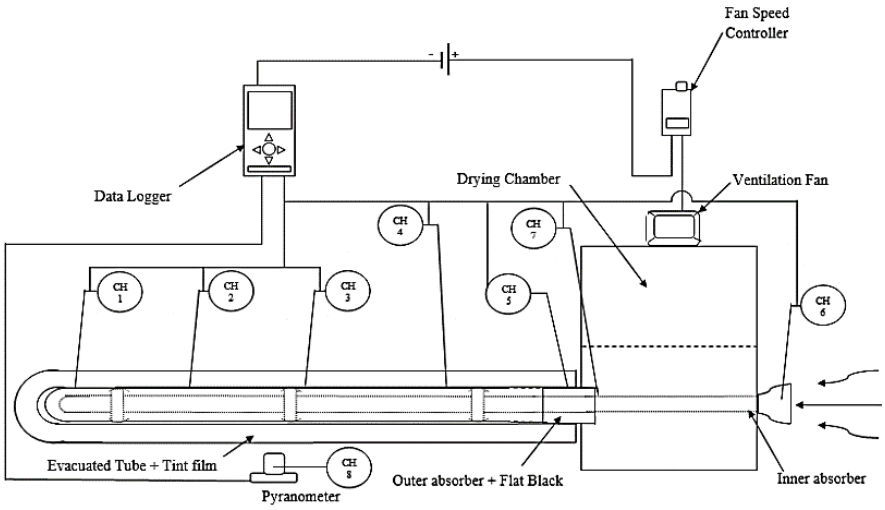

Label	Description	Label	Description
CH1	Absorber temperature 1	CH5	Absorber temperature 5
CH2	Absorber temperature 2	CH6	Air inlet temperature
CH3	Absorber temperature 3	CH7	Air outlet temperature
CH4	Absorber temperature 4	CH8	Solar radiation

Figure 3.4: The design and fabrication of the preliminary experimental rig combined with the development of DAQ (data Acquisition) system installation and setup

3.4 PRELIMINARY EXPERIMENTAL RIG (OUTDOOR)

The preliminary experiments were conducted to ensure the design was on the right path by monitoring the theoretical statements that were similar to the experimental results. The experiments were conducted under real ambient conditions. According to Q. Li et al. (2020), a typical HP ETC system requires a slope angle during installation for the heat pipe to operate efficiently. Consequently, the preliminary experiment was done at an 8° slope angle. The first preliminary experiment was conducted to verify that the outlet temperature gained from EGATC is capable of drying the agricultural product. The experiment was held on May 2019 from 8.30 am until 5.00 pm (refer to **Figure 3.5**).

Figure 3.5: Preliminary experimental rig on EGATC

Another preliminary experiment was conducted in July 2019 from 8.45 am until 5.30 pm (refer to **Figure 3.6**). The experiment was conducted to monitor the outlet temperature between the Evacuated Glass-Thermal Absorber Tube Collector (EGATC) and Heat Pipe Evacuated Tube Collector (HP ETC).

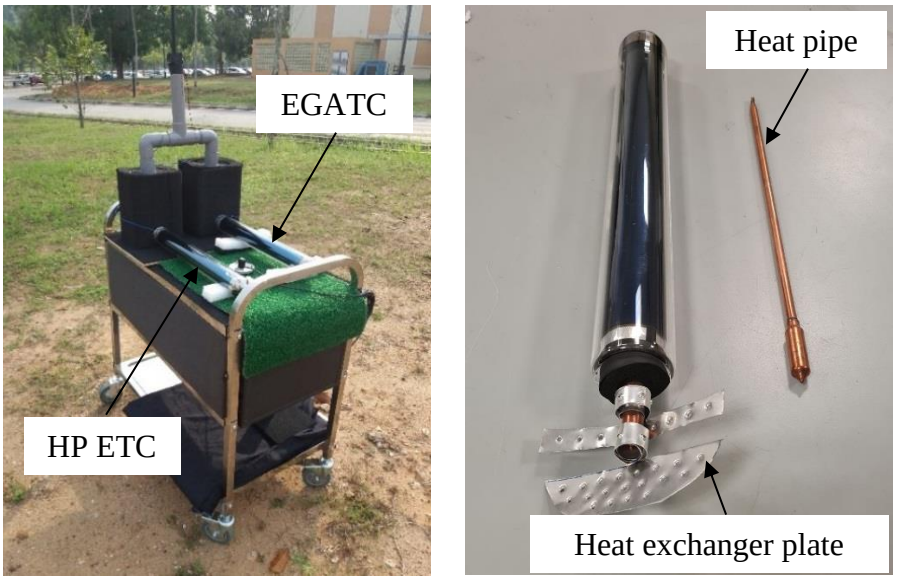

(a) (b)

Figure 3.6: (a) Preliminary experimental rig between EGATC and heat pipe ETC (b) Heat exchanger plate attached to the header of heat pipe

3.5 PREPARING BILLS OF MATERIAL AND COMPONENTS PURCHASING

After the positive results obtained from the preliminary experiments, the detailed bills of materials (BOM) were prepared according to the technical drawing and components specifications needed, as stated in **Table 3.1**. Then only, the purchasing process will be started. The materials selection involved in this project also were recorded in detail.

3.6 FABRICATION OF EXPERIMENTAL RIG AND DEVELOPMENT

Fabrication work is started only if the results obtained from the preliminary experiment are satisfied theoretically and after the completion of item purchasing. The fabrication process is divided into two, i.e., indoor for the experimental parameter rig and outdoor for the experimental performance rig.

3.7 PARAMETER EXPERIMENTAL RIG (INDOOR)

Determination of the design parameters effect, i.e., inner absorber surface area air contact (perforated fins), outer absorber selective coating surface, outer absorber wall thickness, double layer non-vacuum glass tube, single layer transparent outer glass tube and single layer thin film inner glass tube on thermal performance enhancement was conducted, and the parameter experiment was setup including sensor location as shown in **Figure 3.7**. Two (2) units of data Logger, an 8-Channel Temperature Meter, Data Logger A, and Data Logger B were used to record the data during the experiment. Out of 16 channels, 6 channels were unused, and ten (10) channels were allocated for temperature data.

Table 3.1: Bill of materials (BOM) in regard to the experimental rig fabrication

Nos.	Specification/ Dimension	Type/ Material	Component	Nos. of Unit	Price (RM)
1	O. D = 58mm, I. D = 48mm t = 5mm, L = 500mm	High Borosilicate, Vacuum tightness = 5.0×10^{-2}Pa	MISOLIE Technology, Double Layer Glass- Evacuated Tube	3	160.35
2	O. D = 38.5mm, t= 1.0mm, L = 550mm	Stainless Steel 304	Pipe (Outer absorber)	2	40.00
3	O. D = 38.5mm, t = 2.0mm, L = 550mm	Stainless Steel 304	Pipe (Outer absorber)	1	30.00
4	O. D = 12.7mm, t = 1.0mm, L = 615mm	Stainless Steel 304	Pipe (Inner absorber)	5	50.00
5	O. D = 36.3mm, I.D = 12.9mm, t = 1.0mm	Stainless Steel 304	Perforated fins, Dia. 6 mm x 8 holes	24	180.00
6	V = 9V, I = 1000mA	N/A	APPLENT Technologies, Multi-Channel Temp. Meter (8-CH) (AT4208)	2	2400.00
7	N/A	N/A	APOGEE INSTRUMENTS, Pyranometer	1	1500.00
8	V = 12V, P = 6.8watt	N/A	SUNON, D.C Brushless Ventilation Fan (PMD1204PQBX-A)	1	20.00
9	V = 5V, I = 2.1A	N/A	Fan Speed Controller	1	40.00
10	Thickness = 5mm, k value = 0.035W/ mK	High quality flexible elastomeric closed cell nitrile rubber insulation	Insulflex®, High quality Insulation – Class 1	1	30.00
11	L = 250mm, W = 150mm, H = 300mm	Mild Steel	Steel box	1	20.00
12	L = 850mm, W = 450mm, H = 900mm	Stainless Steel 304	Trolley	1	300.00
13	BS4514, O.D = 110mm	PVC	Piping (drying chamber), fittings	4	80.00
14	BS4346, O.D = 32mm	PVC	Piping, fittings	8	40.00
15	BS4346, O.D = 50mm	PVC	Piping, fittings	4	60.00
16	L = 200mm, W = 1200mm, H = 1500mm, (12-volt 35Ah)	Industrial Power Battery, POWERBATT PS35-12, Sealed lead acid type	Maintenance free, rechargeable battery	1	200.00
17	L = 400mm, Header dia. = 14mm, Pipe dia. = 8mm	Copper	MISOLIE Technology, Heat Pipe	1	150.00
18	L = 297mm, W = 210mm (100 watts, 12-volt)	Monocrystalline	Radtech, Solar Panel	1	50.00
				Total	**5350.35**

Ten (10) units of K-type thermocouple were used to record the temperature data, namely, T1A until T8A were used for Data Logger A while T1B and T2B were used for Data Logger B. T1A and T2A were allocated to sense the air inlet and outlet temperature respectively while T3A, T1B, T4A, T2B, and T5A were allocated to sense the outer absorber temperature at five (5) different locations. T6A and T7A were used to sense an evacuated tube's outer glass surface temperature. Meanwhile, T8A was used to record the ambient temperature. The experiment was run as an indoor experiment under artificial solar radiation for charging and discharging. The data logger recorded the temperature data every one (1) minute.

As the test rig calibration setup, the artificial solar radiation was calibrated before each experiment was run. The artificial solar radiation was designed to consist of nine (9) halogen lamps (150W, 220-240V, 50/60Hz) in series-parallel connection with a matrix 3x3 arrangement. The current reading measured by UNI-T Mini Clamp Meter (UT210E) was set up to 7.57Amp to produce the value of solar radiation 700 w/m². The readings were monitored every five (5) minutes at three (3) different points until the end of the experiment, and the data was recorded manually. For the first experimental setup, EGATC was inserted with zero (0) perforated fin at the inner absorber. For each zero (0) perforated fin, the experiment was carried out with air velocities 0.0 m/s, 0.7 m/s, 0.9 m/s, 1.1 m/s, 1.3 m/s, 1.5 m/s, and 1.7 m/s. Before running each experiment, the initial temperature had to be controlled to 28°C. The controlled parameters involved are listed in **Table 3.2**.

Table 3.2: The controlled parameters involved in each experimental parameter setup

Nos.	**Parameters**	**Value**
1	Artificial solar radiation, S_R	700 w/m^2
2	Initial temperature, T_i	28°C
3	Air velocity, V	0.0 m/s, 0.7 m/s, 0.9 m/s, 1.1 m/s, 1.3 m/s, 1.5 m/s and 1.7 m/s

A similar working procedure was followed for the other parameter experiments with the seven (7) perforated fins. The data of each wind speed experiment on zero (0) and seven (7) perforated fins were compared to determine the ideal design of the perforated fin and appropriate wind speed. The selected design was then set up for the next parameter experiments, namely outer absorber selective coating and outer absorber wall thickness. Other parameter experiments also were reported on evacuated tubes, i.e., double-layer non-vacuum glass tubes, single-layer transparent outer glass tubes, and single-layer thin film inner glass tubes. All the recorded data were analyzed, and the graph was plotted after the experiment was conducted.

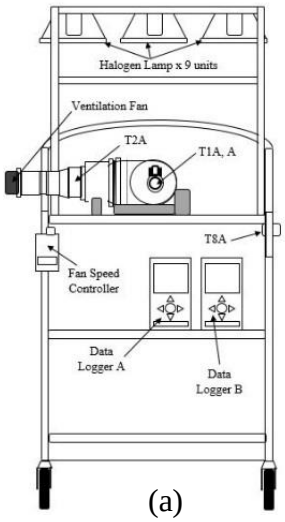

(a)

Label	Description
T1A	Ideal EGATC inlet temperature
T2A	Ideal EGATC outlet temperature
T3A	Ideal EGATC front thermal absorber temperature
T4A	Ideal EGATC middle thermal absorber temperature
T5A	Ideal EGATC rear thermal absorber temperature
T6A	Ideal EGATC middle outer glass surface temperature
T7A	Ideal EGATC rear outer glass surface temperature
T8A	Ambient temperature
T1B	Ideal EGATC front-middle thermal absorber temperature
T2B	Ideal EGATC middle-rear thermal absorber temperature
A	Area of inlet duct, (m^2) (Area of inlet duct, A = 5.47×10^{-4} m^2)

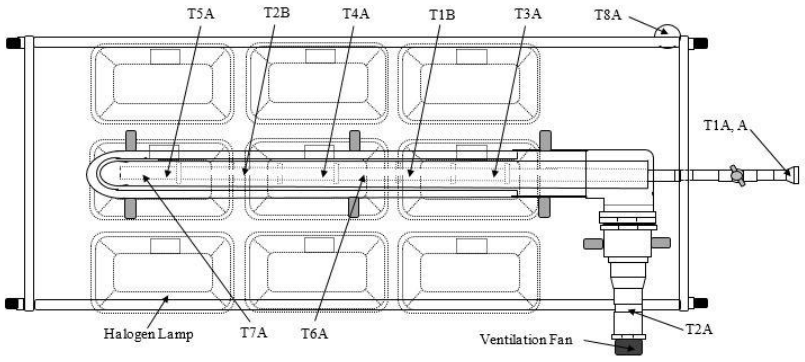

(b)

Figure 3.7: Experimental setup for determining the effect of design parameters on thermal performance enhancement. (a) Side view and (b) Top view of the test rig

3.7.1 Device and Apparatus

The parameter experiment investigated the effects of perforated fins, coated outer absorber, 2mm outer absorber wall thickness, insulation material inner absorber, double layer non-vacuum glass tube, single layer transparent glass tube, and single layer thin film glass tube on thermal performance enhancement of EGATC. The apparatus was exposed to artificial solar radiation with 700 W/m² for 30 minutes on charging and the other 30 minutes on discharging. The artificial solar radiation flux was measured using TES ELECTRICAL ELECTRONIC CORPORATION, Datalogging Solar Power Meter (TES-1333R). The readings were recorded every five (5) minutes at three (3) different locations along the experiment to monitor the consistency of flux produced by the simulator. The APPLENT TECHNOLOGIES, Multi-Channel Temperature Meter (8-CH) (AT4208) was utilized to measure the temperature. The wind speed was measured by UNI-T Mini Digital Anemometer (UT363).

The thermal absorber acted as heat storage material comprising of the inner absorber and outer absorber. For the experimental parameter setup, the inner absorber was made up of stainless steel pipe (with dimensions of 15mm outside diameter x 1.0mm thickness x 600mm length) attached with stainless steel perforated fins, i.e. (0) zero and seven (7) perforated fins (with dimensions of each fin 36.3mm outside diameter x 12.9mm inside diameter x 1.0mm thickness, 6mm diameter x 8 holes), while outer absorber was made up by stainless steel pipe (with dimensions of 38mm outside diameter x 1.0mm thickness x 550mm length). These thermal absorbers were assembled inside MISOLIE TECHNOLOGY, with high borosilicate glass evacuated tube (with dimensions of 58mm outside diameter x 48mm inside diameter x 500mm length) by one-sided refraction/reflection characteristic coating to eliminate heat loss through convection and radiation between the solar thermal absorber and ambient.

The indoor experiment was conducted for 12 days from November 2020 to December 2020 (refer to **Figure 3.8**). The experiment was done to monitor the outlet temperature of the EGATC air heater.

(a) (b)

Figure 3.8: The setup of indoor experiment under the artificial solar radiation during (a) Charging (b) Discharging

3.7.2 Parameter Experimental Setup on Energy Storage

For the first parameter experiment setup on inner absorber surface area air contact (perforated fins), the inner absorber was made up of stainless-steel pipe attached with stainless steel perforated fins, i.e. (0) zero and seven (7) perforated fins. The fin array under consideration was made of seven (7) stainless steel fins with 1mm thickness**. Figure 3.9(a)** shows the schematic of the fin showing its perforations configuration with dimensions (in mm). Drilling for eight (8) arrays holes of 6mm diameters in the solid rounded fins was done to form the perforated fins. These configurations were attached to the inner absorber, as shown in **Figure 3.9(b)**. It also compares the inner absorber without a perforated fin experimental setup.

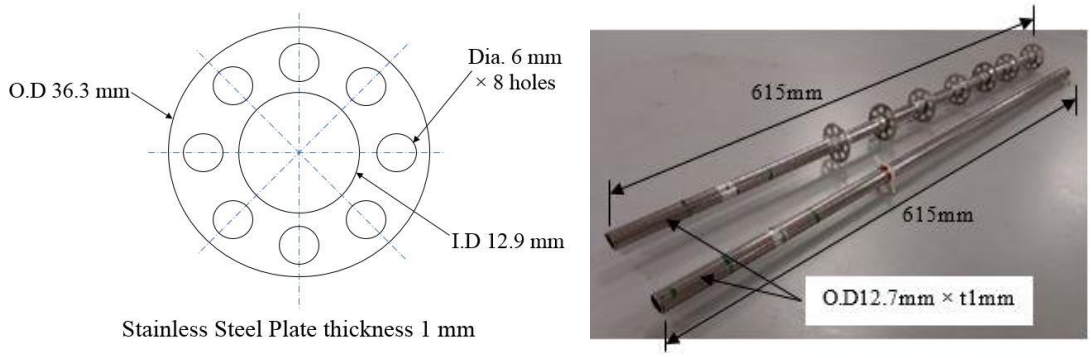

Figure 3.9: The perforated fins used in the parameter experimental setup. (a) Schematic diagram of the perforated fin (b) Two types of perforated fins experimental setup i.e., inner absorber without perforated fin and inner absorber with 7 perforated fins

For the second parameter experimental setup on the outer absorber selective coating surface, the outer absorber was made up of stainless-steel pipe coated with a selective coating surface (flat black colour). This outer absorber was compared with the same configuration of the outer absorber without a selective coating surface (standard stainless-steel finishes). **Figure 3.10** shows the coated outer absorber and non-coated outer absorber.

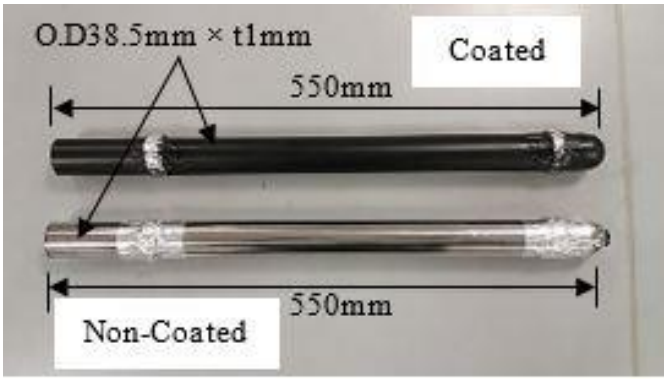

Figure 3.10: Non-coated and coated outer absorber used for the parameter experimental setup

The parameters and properties involved in the respective experiment are given in **Table 3.3**.

Table 3.3: Hollow pipe physical properties (Cengel, Yunus A. , Ghajar, 2016)

Parameters	Length, L	Absorptivity, α	Emissitivity, ε	Reflectivity, ρ	Transmitivity, τ
Non-coated Stainless steel	550 mm	0.41	0.05	0.59	-
Coated Stainless steel	550 mm	0.98	0.98	0.02	-

While for the third parameter experimental setup on outer absorber wall thickness, the outer absorber was made up of 1 mm wall-thickness stainless-steel pipe and was compared with a 2 mm wall-thickness stainless-steel pipe. The outer absorber used in the experiment is shown in **Figure 3.11**.

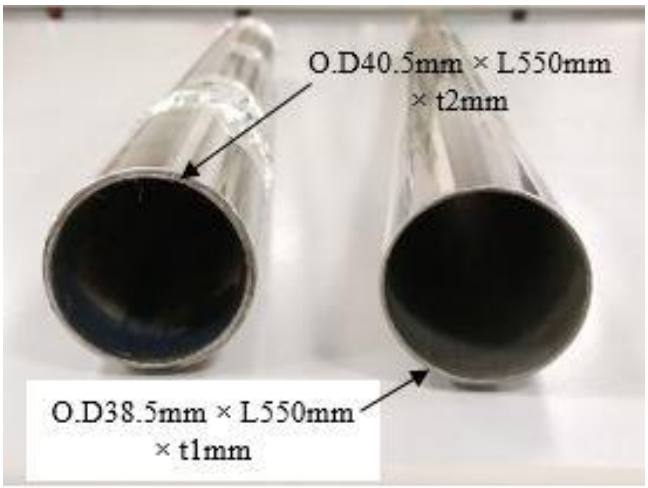

Figure 3.11: Outer absorber wall thickness 1mm and 2mm used for the parameter experimental setup

A typical double glass evacuated tube design consists of an inner and outer glass tube. The double glass evacuated tube used in other experimental setups was manufactured by MISOLIE TECHNOLOGY and made from high borosilicate 3.3 glass with thermal conductivity of 1.2 $Wm^{-1}K^{-1}$, specific heat capacity 0.83 $kJkg^{-1}K^{-1}$, coefficient of thermal expansion 3.3 x 10^{-6} K^{-1} and vacuum tightness 5.0×10^{-3}Pa. Both the outer and inner tubes were transparent tempered glass with a thickness of 1.6mm, and the outer surface of the inner tube was coated with a thin film-selective surface coating (anti-reflection- absorptance layer / infrared-reflection layer) property i.e. Aluminium nitride - Stainless steel/ Cuprum (Al N- SS/ Cu). For experimental parameter setup, this standard configuration of the evacuated tube was compared with another three (3) design parameters, i.e., double layer non-vacuum glass tube, single layer transparent outer glass tube, and single layer thin film inner glass tube as shown in **Figure 3.12**.

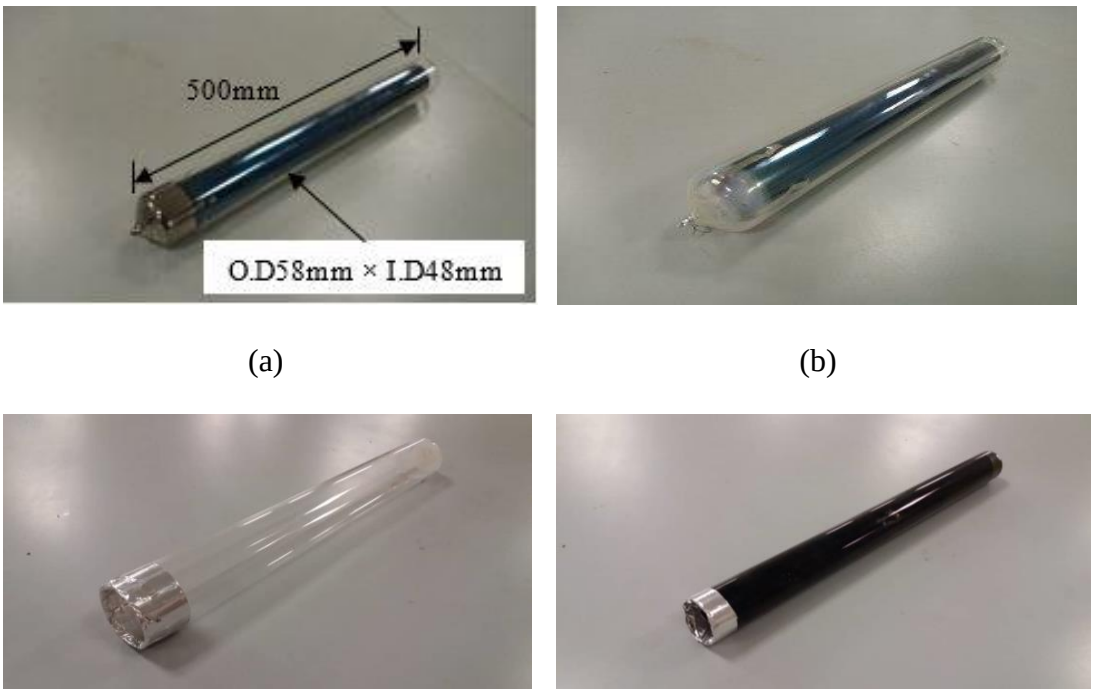

Figure 3.12: The parameters involved in the experimental setup (a) Standard configuration of evacuated tube available in the market (b) Double layer non vacuum glass tube (c) Single layer transparent outer glass tube (d) Single layer thin film inner glass

The parameters and properties involved in the respective experiment are given in **Table 3.4**.

Table 3.4: Evacuated glass physical properties (Arvind Kumar et al., 2020)

Parameters	Length, L	Absorptivity, α	Emissivity, ε	Reflectivity, ρ	Transmittivity, τ
High Borosilicate Glass	500 mm	0.05	0.02	0.03	0.92
Thin film-Selective Surface Coating	500 mm	0.67	0.05	0.03	0.3

The thermal absorber acts as heat storage material comprising the inner absorber and outer absorber. These thermal absorbers were assembled inside the evacuated tube, as shown in **Figure 3.13**.

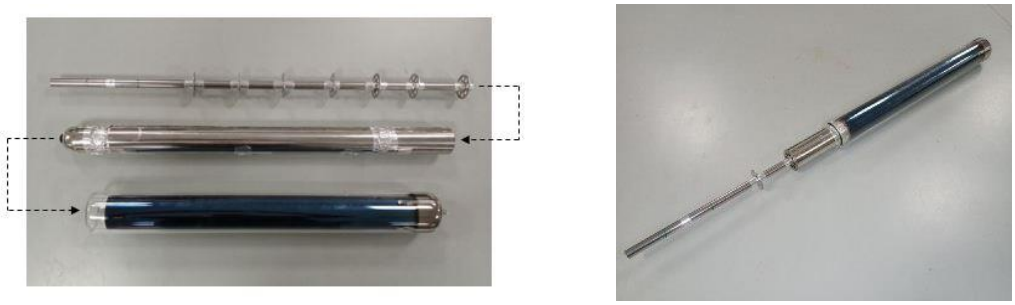

(a) (b)

Figure 3.13: (a) Design arrangement of EGATC (b) EGATC assembled components

3.7.3 Parameter Experimental Setup on Double Pass Flow

Polyvinyl Chloride, also referred to as PVC, is a thermoplastic material. PVC is very versatile and a widely known and used compound. PVC has a good combination of characteristics, as the reason why it is so commonly used for wire insulation and cable jacketing. PVC is flexible, durable, UV resistant, and highly resistant to chemicals,

water, and fire within its nominal temperature ratings between -20°C to 105°C. This Industrial Grade PVC type of material was used to replace the stainless-steel inner absorber to prove whether a double pass flow arrangement occurred inside the inner absorber and was able to enhance the thermal performance.

The double pass flow experiment was conducted as an indoor experiment (refer to **Figure 3.14**) by monitoring the outlet temperature between zero (0) perforated fin EGATC (with a specification of zero (0) perforated fin, non-coating stainless-steel inner absorber, non-coating outer absorber with 1mm wall thickness) and zero (0) fin (insulation material inner absorber) EGATC (with a specification of zero (0) perforated fin, insulation material inner absorber, non-coating outer absorber with 1mm wall thickness).

Figure 3.14: The double pass flow experiment of zero (0) fin (insulation material inner absorber) EGATC during charging and discharging

Meanwhile, **Figure 3.15** shows the insulation material and stainless-steel inner absorber without a perforated fin. The double pass flow experiment was conducted with a similar arrangement, device, and apparatus of other parameter experimental setups.

Figure 3.15: The insulation material and stainless-steel inner absorber without perforated fin

3.8 PERFORMANCE OF EXPERIMENTAL RIG (OUTDOOR)

The determination of EGATC performance and efficiency was conducted, and the experiment was set up, including sensor location, as shown in **Figure 3.16**. Two (2) units of data Logger, 8-Channel Temperature Meter were used to record the data during the experiment. Out of 16-channels, five (5) channels were unused; one (1) channel was allocated for global solar radiation, G_t and other ten (10) channels were allocated for temperature data. Ten (10) units of K-type thermocouple were used to record the temperature data, namely, T1 until T10. T1, T2, T3, and T4 were used to sense the air inlet temperature and air outlet temperature (inside the dryer chamber) for both HP ETC and EGATC, while T5 until T9 was used to sense the temperature of the thermal absorber and heat pipe at five (5) different locations respectively. Meanwhile, T10 was used to record the ambient temperature.

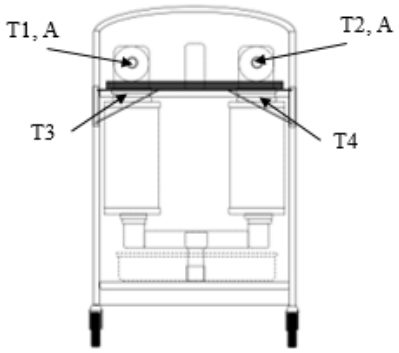

Label	Description	Label	Description
T1	HP ETC inlet temperature	T8	Center thermal absorber temperature
T2	EGATC inlet temperature	T9	Bottom thermal absorber temperature
T3	HP ETC outlet temperature	T10	Ambient temperature
T4	EGATC outlet temperature	G_t	Global Solar radiation (Pyranometer)
T5	Heat pipe condenser temperature	PV Panel	Photo Voltaic Panel
T6	Heat pipe evaporator temperature	EGATC	Evacuated Glass-Thermal Absorber Tube Collector
T7	Top thermal absorber temperature	HP ETC	Heat Pipe Evacuated Tube Collector
		A	Area of inlet duct, (m^2) (A = 5.47 × 10^{-4} m^2)

(a)

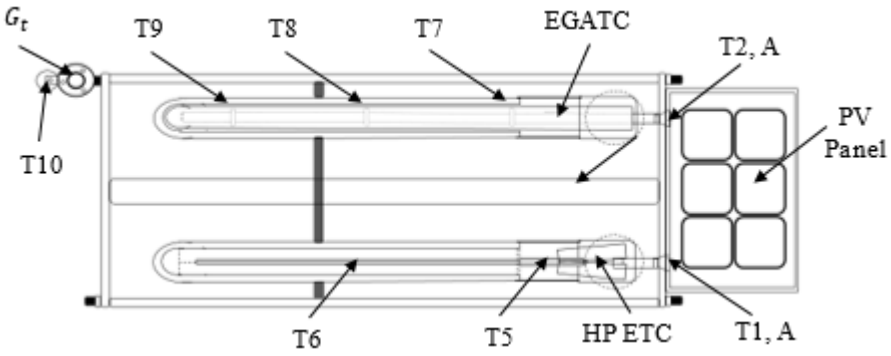

(b)

Figure 3.16: Experimental setup for determining EGATC performance and efficiency. (a) Side view and (b) Top view of the test rig

The experiment was run under real solar radiation conditions. The temperature and solar radiation data were recorded by data logger every one (1) minute interval. On Day 1, during the initial setup, the fan speed controller was adjusted to 5.0V with the air velocity data of 0.74 m/s. As the data constantly changed during the experiment, the air velocity data were recorded every four (4) hours intervals to find its average value of 0.67 m/s. The same procedure was followed for the next 2 days, where the voltage of the fan speed controller and average air velocity value remained for both day 2 and day 3. All the recorded data were analyzed, and the graph was plotted after the experiment was done.

3.8.1 Device and Apparatus

The performance experiment was conducted to compare the thermal efficiency and performance between EGATC and HP ETC as a control reference. The apparatus was exposed to real solar radiation within the range of 0.1 W/m² to 969.3 W/m² for three (3) days. In order to measure the temperature at the thermal absorber wall and the solar radiation flux, APPLENT TECHNOLOGIES, Multi-Channel Temperature Meter (8-CH) (AT4208) and APOGEE INSTRUMENTS, Silicon-Cell: Self Powered Pyranometer (SP-110-SS) were utilized. While for calibration purposes, the real-time solar radiation flux was measured using TES ELECTRICAL ELECTRONIC CORPORATION, Datalogging Solar Power Meter (TES-1333R). The readings taken by both Pyranometer and datalogger were calibrated for their validity and reliability before conducting the experiment. The air velocity was measured by TESTO, Digital Display Hot-Wire Anemometer (405-V1).

Since the parameter experiment showed no significance on the number of fins towards the design of shortened evacuated tube collector (ETC), for commercial purposes, the inner absorber was attached with several PVC fins as the saddle. The inner absorber was made up of stainless steel pipe (with dimensions of 15mm outside diameter x 1.0mm thickness x 600mm length) attached with three (3) Polyvinyl Chloride (PVC) fins as the saddle (with dimensions of 36.3mm outside diameter x 12.9mm inside diameter x 1.0mm thickness, 6mm diameter x 8 holes), while outer absorber was made up by stainless steel pipe (with dimensions of 38mm outside diameter x 1.0mm thickness x 550mm length). Both inner and outer absorbers were assembled inside MISOLIE TECHNOLOGY, high borosilicate glass evacuated tube (with dimensions of 58mm outside diameter x 48mm inside diameter x 500mm length) by one-sided refraction/reflection characteristic coating to eliminate heat loss through convection and radiation between the solar thermal absorber and ambiance.

As per HP ETC, the MISOLIE TECHNOLOGY heat pipe (with a dimension of 400mm length (including header) x 14mm header diameter x 8mm pipe diameter)

attached with an aluminium fin was assembled together inside the same specification of an evacuated tube with EGATC arrangement. The heat pipe header was attached to the stainless-steel plate (with dimensions of 60mm length x 40mm width) to extend the surface area contact with air. The energy collected by both solar thermal collectors was stored inside the separated ventilated drying chamber (with dimensions of 110mm outside diameter x 320mm length). In order to avoid heat losses through the bottom and sides of the chamber, the insulation layer with a thickness of 4 mm was applied. Experimental work was conducted as an outdoor experiment for three (3) days and was exposed to ambient conditions, i.e., clouds and rain. The details of the experiment conducted will be explained in the following sub-sections.

The outdoor experiment was conducted for 3 days from 12th to 14th November, from 9.30 am until 5.30 pm (refer to **Figure 3.17**). The experiment was run at International Islamic University (IIUM), Kuantan Campus **(**GPS Coordinate**:** N 3°50'42.47", E 103°18'11.76") to monitor the outlet temperature between EGATC and HP ETC. (Shailendra Singh et al., 2021) had mentioned it was essential as the tilted angle at latitude orientation would be transferring the maximum amount of solar radiation to the water with regards to ETC solar water heater system. Previously, the preliminary experiment was done at 8° slope angle. Since the result shows a non-significant effect due to the slope of the outlet temperature, the slope angle was considered insignificant in this study. The installation angle depended on the latitude of the site location and was found to be too small at Latitude: 3°50'42.47″N during the experiment.

Figure 3.17: The outdoor experiment between EGATC air heater and HP ETC air heater

3.9 ANALYTICAL MATHEMATICAL MODELING ASSUMPTIONS

The physical component models of the collector are described by equations (3.6) to (3.13). Four (4) nodes model for each main collector component level were selected, starting with evacuated glass, outer absorber, inner absorber, and working fluid inside the absorber. For each node, equations related to the respective components were developed based on the first law of thermodynamics, which describes the energy conservation equations. Combining the developed equation forms a solar thermal collector model for the system.

The proposed model is considered as the distributed parameters of the thermal collector. The method was based on solving the energy conservation equation for the evacuated glass and both the outer and inner absorber and working fluid. Listed below are the assumptions for modelling purposes:

i. The airflow from the inlet to the outlet was in a steady state condition.
ii. The convective heat transfer coefficient and thermal conductivity of the thermal absorber were constant along the path of the working fluid.

iii. The thermal losses via convection around the evacuated glass tube were eliminated and can be neglected.
iv. The wall thickness of the evacuated glass tube (T=1.6mm) was small and can be neglected.
v. The thermal collector was assumed as a short collector (≤ 1 meter). (Ong, 1995)
vi. The temperature gradients in the direction of flow can be neglected.
vii. Lumped-type analysis was used for the evacuated tube.

3.10 ENERGY BALANCE OF EGATC

In a steady state system with a single inlet and outlet entrance, the flowing in mass flow rate was identical to flowing out of the control volume where.

$$\dot{m}_{\text{in}} = \dot{m}_{\text{out}} \tag{3.1}$$

With changes of kinetic and potential energy introduced into or out of the control volume is considered as negligible, the energy balance of the system was described by the changes in the fluid temperature as defined in equation (3.2)

$$\dot{E}_{\text{in}} - \dot{E}_{\text{out}} = \frac{dE_{system}}{dt} \tag{3.2}$$

The amount of energy entered into the control volume was equal to the energy leaving the control volume. Hence, the difference in energy entering and leaving the control volume will equal the total energy change within the control volume, as illustrated in **Figure 3.18**.

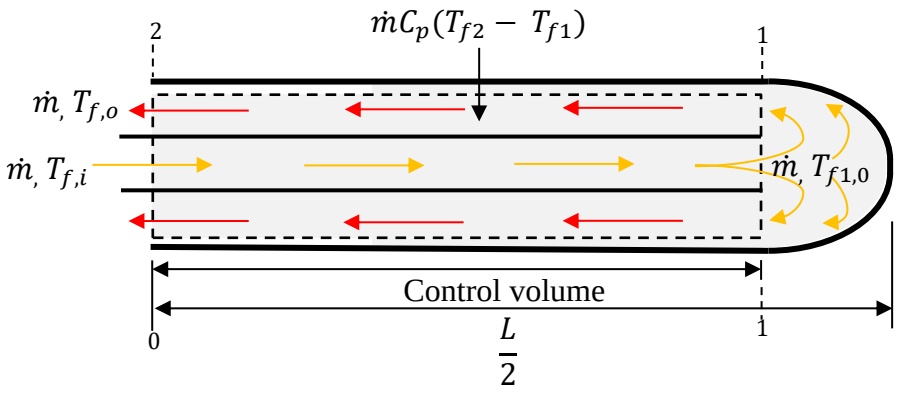

Figure 3.18: Energy balance in a control volume

It was assumed that the constant heat transfer occurred between the thermal absorber and the fluid along the length of the heater. This assumption suggests the fluid temperature varies linearly along the short collectors (less than 10 m), as proposed by (Ahmad Fudholi et al., 2013). Thus, the mean temperature can be obtained based on the following:

$$T_f = T_{f1,0} = \frac{T_{f,i} + T_{f,o}}{2} \tag{3.3}$$

Hence, the defined boundary condition for the fluid temperature is given as follows:

$$T_{f1}\left(0 < x < \frac{L}{2}\right) = \frac{T_{f,i} + T_{f1,0}}{2} \tag{3.4}$$

$$T_{f2}\left(\frac{L}{2} < x < L\right) = \frac{T_{f1,0} + T_{f,o}}{2} \tag{3.5}$$

Figure 3.19 illustrates the schematics diagram of heat transfer in EGATC system, where the energy balance equation was derived. Each evacuated glass element was lumped into one node because of the temperature measurement difficulties at the vacuum pocket. (Njomo & Daguenet, 2006) also had neglected the heat exchange between the two covers in their mathematical model study.

The energy balance is divided into four collector components: evacuated glass, outer absorber, inner absorber, and airflow. The model's boundary conditions assumed that steady air flow was taking place along the solar thermal collector, with convection and radiation heat transfer as well as the thermal conductivity of the thermal absorber being constant along the solar thermal collector length. Based on the assumption, the energy analysis based on the 1st law of thermodynamics is presented as follows:

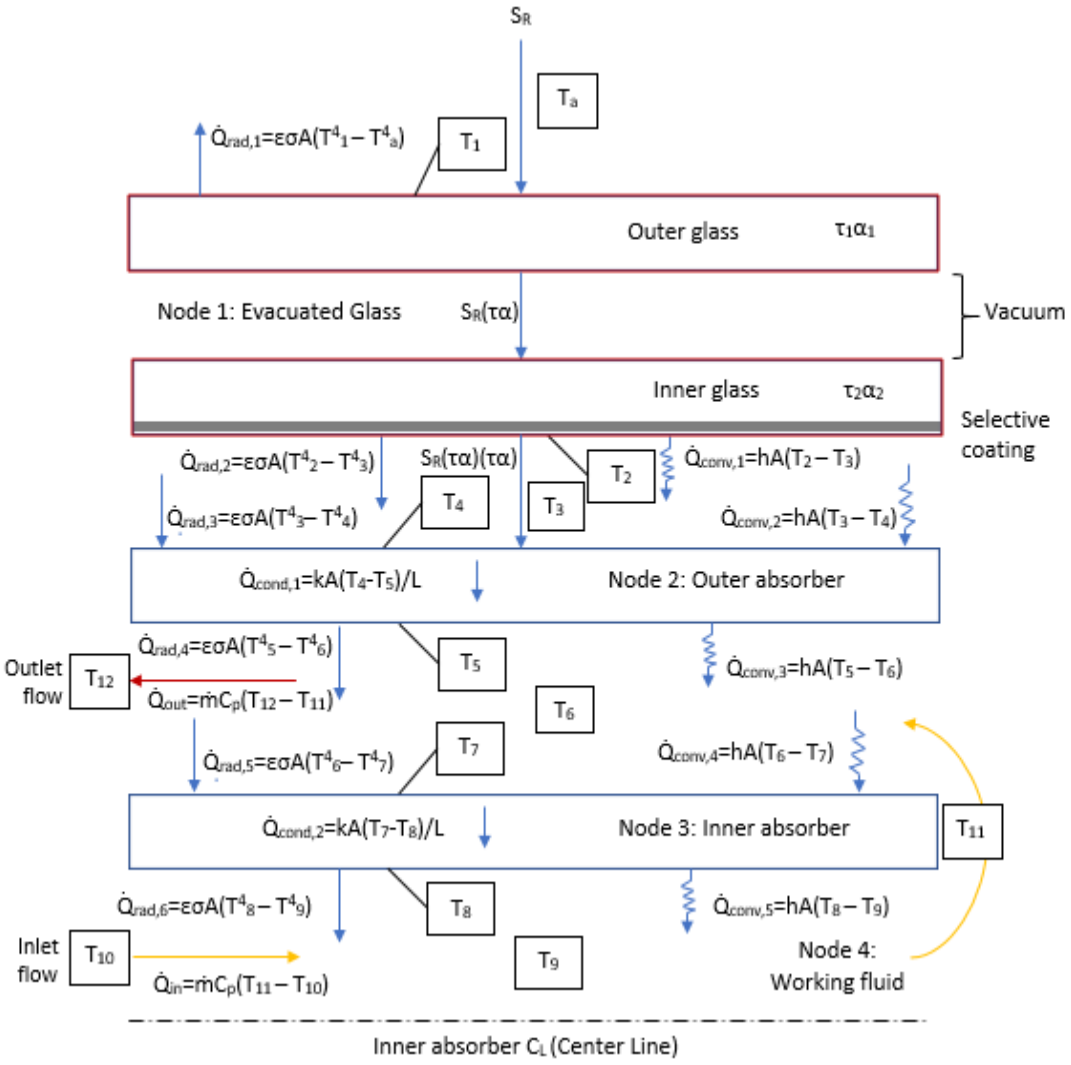

Figure 3.19: Schematics diagram of heat transfer coefficient

For evacuated glass,

Energy in to the outer glass = Energy out of the inner glass (Watt)

$$S_R + S_R(\tau\alpha) = \dot{Q}_{rad,1} + \dot{Q}_{rad,2} + \dot{Q}_{conv,1} \quad (3.6)$$

$$G_t A_c + G_t A_c(\tau\alpha) = \varepsilon\sigma A_s({T_1}^4 - {T_a}^4) + \varepsilon\sigma A_s({T_2}^4 - {T_3}^4) + hA_s(T_2 - T_3) \quad (3.7)$$

For the outer absorber,

Energy in to the outer absorber = Energy out of the outer absorber

$$S_R(\tau\alpha)(\tau\alpha) + \dot{Q}_{cond,1} + \dot{Q}_{rad,3} + \dot{Q}_{conv,2} = \dot{Q}_{rad,4} + \dot{Q}_{conv,3} \quad (3.8)$$

$$G_t A_c(\tau\alpha)(\tau\alpha) + \frac{kA(T_4 - T_5)}{L} + \varepsilon\sigma A_s({T_3}^4 - {T_4}^4) + hA_s(T_3 - T_4) = \varepsilon\sigma A_s({T_5}^4 - {T_6}^4) + hA_s(T_5 - T_6) \quad (3.9)$$

For the inner absorber,

Energy in to the inner absorber = Energy out of the inner absorber

$$\dot{Q}_{cond,2} + \dot{Q}_{rad,5} + \dot{Q}_{conv,4} = \dot{Q}_{rad,6} + \dot{Q}_{conv,5} \quad (3.10)$$

$$\frac{kA(T_7 - T_8)}{L} + \varepsilon\sigma A_s({T_6}^4 - {T_7}^4) + hA_s(T_6 - T_7) = \varepsilon\sigma A_s({T_8}^4 - {T_9}^4) + hA_s(T_8 - T_9) \quad (3.11)$$

For working fluid,

Energy in to air = Energy out of air

$$\dot{Q}_{in} = \dot{Q}_{out} \quad (3.12)$$

$$\dot{m}C_p(T_{11} - T_{10}) = \dot{m}C_p(T_{12} - T_{11}) \quad (3.13)$$

Where,

S_R	=	Solar energy (W)
G_t	=	Solar radiation (W/m^2)
A_c	=	Surface area of collector (m^2)

τ	=	Surface transmittivity
α	=	Surface absorptivity
ε	=	Surface emissivity
σ	=	Stefan-Boltzmann constant (5.67 x 10^{-8} W/m^2 K^4)
h	=	Convective heat transfer coefficient (W/m^2 K)
A_s	=	Surface area (m^2)
T_a	=	Ambient temperature (K)
k	=	Thermal conductivity (W/m.K)
A	=	Cross-sectional area (m^2)
L	=	Length (m)
$\dot{m}$	=	Mass flow rate (kg/s)
C_p	=	Specific heat capacity for air (KJ/ Kg.K)
$T_1, T_2, T_4, T_5, T_7, T_8$	=	Surface temperature (K)
$T_3, T_6, T_9, T_{10}, T_{11}, T_{12}$	=	Convection air temperature (K)

3.11 REYNOLD NUMBER AND NUSSELT NUMBER DETERMINATION

The value of Reynold's number was beneficial in classifying the type of fluid flow inside the pipeline. By using the Reynolds number, the degree of flow behavior can be determined. The basic equation of Reynolds number is given by equation (3.14) using fluid velocity and kinematic viscosity:

$$Re = \frac{D_h V}{v_{air}} \tag{3.14}$$

Derivation of Reynold number incorporating mass flow rate and dynamic viscosity of the fluid in an open channel conduit is presented in Equation (3.15).

$$Re = \frac{4\dot{m}_f}{\pi D_h \mu_{air}} \tag{3.15}$$

The fluid flow characteristics can be categorized into three parts, namely laminar, transition, and turbulent. For the enclosed tube, the range of Reynolds number value for each category was defined in **Table 3.5** (Shankar Subramanian, 2006).

Table 3.5: Reynold number range for various flow types

Flow category	**Re number range**
Laminar	Re < 2300
Transition	2300 < Re < 4000
Turbulence	Re > 4000

To adapt the equation with EGATC at ideal design parameters (air velocity at 0.9 m/s with zero (0) fin resulting in outlet temperature 47.7°C), the Re was determined as follows:

$$Re = \frac{4\dot{m}_f}{\pi D_h \mu_{air}} \tag{3.16}$$

Where,

$\dot{m}_f$ = Mass flow rate (kg/s)

D_h = Inner Diameter of the outer absorber, 0.0365m x 3 = 0.1095m

μ_{air} = Dynamic viscosity of the fluid at 40°C = $1.87x\ 10^{-5}$ kg. s/m^2

From Equation 3.16,

$$Re = \frac{4(5.474\ x\ 10^{-4})}{(3.142)(0.1095)(1.87x\ 10^{-5})}$$

$$Re = \frac{2.1896\ x\ 10^{-3}}{6.4337x\ 10^{-6}}$$

$$Re = 340.33$$

Thus, the type of flow inside the EGATC system was laminar.

On the other hand, the Nusselt number (Nu) is the ratio of convective to conductive heat transfer in a fluid. Nusselt number was used to determine the dominant heat transfer that occurs at a boundary in a fluid, whether conduction or convection. It can be represented by the dimensionless coefficient of the Nusselt number (Nu) (Duffie et al., 1985).

$$Nu = \frac{\dot{q}\ convection}{\dot{q}\ conduction} \tag{3.17}$$

$$Nu = \frac{h\,\Delta T}{k\,\frac{\Delta T}{L}} \tag{3.18}$$

$$Nu = \frac{hL}{k} \tag{3.19}$$

Where,

h	=	Convective heat transfer coefficient (W/m^2 K)
L	=	Length (m)
k	=	Thermal conductivity (W/m. K)

From Equation 3.19, the Nusselt number inside the thermal absorber is determined as follows:

$$Nu = \frac{(720)(0.5)}{(15)}$$

$$Nu = 24$$

.

The Nusselt number (Nu) calculation shows the value is small, which means there was high conductive heat transfer energy. This is due to the effect of conduction versus the heat transfer, which resulted in the convection inside the thermal absorber.

3.12 EGATC VALIDATION ANALYSIS

In this subchapter, the performance analysis was done based on the obtained data from two different EGATC experiments. The temperature value which meets the process criteria were used to compute the thermal performance of the solar thermal collector for the validation process. The theoretical thermal performance was validated with another actual experiment with a similar arrangement. The efficiency, η of the collector was determined as follows (Ahmad Fudholi et al., 2015):

$$\eta_{Collector} = \frac{\dot{Q}_u}{G_t A_c} \times 100\% \tag{3.20}$$

where G_t was solar radiation in W/m^2 and A_c was surface area of the solar thermal collector in m^2. The useful energy gain, $\dot{Q}_u$ was determined based on the following expression (Duffie & Beckman, 2013):

$$\dot{Q}_u = \dot{m} C_p (T_o - T_i) \tag{3.21}$$

with $T_o - T_i$ was temperature difference between the inlet and outlet, C_p was air specific heat capacity in kJ/ kg.K and mass flow rate, $\dot{m}$ was calculated in kg/s using the following:

$$\dot{m} = \rho A V \tag{3.22}$$

where ρ, A, and V were the air density (kg/m^3), the cross-sectional area of the inlet duct (m^2), and the average air velocity (m/s), respectively.

3.13 THEORETICAL SOLUTION METHOD

Numerous researchers have studied solar collector modeling, which includes detailed numerical models, such as Tchinda (2009), Parker et al. (1982), and Hollands &

Shewen (1981). Almost similar to the research, a numerical model has been developed by Kotian, Methekar, et al. (2022) to analyze the performance of the double pipe galvanized iron heat exchanger. A numerical solution for the collector that assumes an adequately short collector under steady-state (Choudhury et al., 1995) was sufficient in solving the theoretical model for Evacuated Glass-Thermal Absorber Tube Collector (EGATC).

During the initial stage, all the required constants and parameters need to be determined. These include surrounding conditions such as solar radiation, ambient temperature, physical properties of the evacuated glass, both outer and inner thermal absorber, thermophysical of the working fluid, and the dimension of the solar thermal collector. The design parameters were:

At the evacuated glass,			
	$\tau = 0.92$	|	$A_s = 0.0455 m^2$
	$\alpha = 0.05$ (High borosilicate glass)	|	$\varepsilon_2 = 0.05$
	$\varepsilon_1 = 0.02$	|	$h = 250\ W/m^2.K$
	$\sigma = 5.67 \times 10^{-8}\ W/m^2.K^4$	|	
At outer absorber,			
	$\tau = 0.3$	|	$\varepsilon = 0.05$
	$\alpha = 0.67$ (Selective surface coating)	|	$A_s = 0.0308 m^2$
	$k = 15\ W/m.K$	|	$h = 250\ W/m^2.K$
	$A = 0.0615 m^2$	|	$A_s = 0.0333 m^2$
	$L = 0.5m$	|	$h = 720\ W/m^2.K$
At inner absorber,			
	$k = 15\ W/m.K$	|	$\varepsilon = 0.05$
	$A = 0.0199 m^2$	|	$A_s = 0.0122 m^2$
	$L = 0.5m$	|	$h = 720\ W/m^2.K$
At working fluid,			
	$C_p = 1.005\ kJ/kg.K$	|	$\dot{m} = 0.0005\ kg/s$

The energy conservation equations were developed for each node, i.e., evacuated glass, outer absorber, inner absorber, and working fluid, based on the first law of thermodynamics. The value obtained from the respective experiment was stated

while computing the energy conservation equations (3.6-3.13). Microsoft Excel® software was used for solving the equation. The solution needs to ensure the amount of energy entered each node should equal the energy leaving the node during charging. The temperature value which meets the process criteria will then be used to compute the thermal performance of the solar thermal collector. The theoretical thermal performance was validated with another actual experimental value with a similar arrangement. The algorithm flowchart for the theoretical solution process is outlined in **Figure 3.20**.

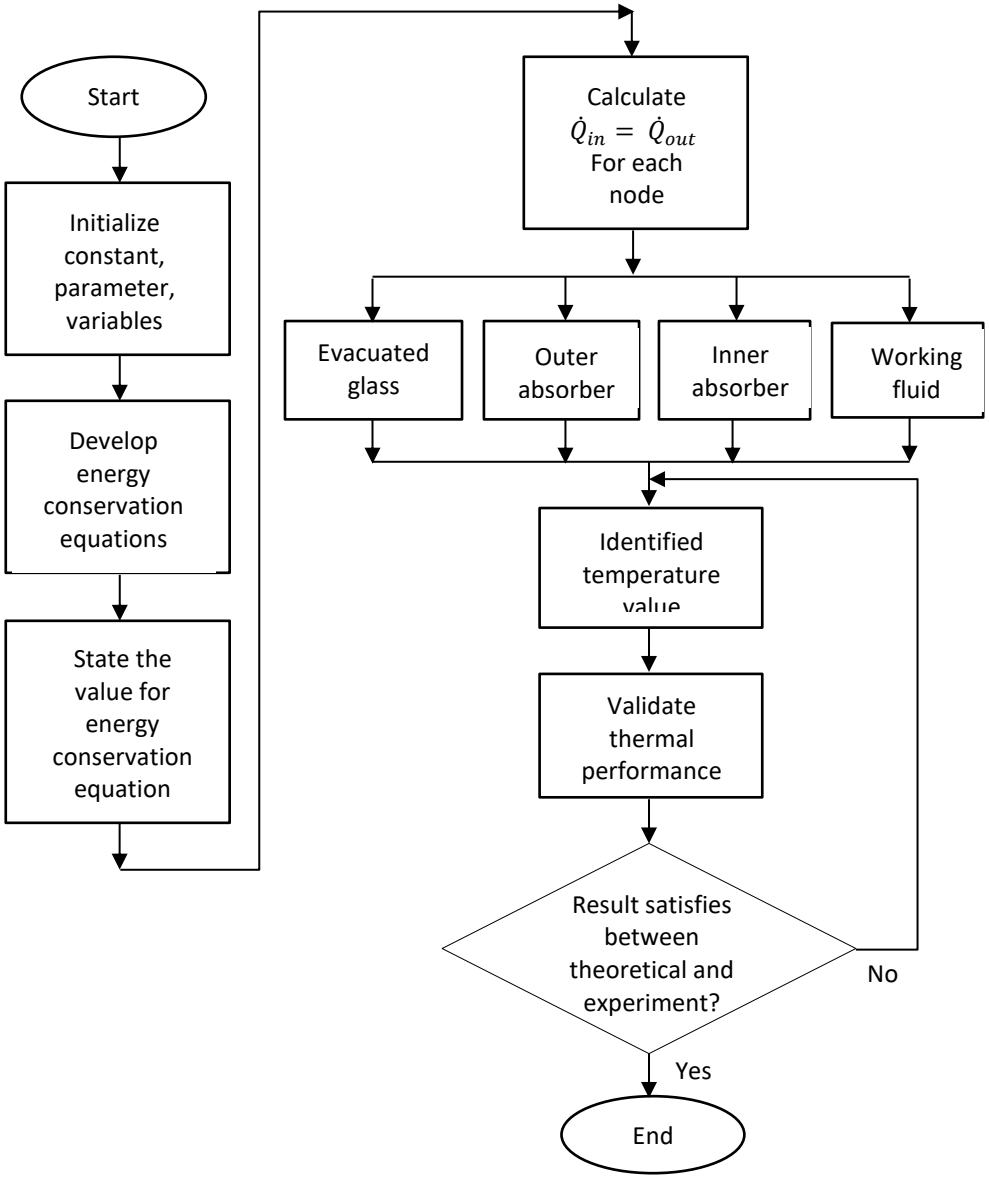

Figure 3.20: Flow chart for theoretical solution process

3.14 CHAPTER SUMMARY

The research method starts with studying the current design of solar thermal collectors and dryers, namely, heat-pipe evacuated tube collectors (HP ETC), and the gaps existing between them were defined. There were three (3) experiments involved in the research, i.e., preliminary experiment, parameter experiment, and performance experiment. Each experiment involved design, development, and investigation process and was reliable to each other. Purchasing components proceeded only after the preliminary experiment showed significant results. Several parameters were investigated on their thermal enhancement performance to determine the ideal design. After all, the performance experiment apparatus was assembled based on the identified design to evaluate the performance and efficiency. Lastly, the results from the experiment were compared with mathematical modeling. If the results are satisfied, then only the process is continued to the end.

The end of this chapter also discussed in detail the mathematical modeling of EGATC, their configuration, application, and also an analytical model assumption. The energy balance of EGATC was developed, and the temperature value was identified. The thermal performance was validated and compared between theoretical and experimental values.

CHAPTER FOUR

RESULTS AND DISCUSSION

4.1 INTRODUCTION

This results and findings of the study are presented in the preceding chapter in light of prior research. The findings discussion is guided by the three (3) major experiments posed in the study, i.e., preliminary experiment, parameter experiment, and performance experiment. However, the focus of the discussion was effectively geared toward significant findings and their theoretical, methodological, and practical contributions to the standing body of knowledge on solar thermal technology, especially within Evacuated Glass-Thermal Absorber Tube Collectors (EGATC).

4.2 PRELIMINARY EXPERIMENTAL RESULTS OF EGATC AND HP ETC: TEMPERATURE AND ENERGY BUFFER

The preliminary experiment on an Evacuated Glass-Thermal Absorber Tube Collector (EGATC) was conducted to prove that EGATC could increase the outlet temperature by converting solar radiation into heat. The findings of the one (1) day experimental results observed that the outlet temperature gained had increased and could dry agricultural products (refer to **Figure 4.1**). Before entering the drying chamber, the air outlet temperature was recorded between 30.6°C to 64.3°C within the range of solar radiation at 91.2 W/m² to 338.9 W/m². According to M. Kumar et al. (2016), in solar drying agricultural products, the moisture was removed by solar air heating with a temperature range of 50 to 60°C. To ensure perfect drying and desirable product quality, the solar drying temperature and moisture removing rate should be under controlled conditions. The percentage of moisture content for different agricultural products was different and varied between products.

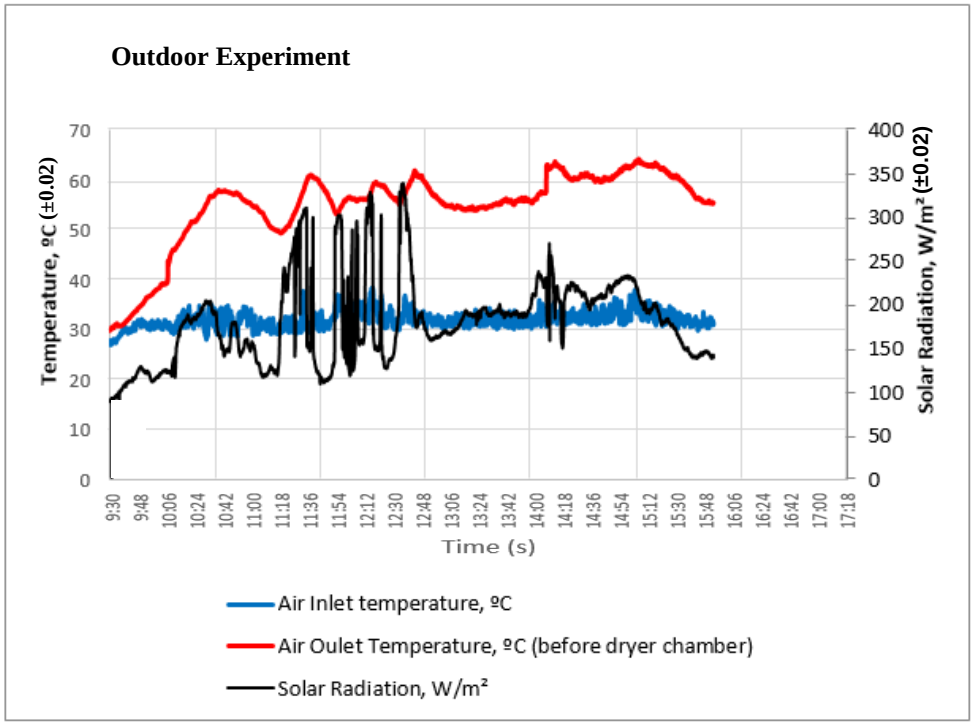

Figure 4.1: Air inlet and outlet temperature differences of EGATC

A preliminary experiment was also conducted to certify the outlet temperature between the Evacuated Glass-Thermal Absorber Tube Collector (EGATC) and Heat Pipe Evacuated Tube Collector (HP ETC). From **Figure 4.2**, the results show the outlet and ambient temperature profile for both EGATC and HP ETC during the whole duration of the experiment. It can be seen that the solar radiation profile during the one (1) day of experimental work was cloudy, with the radiation value fluctuating for the selection of solar radiation between 109 – 309 W/m^2. The experiment was conducted for both collectors, starting at an outlet temperature of 30°C and an ambient temperature of 28°C. As the experiment continued, the solar radiation's heavy fluctuation affected the performance of both collectors. At 11:15 am, when solar radiation was at 312.1 W/m^2, the outlet temperature for EGATC and HP ETC was 43.0°C and 40.7°C, respectively, with a difference of 5.3%.

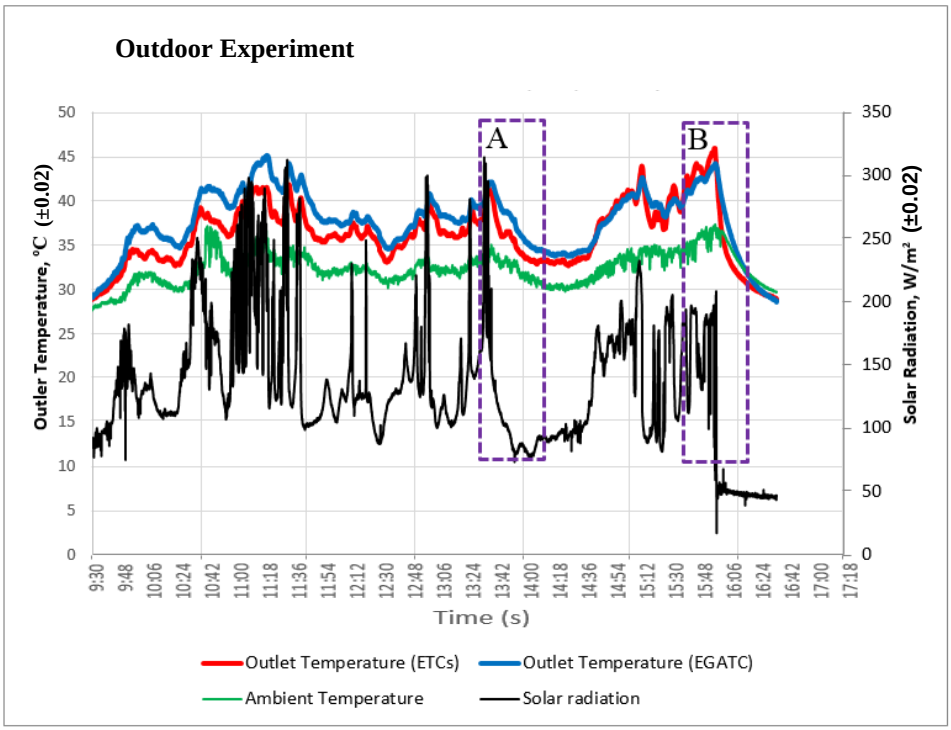

Figure 4.2: Outlet temperature difference between EGATC Air Dryer and HP ETC

The outlet temperature of the EGATC profile was more consistent compared to the one with HP ETC, which contributed to the thermal buffer effect. This can be seen by the discharge rate of each air dryer's outlet temperature profile as labeled by selection Areas A and B. As per Area A, the discharge rate of EGATC and HP ETC were -0.00283 ^{o}C/s and -0.00333 ^{o}C/s, respectively, with solar radiation dropping from 309.3 W/m^2 to 83.8 W/m^2; meanwhile, for Area B, 151.6 W/m^2 radiation drop produced heat discharge rate of -0.01026 ^{o}C/s and -0.01329 ^{o}C/s for EGATC and HP ETC, respectively.

Table 4.1 summarizes the solar radiation range and discharge rate obtained from the experimental runs. Based on these results and observations, it was concluded that EGATC obtained greater heat storage capability as compared to HP ETC. It was observed that the thermal buffer effect was very useful for drying applications in conditions with intermittent solar radiation and during the unavailability of solar

radiation. As for EGATC, the temperature difference between outlet and ambiance after 04.00 p.m. was 2 ^{o}C for about 19 minutes during solar radiation of 52.2 W/m^2.

Table 4.1: Summary of the calculated values of solar radiation range and discharge rate obtained from the preliminary experimental runs

Box	Parameters	EGATC	HP ETC
A	Solar Radiation range, W/m^2 (±0.02)	309.3 – 83.8	
	Discharge rate, ^{o}C/s (±0.000002)	-0.00283	-0.00333
B	Solar Radiation range, W/m^2 (±0.02)	201.3 – 49.7	
	Discharge rate, ^{o}C/s (±0.000002)	-0.01026	-0.01329

4.3 PARAMETER EXPERIMENTAL RESULTS

The experimental results, as well as the observations, indicate that changing in the outlet temperature of the fluid occurred, and the results of fins, fan speed, and fan power obtained from indoor experiments are shown in **Table 4.2**.

Table 4.2: The relationship between fins, fan speed, and fan power obtained from experiments

Fin	Fan speed, V (m/s)						
	0.00	0.70	0.90	1.10	1.30	1.50	1.70
	Fan power (watt)						
0	0.00	2.38	2.61	3.06	3.63	4.59	5.67
1	0.00	2.44	2.67	3.13	3.72	4.70	5.81
3	0.00	2.54	2.78	3.27	3.87	4.90	6.05
5	0.00	2.62	2.87	3.37	3.99	5.06	6.24
7	0.00	2.69	2.95	3.46	4.10	5.19	6.41

It was observed that as the temperature difference between the inlet and outlet increased, the heat transfer rate also increased. By increasing the fan speed, increasing the power of the fan, increasing the number of fins, and increasing the backflow simultaneously lowers the outlet temperature. The results were similar to Kotian, Jain, et al. (2022). They found that as the fluid flow rate increased at the inlet for a fixed

outlet flow rate, the temperature of the fluid at the outlet decreased. At a certain saturation value, the outlet temperature no longer decreases, even when the fluid flow rate at the inlet is increased.

Hence further temperature decreases were not possible. With a higher initial temperature difference, the heat transfer rate was higher but decreased and became almost constant as the flow rate increased. Thus, the hot fluid may cool only up to a certain temperature within specified limits. Figure 5.3(a) and Figure 5.3(b) show the results for the first experimental setup to determine the ideal design of the perforated fin and appropriate air velocity at solar radiation (simulator) 700 watt/m² between zero (0) perforated fin and seven (7) perforated fins with air velocity of 0.0 m/s, 0.7 m/s, 0.9 m/s, 1.1 m/s, 1.3 m/s, 1.5 m/s, and 1.7 m/s. Considering the maximum outlet temperature at minute 30, air velocity at 0.9 m/s was chosen with outlet temperature 47.7 ºC for zero (0) perforated fins and 48.0 ºC for seven (7) perforated fins.

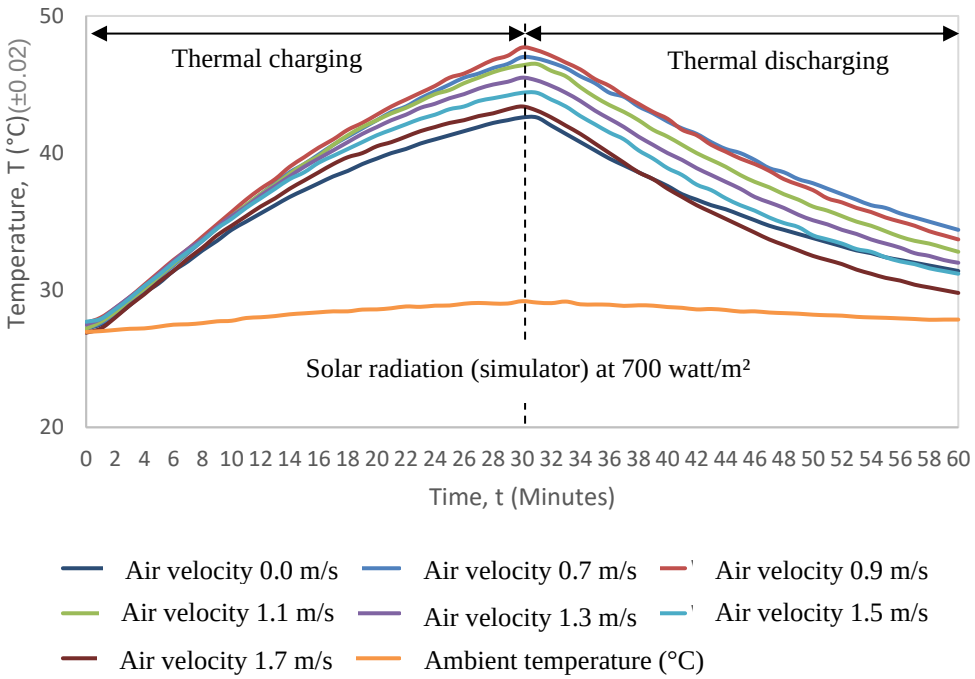

(a)

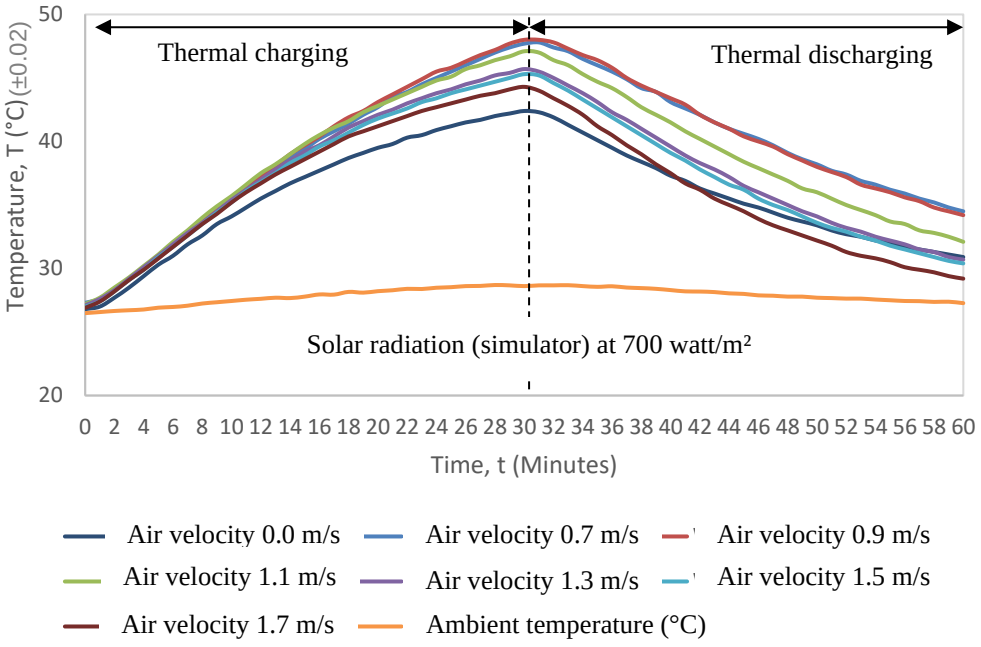

(b)

Figure 4.3: Results of outlet temperature records to determine the ideal design of fin and appropriate air velocity (a) Experiment of zero (0) perforated fin EGATC (b) Experiment of seven (7) perforated fin EGATC

A lower mass flow rate results in a higher air outlet temperature. This is because, at a lower mass flow rate, the higher the residential time of the flowing air around the surface of the thermal absorber increases the heat transfer amount between them. Since zero (0) perforated fin showed the highest daily energy store, Q_{Store}(Daily), it was chosen as the ideal design with 4.46 kJ compared with seven (7) perforated fins at 3.42 kJ. Zero (0) perforated fin may produce laminar air flow resulting in lower outlet temperature at minute 30 but gain better energy store, Q_{Store} value. On the other side, seven (7) perforated fins with turbulence air flow built up the outlet temperature at minute 30 but lowered the energy store, Q_{Store} value.

From the analysis, **Table 4.3** shows the parameter experimental results between zero (0) perforated fin and seven (7) perforated fins with varied air velocity but similar global solar radiation, Gt hour per day and total daily collected energy from global solar radiation, E($GtAc$), which were 0.71 hours and 73.79 kJ respectively.

Table 4.3: The results for parameter experimental between zero (0) perforated fin and seven (7) perforated fins with varied air velocity involved in the study

No.	Optimization Parameters	Gt hour per day (hour) (±0.002)	Vair (avg) (m/s) (±0.02)	E($GtAc$) (kJ) (±0.002)	E ($\dot{Q}$ $Collector$) (kJ) (±0.002)	Efficiency (collector) (%) (±0.02)	Q_{Store} (Daily) (kJ) (±0.002)	Efficiency (collector + storage) (%) (±0.02)
1 (a)	0 Perforated Fin EGATC (V=0.0 m/s)	0.71	0.0	73.79	0.00	0.0	15.01	20.3
	0 Perforated Fin EGATC (V=0.7 m/s)	0.71	0.7	73.79	17.83	24.2	4.81	30.7
	0 Perforated Fin EGATC (V=0.9 m/s)	0.71	0.9	73.79	23.23	31.5	4.46	37.5
	0 Perforated Fin EGATC (V=1.1 m/s)	0.71	1.1	73.79	27.55	37.3	3.59	42.2
	0 Perforated Fin EGATC (V=1.3 m/s)	0.71	1.3	73.79	29.50	40.0	2.59	43.5
	0 Perforated Fin EGATC (V=1.5 m/s)	0.71	1.5	73.79	31.28	42.4	1.87	44.9
	0 Perforated Fin EGATC (V=1.7 m/s)	0.71	1.7	73.79	34.97	47.4	1.72	49.7
1 (b)	7 Perforated Fins EGATC (V=0.0 m/s)	0.71	0.0	73.79	0.00	0.0	16.19	21.9
	7 Perforated Fins EGATC (V=0.7 m/s)	0.71	0.7	73.79	19.58	26.5	4.27	32.3
	7 Perforated Fins EGATC (V=0.9 m/s)	0.71	0.9	73.79	23.87	32.4	3.42	37.0
	7 Perforated Fins EGATC (V=1.1 m/s)	0.71	1.1	73.79	29.23	39.6	2.40	42.9
	7 Perforated Fins EGATC (V=1.3 m/s)	0.71	1.3	73.79	31.44	42.6	1.62	44.8
	7 Perforated Fins EGATC (V=1.5 m/s)	0.71	1.5	73.79	34.34	46.5	1.39	48.4
	7 Perforated Fins EGATC (V=1.7 m/s)	0.71	1.7	73.79	37.44	50.7	0.92	52.0

As the parameters (air velocity at 0.9 m/s and zero (0) perforated fin) were chosen as the ideal design, it was setup for the next parameter experiment. The next experiment was conducted with air velocity at 0.9 m/s and zero (0) perforated fin with outer absorber selective coating surface, outer absorber with 2mm wall thickness, double layer non-vacuum glass tube, single layer transparent outer glass tube and single layer thin film inner glass tube. These experiments were compared to a similar arrangement of zero (0) perforated fin, non-coating outer absorber with 1mm wall thickness, also known as zero (0) perforated fin EGATC at wind speed 0.9 m/s. **Figure 4.4** shows the outlet temperature histories for each parameter experiment at solar radiation (simulator) 700 watt/m². The maximum outlet temperature at minute 30 shows zero (0) perforated fin EGATC with 47.7 ^{o}C, zero (0) perforated fin with outer absorber selective coating surface 48.4 ^{o}C, zero (0) perforated fin with 2mm Outer

absorber wall thickness 46.0 ^{o}C, zero (0) perforated fin with Double layer nonvacuum glass tube 43.8 ^{o}C, zero (0) perforated fin with Single layer transparent outer glass tube 44.1 ^{o}C and zero (0) perforated fin with single layer thin film inner glass tube 43.6 ^{o}C.

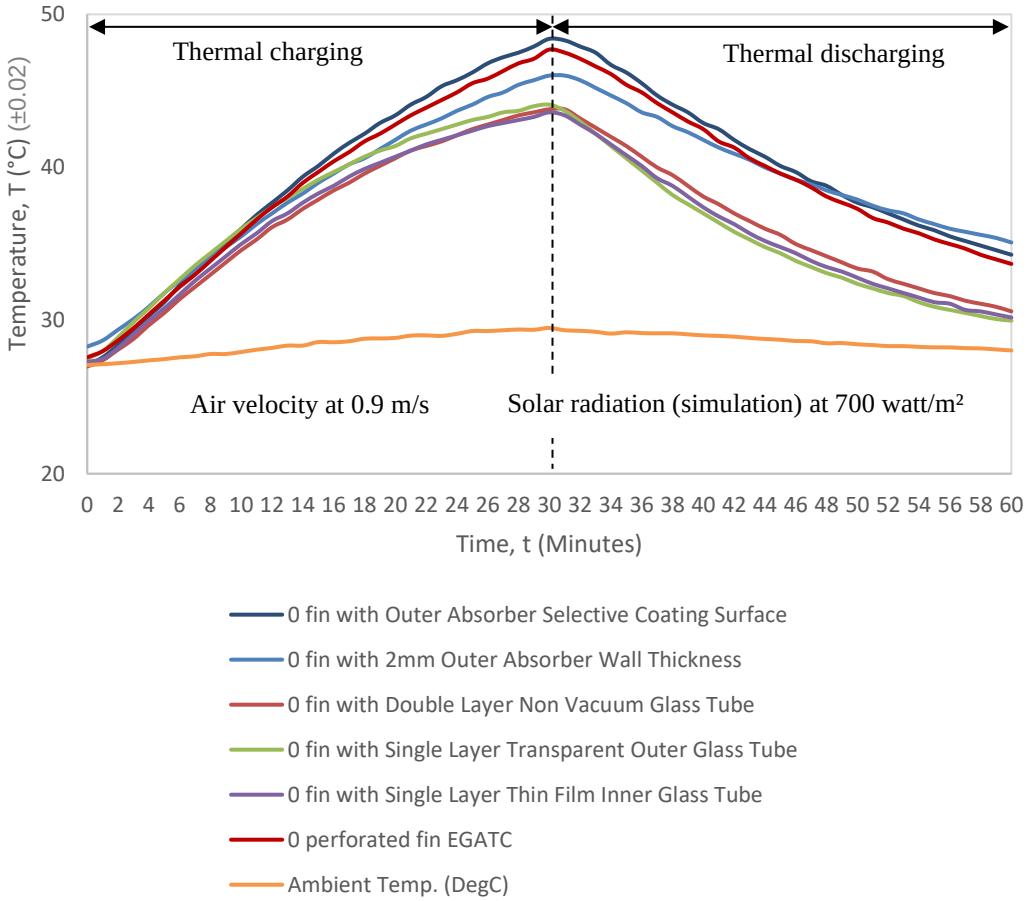

Figure 4.4: Results of the outlet temperature histories for each parameter experiments

The analysis in **Table 4.4** shows the parameter experimental results between zero (0) perforated fin EGATC and zero (0) perforated fin with various parameters. The experiments were conducted with the same solar radiation (simulator) at 700 w/m² and area of collector, 0.0288 m² resulting in a similar value of global solar radiation, Gt hour per day and total daily collected energy from global solar radiation, E($GtAc$), which were 0.71 hours and 73.79 kJ respectively.

Table 4.4: The results between zero (0) perforated fin EGATC and zero (0) perforated fin with varied parameters involved in the experiment

No.	Optimization Parameters	Gt hour per day (hour) (±0.002)	Vair (avg) (m/s) (±0.02)	E($GtAc$) (kJ) (±0.002)	E ($\dot{Q}$ $Collector$) (kJ) (±0.002)	Efficiency (collector) (%) (±0.02)	Q_{Store} (Daily) (kJ) (±0.002)	Efficiency (collector + storage) (%) (±0.02)
1	0 Perforated Fin EGATC (V=0.9 m/s)	0.71	0.9	73.79	23.23	31.5	4.46	37.5
2	0 FIN (Outer absorber selective coating surface) EGATC (V=0.9 m/s)	0.71	0.9	73.79	24.17	32.8	4.17	38.4
3	0 FIN (2mm outer absorber wall thickness) EGATC (V=0.9 m/s)	0.71	0.9	73.79	22.07	29.9	8.54	41.5
4	0 FIN (Double layer Non-Vacuum glass tube) EGATC (V=0.9 m/s)	0.71	0.9	73.79	18.54	25.1	1.39	27.0
5	0 FIN (Single layer transparent outer glass tube) EGATC (V=0.9 m/s)	0.71	0.9	73.79	17.07	23.1	0.44	23.7
6	0 FIN (Single layer thin film inner glass tube) EGATC (V=0.9 m/s)	0.71	0.9	73.79	17.24	23.4	0.74	24.4

4.3.1 Thermal Energy Storage and Performance

In thermal energy storage (TES), extended surfaces were one of the most favorable methods due to their important application in many fields, including electrical conductors, computer chips, automobile engines, heaters, refrigerators, hot water and steam pipes, heat exchanger, etc. The extended surface, also known as fins, was commonly used to enhance the heat transfer rate in many industries. Optimizing the heat transfer rates results in saving power supplied and increased efficiency. TES ability may also be enhanced by increasing the mass of high-heat capacity material.

For assumption, the system in this study was considered a closed system and did not involve any velocity and elevation change. Hence, the heat transfer rate of the collector was expressed by Ahmad Fudholi et al. (2015) and Duffie & Beckman (2013). **Equation 4.1** was used to convert energy from solar radiation into heat to increase the collector's outlet temperature by referring to the inlet temperature.:

$$\dot{Q}_{Collector} = \rho A v C_{p(air)}(T_o - T_i) \tag{4.1}$$

While **Equation 4.2** was used to calculate energy from solar radiation that was converted into thermal energy storage (TES) at the thermal absorber by referring to instantaneous energy accumulation for each second. The heat transfer rate of the thermal absorber storage was expressed by Ahmad Fudholi et al. (2015) and Duffie & Beckman (2013):

$$Q_{Store} = \frac{m_{ab} C_{p(ab)} (T_2 - T_1)}{t_2 - t_1} \quad (4.2)$$

Where

ρ	=	Density of air (kg/m^3)
A	=	Area of inlet duct (m^2)
v	=	Velocity of air at inlet duct (m/s)
$C_{p(air)}$	=	Specific heat of air (kJ/kgK)
T_o	=	Air outlet temperature (K)
T_i	=	Air inlet temperature (K)
m_{ab}	=	mass of thermal absorber (kg)
$C_{p(ab)}$	=	Specific heat of thermal absorber (kJ/kgK)
T_2	=	Temperature of thermal absorber after heat gain (K)
T_1	=	Temperature of thermal absorber before heat gain (K)
t_2	=	Time after heat gain (s)
t_1	=	Time before heat gain (s)

Table 4.5 summarizes the results for all parameter experiments involved in the study. Based on the outlet temperature (47.7°C) at minute 30, the increasing of fin number (7 fins) increases the pressure drop between the inlet and outlet, simultaneously decreasing the wind speed (0.7m/s) by comparing with 0 fins at wind speed 0.9 m/s. The findings were similar to those of (Pavan Kumar et al., 2021) and (Yan et al., 2022). The analysis of energy buffer between zero (0) perforated fin EGATC and zero (0) fin with Outer absorber selective coating demonstrated that zero (0) perforated fin EGATC had better energy buffer, -0.00778 ^{o}C/s compared to zero (0) perforated fin with Outer

absorber selective coating, -0.00783 °C/s. From **Equation 4.2**, in terms of energy store, Q_{Store}, zero (0) perforated fin EGATC also had an advantage with 4.46kJ compared to zero (0) perforated fin with Outer absorber selective coating surface with 4.12kJ.

Table 4.5: Summary of the result for all parameter experiments involved in the study. Red dotted line indicates the comparison experiment

No.	Optimization Parameters	$\dot{Q}_{Collector}$ (KJ) (±0.002)	Q_{Store} (Daily) (kJ) (±0.002)	Tout @ mins 30 (°C) (±0.02)	Tout @ mins 60 (°C) (±0.02)	Temp. different (°C) (±0.02)	Energy buffer (°C/Sec) (±0.000002)
1 (a)	0 Perforated Fin EGATC (V=0.0 m/s)	0.00	15.01	42.6	31.4	11.2	-0.00622
	0 Perforated Fin EGATC (V=0.7 m/s)	17.83	4.81	47.0	34.4	12.6	-0.00700
	0 Perforated Fin EGATC (V=0.9 m/s)	23.23	4.46	47.7	33.7	14.0	-0.00778
	0 Perforated Fin EGATC (V=1.1 m/s)	27.55	3.59	46.4	32.8	13.6	-0.00756
	0 Perforated Fin EGATC (V=1.3 m/s)	29.50	2.59	45.5	32.0	13.5	-0.00750
	0 Perforated Fin EGATC (V=1.5 m/s)	31.28	1.87	44.4	31.2	13.2	-0.00733
	0 Perforated Fin EGATC (V=1.7 m/s)	34.97	1.72	43.4	29.8	13.6	-0.00756
1 (b)	7 Perforated Fins EGATC (V=0.0 m/s)	0.00	16.19	42.4	30.9	11.5	-0.00639
	7 Perforated Fins EGATC (V=0.7 m/s)	19.58	4.27	47.7	34.5	13.2	-0.00733
	7 Perforated Fins EGATC (V=0.9 m/s)	23.87	3.42	48.0	34.2	13.8	-0.00767
	7 Perforated Fins EGATC (V=1.1 m/s)	29.23	2.40	47.1	32.1	15.0	-0.00833
	7 Perforated Fins EGATC (V=1.3 m/s)	31.44	1.62	45.7	30.7	15.0	-0.00833
	7 Perforated Fins EGATC (V=1.5 m/s)	34.34	1.39	45.3	30.4	14.9	-0.00828
	7 Perforated Fins EGATC (V=1.7 m/s)	37.44	0.92	44.3	29.2	15.1	-0.00839
2	0 FIN (Outer absorber selective coating surface) EGATC (V=0.9 m/s)	24.17	4.12	48.4	34.3	14.1	-0.00783
3	0 FIN (2mm outer absorber wall thickness) EGATC (V=0.9 m/s)	22.07	8.54	46.0	35.1	10.9	-0.00606
4	0 FIN (Double layer Non-Vacuum glass tube) EGATC (V=0.9 m/s)	18.54	1.39	43.8	30.6	13.2	-0.00733
5	0 FIN (Single layer transparent outer glass tube) EGATC (V=0.9 m/s)	17.07	0.44	44.1	30.0	14.1	-0.00783
6	0 FIN (Single layer thin film inner glass tube) EGATC (V=0.9 m/s)	17.24	0.74	43.6	30.2	13.4	-0.00744

While on outlet temperature, T_{out}, zero (0) fin with Outer absorber selective coating attained 48.4°C compared with zero (0) perforated fin EGATC with 47.7°C. The value was not similar to the outdoor experiment (para 5.6) which non-coated EGATC showed better thermal efficiency in terms of high temperature gained, followed by coated EGATC and HP ETC. Solar radiation by direct sunlight has a different light spectrum, providing a larger frequency range and giving as much incoming shortwave solar radiation as possible compared with artificial solar radiation by a halogen lamp. According to Planck's Law, the energy of a photon is inversely proportional to the wavelength of light. This shortwave radiation contained more

energy than the photon, thus raising the solar intensity (Kaiser et al., 2019)(Seidlitz et al., 2001). The solar intensity also increased with a small surface area of EGATC since Inverse Square Law states the intensity was inversely proportional to the surface area.

Furthermore, in this research, the selection of the efficiency and performance should focus either on high outlet temperature or heat storage capacity. If focusing on the high outlet temperature, the energy storage could be low, while efficiency will be good due to the lower fan speed. While if focusing on the largest heat storage capacity, the outlet temperature could be low with a higher fan speed. This indicates the system has a good performance.

On zero (0) perforated fin with 2mm Outer absorber wall thickness experiment, the comparison on energy store, Q_{Store} show zero (0) perforated fin EGATC attained 4.46kJ, and zero (0) perforated fin with 2mm Outer absorber wall thickness attained 8.54kJ while on energy buffer, both attained -0.00778 ^{o}C/s and -0.00606 ^{o}C/s respectively. In other experiments, the energy store, Q_{Store} for zero (0) perforated fin with Double layer non-vacuum glass tube attained 1.39kJ, zero (0) perforated fin with Single layer transparent outer glass tube 0.44kJ, and zero (0) perforated fin with Single layer thin film inner glass tube 0.74kJ compared to zero (0) perforated fin EGATC 4.46kJ. Meanwhile, on the energy buffer, there were -0.00733 ^{o}C/s, -0.00783 ^{o}C/s, and -0.00744 ^{o}C/s compared to -0.00778 ^{o}C/s, respectively.

4.4 DOUBLE PASS FLOW EXPERIMENT RESULTS

The double pass flow experiment was conducted to determine whether the double pass flow arrangement that occurred inside the inner absorber was able to enhance the thermal performance. From the results, zero (0) perforated fin with stainless-steel inner absorber EGATC showed better results (refer to **Figure 4.5**) in terms of outlet temperature.

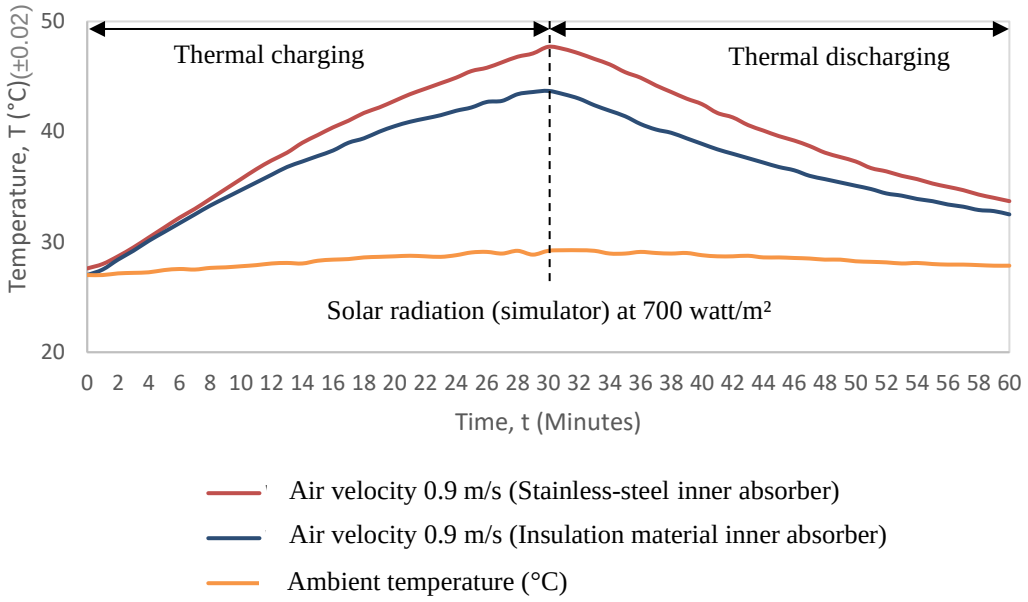

Figure 4.5: Outlet temperature records between stainless steel inner absorber and insulation material inner absorber for double pass flow experiment

After 30 minutes of charging, the outlet temperature of zero (0) perforated fin with stainless-steel inner absorber EGATC was 47.7°C compared with zero (0) fin with insulation material inner absorber 44.7°C with differences of 3°C. In terms of energy store, Q_{Store}, stainless-steel inner absorber also had an advantage with 4.46kJ compared to insulation material inner absorber 4.40kJ. At the end of discharging period at 60 minutes, the outlet temperature of both inner absorbers was 33.7°C and 33.5°C, respectively. With differences in outlet temperature between minute 30 and minute 60 for the stainless-steel inner absorber of 14.0°C and insulation material inner absorber of 11.2°C affected the energy buffer for both inner absorbers, -0.00778°C/s and -0.00622°C/s respectively. **Table 4.6** shows the calculated values obtained from the experiment.

Table 4.6: The calculated values obtained from the double pass flow experimentantal runs

No.	Optimization Parameters	$\dot{Q}_{Collector}$ (KJ) (±0.002)	Q_{Store} (Daily) (kJ) (±0.002)	Tout @ mins 30 (°C) (±0.02)	Tout @ mins 60 (°C) (±0.02)	Temp. different (°C) (±0.002)	Energy buffer (°C/Sec) (±0.000002)
1	0 Perforated Fin EGATC (V=0.9 m/s) (Stainless steel Inner Absorber)	23.23	4.46	47.7	33.7	14.0	-0.00778
2	0 FIN (Insulation Material Inner Absorber) EGATC (V=0.9 m/s)	18.53	4.40	44.7	33.5	11.2	-0.00622

The analysis in **Table 4.7** shows the results between zero (0) perforated fin EGATC with stainless steel inner absorber and zero (0) perforated fin with insulation material of the inner absorber involved in the parameter experiment. This experiment also was conducted with a similar arrangement to previous parameters experiments.

Table 4.7: The parameter experimental result between zero (0) perforated fin EGATC with stainless steel inner absorber and zero (0) perforated fin with insulation material inner absorber

No.	Optimization Parameters	Gt hour per day (hour) (±0.002)	Vair (avg) (m/s) (±0.02)	E($GtAc$) (kJ) (±0.002)	E ($\dot{Q}$ $Collector$) (kJ) (±0.002)	Efficiency (collector) (%) (±0.02)	Q_{Store} (Daily) (kJ) (±0.002)	Efficiency (collector + storage) (%) (±0.02)
1	0 Perforated Fin EGATC (V=0.9 m/s) (Stainless steel Inner Absorber)	0.71	0.9	73.79	23.23	31.5	4.46	37.5
2	0 FIN (Insulation Material Inner Absorber) EGATC (V=0.9 m/s)	0.71	0.9	73.79	18.53	25.1	4.40	31.1

The stainless-steel inner absorber EGATC consists of conductive inner absorber material, which affected the mass of the total absorber and was set as a double pass arrangement. These were the main factors that initiated the initial heat convection inside the inner absorber before the airflow moved towards the outer absorber. It also acts as heat storage material as it stores maximum heat from the thermal absorber, and it can be efficiently transferred to the air due to the increased contact area between air and thermal absorber. The airflow that moved towards the outer absorber produced the cumulative heat gained inside the outer absorber, thus doubling up the temperature at the outlet. The types, mass, and arrangement of the conductive inner absorber material show that the double pass arrangement inside EGATC was significant.

4.5 EFFECT OF TILTED ANGLE AND SOLAR THERMAL ABSORBER PROPERTIES: 1 MM WALL THICKNESS AND 2 MM WALL THICKNESS

According to Shailendra Singh et al. (2021), the tilted angle at latitude orientation would transfer the maximum amount of solar radiation to the water with regards to ETC solar water heater system. The slope angle installation depended on the site location's latitude and during the experiment it was found to be too small at Latitude: 3°50'42.47″N (KUANTAN, Pahang). For fixed installation, the solar thermal collector should receive solar radiation throughout the year for maximum performance. For that purpose, a 2-axis manual sun tracker may be used for the equinox situation.

Thus, the experiment was conducted at 8° slope angle to ensure the slanting angle occurred at the perfect evaporation. **Figure 4.6** shows the outlet temperature differences at 8° slope angle between HP ETC, 3 fins (1mm absorber wall thickness) EGATC, and 3 fins (2mm absorber wall thickness) EGATC.

At 11:12 am, where the solar radiation was 265.4 W/m^2, the outlet temperature differences for HP ETC, 3 fins (1mm absorber wall thickness) EGATC and 3 fins (2mm absorber wall thickness) EGATC were recorded at 43.3°C, 44.3°C and 53.4°C respectively. During maximum solar radiation, 1082.1 W/m^2 at 11:47 am, the outlet temperature differences for HP ETC were recorded at 40.7°C, 3 fins (1mm absorber wall thickness) EGATC was recorded at 40.9°C and 3 fins (2mm absorber wall thickness) EGATC was recorded at 46.6°C. Lastly, at 16:51 pm, during the diffused solar radiation condition, 50.9 W/m^{2,} the reading of outlet temperature differences for HP ETC, 3 fins (1mm absorber wall thickness) EGATC, and 3 fins (2mm absorber wall thickness) EGATC were recorded at 32.9°C, 34.5°C and 36.2°C respectively.

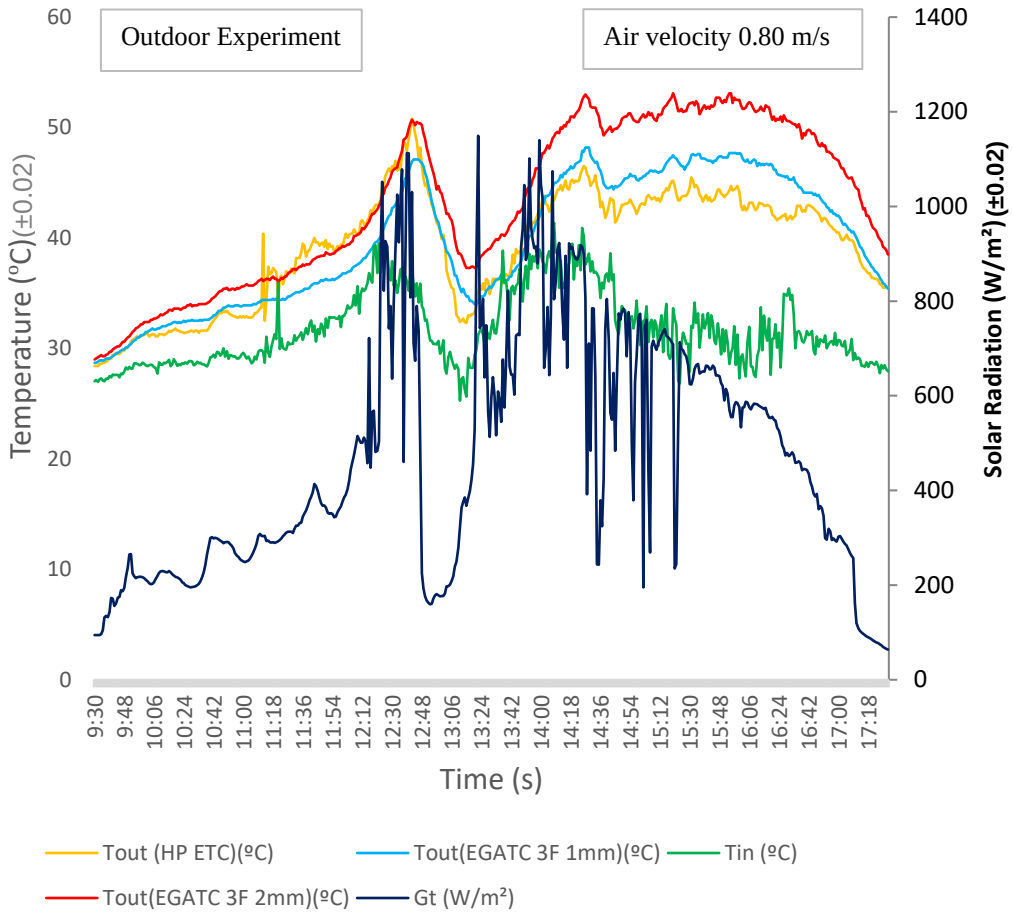

Figure 4.6: The outlet temperature differences at 8° slope angle between HP ETC, 3 Fins (1mm absorber wall thickness) EGATC and 3 Fins (2mm absorber wall thickness) EGATC

From the analysis, the global solar radiation, Gt hour per day, was 2.59 hours, and air velocity, V, was 0.8 m/s. For HP ETC, 3 fins (1mm absorber wall thickness) EGATC and 3 fins (2mm absorber wall thickness) EGATC, the total daily collected energy from global solar radiation, E($GtAc$) was 268.18 kJ. Total daily energy gain produced by solar thermal collector E ($\dot{Q}\ Collector$) for HP ETC were 130.29 kJ, 153.14 kJ for 3 fins (1mm absorber wall thickness) and 170.10 kJ for 3 fins (2mm absorber wall thickness). The efficiency of the collector obtained for HP ETC, 3 fins (1mm absorber wall thickness) and 3 fins (2mm absorber wall thickness) were 48.6%, 57.1%, and 63.4%, respectively. The daily stored energy by the thermal absorber, $QStore$ by HP ETC was 4.66 kJ, 3 fins (1mm absorber wall thickness) was 6.62 kJ and

on the other hand, for 3 fins (2mm absorber wall thickness) was 7.18 kJ. For HP ETC, 3 fins (1mm absorber wall thickness) and 3 fins (2mm absorber wall thickness), the collector's efficiency with storage ability obtained was 50.3%, 59.6%, and 66.1%, respectively.

The results showed there was a non-significant effect due to the slope with regard to outlet temperature at the respective Latitude: 3°50’42.47″N and the slope angle was considered insignificant in this study. The results also proved that 3 fins (2mm absorber wall thickness) EGATC was better than 3 fins (1mm absorber wall thickness) in terms of outlet temperature differences, but both wall thicknesses were better than HP ETC. and EGATC. This experiment was conducted as an outdoor experiment under real solar radiation (see **Figure 4.7**).

Figure 4.7: The outdoor experiment conducted to determine the effect of the slope angle

4.6 EFFECT OF SOLAR THERMAL ABSORBER PROPERTIES: COATED AND NON-COATED

A hollow metal tube in the form of a pipe was the main material used for the Evacuated Glass Thermal- Absorber Tube Collector (EGATC). The thermal behaviour of the pipe for solar thermal absorber application was identified in order to understand thermal interaction under various temperature phases and enhancement to the material. The radiative characteristics of the material used in the experiment were listed in hollow pipe with physical properties (see **Table 3.3)**. While, **Figure 4.8** shows the outlet temperature differences between HP ETC, non-coated EGATC, and coated EGATC.

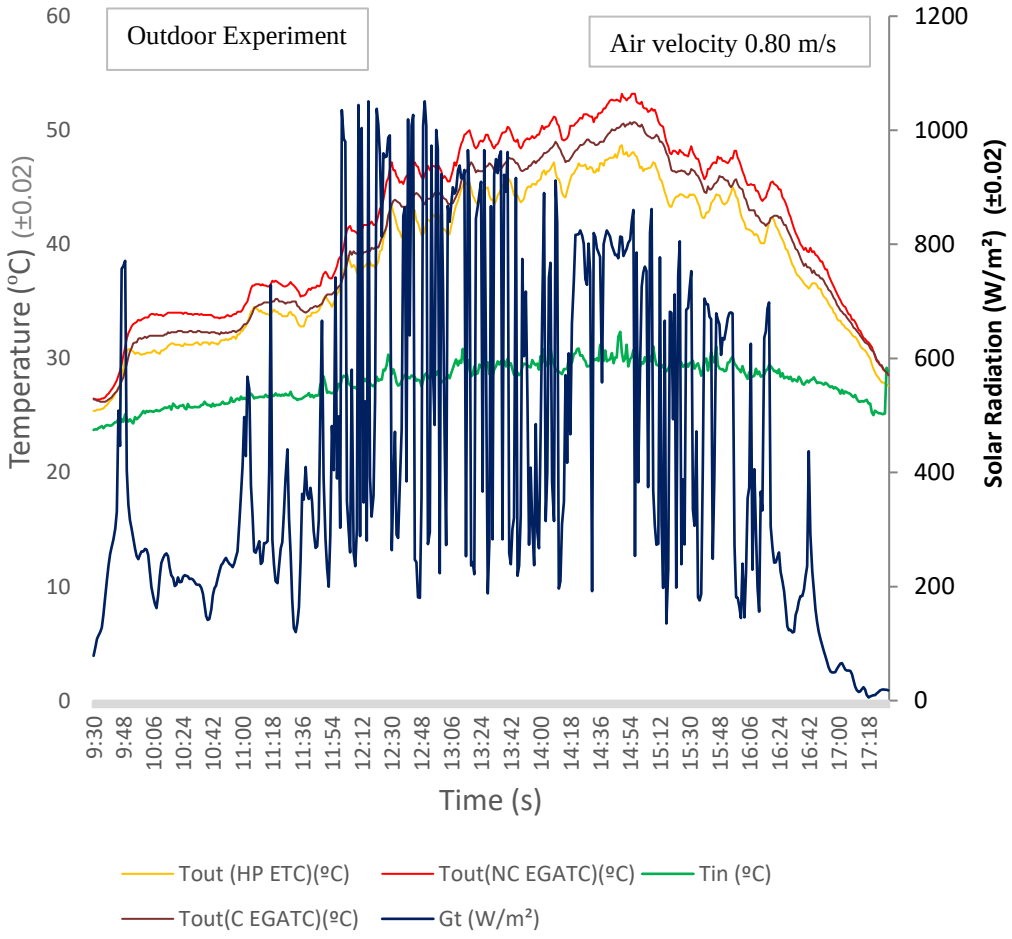

Figure 4.8: The outlet temperature differences between HP ETC, non-coated EGATC, and coated EGATC

At 10:02 am, where the solar radiation was 264.7 W/m^2, the outlet temperature differences for HP ETC, non-coated EGATC, and coated EGATC were recorded at 30.5°C, 31.8°C and 33.6°C respectively. During maximum solar radiation, 1050.7 W/m^2 at 12:50 am, the outlet temperature differences for HP ETC were recorded at 41.2°C, non-coated EGATC was recorded at 43.5°C and coated EGATC was recorded at 46.1°C. Lastly, at 16:55 pm, during the diffused solar radiation condition, 50.9 W/m^{2,,} the reading of outlet temperature differences for HP ETC, non-coated EGATC, and coated EGATC were recorded at 34.5°C, 35.9°C and 36.9°C respectively.

From the analysis, the global solar radiation, Gt hour per day, was 3.40 hours, and air velocity, V, was 0.8 m/s. For HP ETC, non-coated EGATC, and coated EGATC, the total daily collected energy from global solar radiation, E($GtAc$), was 352.63 kJ. Total daily energy gain produced by solar thermal collector E ($\dot{Q}\ Collector$) for HP ETC were 142.34 kJ, 197.03 kJ for non-coated EGATC and 172.56 kJ for coated EGATC. The efficiency of the collector obtained for HP ETC, non-coated EGATC, and coated EGATC were 40.4%, 55.9%, and 48.9%, respectively. The daily stored energy by the thermal absorber, $QStore$ by HP ETC, was 2.18 kJ, non-coated EGATC was 3.17 kJ, and on the other hand, for coated EGATC was 1.11 kJ. For HP ETC, non-coated EGATC, and coated EGATC, the collector's efficiency with storage ability obtained was 41.0%, 56.8%, and 49.2%, respectively.

The results showed that both EGATC coated and non-coated were better than HP ETC due to higher outlet temperature. While in comparison between non-coated EGATC and coated EGATC, Non-coated EGATC showed better thermal efficiency in terms of high temperature gained. Since the radiative characteristics of thin film selective surface coating in evacuated glass physical properties (see **Table 3.4**) allowed higher absorbance and negligible emittance (outer surface of the inner glass tube), the reflection of thermal radiation was reduced (Soteris A. Kalogirou, 2014). The thermal radiation penetrated the thin film selective surface coating and was reflected by the standard stainless-steel finishes of the non-coated absorber. Then, the thermal radiation was reflected again by the mirror reflectance at the selective surface absorbance (inner

surface of the inner glass tube) (Chow et al., 1984) and again to the non-coated absorber.

The characteristic was similar to the conventional ETC design available in the market that uses non-coated Aluminum as the thermal absorber. It could increase the kinetic energy of air molecules, which increases the temperature. These phenomena accumulates the energy at the gap between the evacuated tube inner glass tube and outer stainless-steel absorber, simultaneously increasing the thermal energy storage. Thus, the results showed non-coated thermal absorber was significant.

4.7 EFFECT OF EVACUATED TUBE COLLECTOR PROPERTIES: DOUBLE LAYER NON-VACUUM EGATC AND DOUBLE LAYER VACUUM EGATC

The outlet temperature differences between HP ETC, double-layer non-vacuum EGATC, and double-layer vacuum EGATC are shown in **Figure 4.9**. At 9:40 am, where the solar radiation was 252.9 W/m^2, the outlet temperature differences for HP ETC, double-layer non-vacuum EGATC, and double-layer vacuum EGATC were recorded at 30.7°C, 28.9°C and 31.1°C respectively. During maximum solar radiation, 1047.9 W/m^2 at 12:50 am, the outlet temperature differences for HP ETC were recorded at 50.1°C, double layer non-vacuum EGATC was recorded at 45.4°C and double layer vacuum EGATC was recorded at 55.1°C. Lastly, at 17:23 pm, during the diffused solar radiation condition, 68.1 W/m^{2,,} the reading of outlet temperature differences for HP ETC, double-layer non-vacuum EGATC, and double-layer vacuum EGATC were recorded at 37.5°C, 33.8°C and 40.4°C respectively.

From the analysis, the global solar radiation, Gt hour per day, was 4.91 hours, and air velocity, V, was 0.8 m/s. For HP ETC, double-layer non-vacuum EGATC, and double-layer vacuum EGATC, the total daily collected energy from global solar radiation, E($GtAc$), was 509.21 kJ. Total daily energy gain produced by solar thermal collector E ($\dot{Q}\ Collector$) for HP ETC were 186.41 kJ, 133.91kJ for double layer non-

vacuum EGATC and 188.82 kJ for double layer vacuum EGATC. The efficiency of the collector obtained for HP ETC, double-layer non-vacuum EGATC, and double-layer vacuum EGATC were 36.6%, 26.3%, and 37.1%, respectively. The daily stored energy by the thermal absorber, $QStore$ by HP ETC was 5.30 kJ, double layer non-vacuum EGATC was 1.63 kJ, and on the other hand, for double layer vacuum EGATC was 7.85 kJ. For HP ETC, double-layer non-vacuum EGATC, and double-layer vacuum EGATC, the collector's efficiency with storage ability obtained was 37.6%, 26.6%, and 38.6 %, respectively.

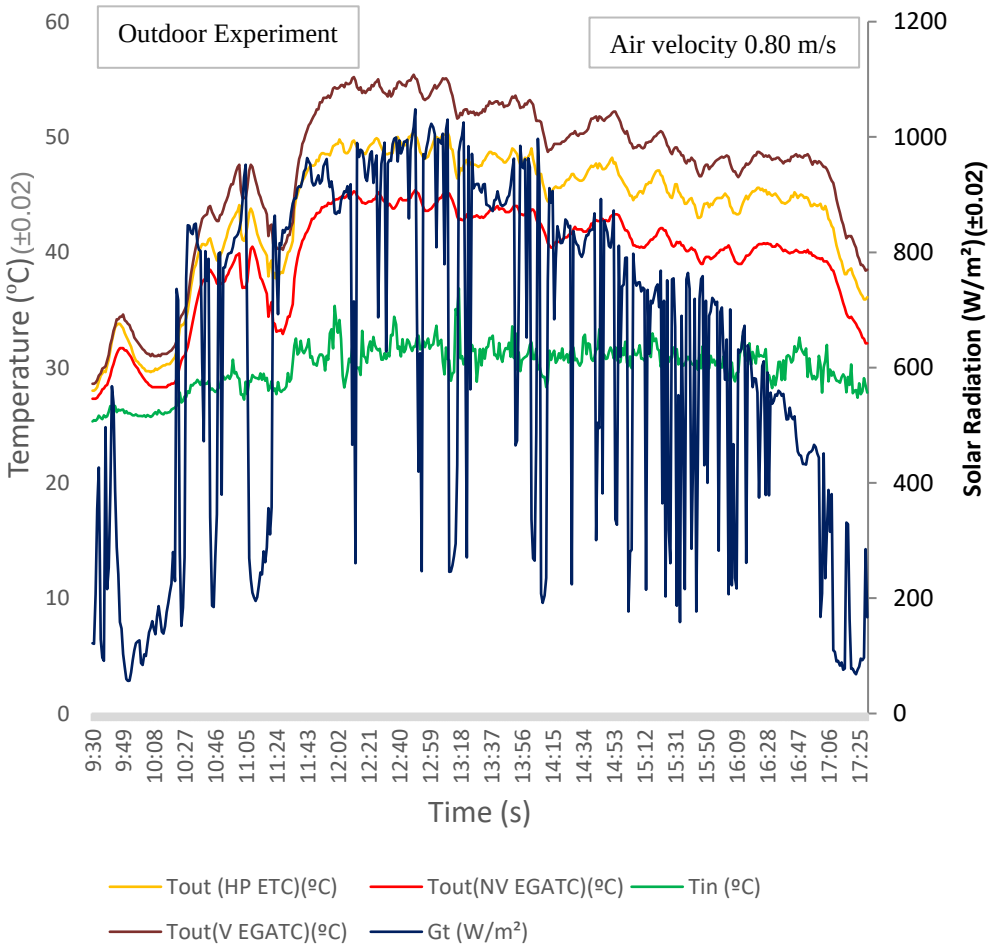

Figure 4.9: The outlet temperature differences between HP ETC, double-layer non-vacuum EGATC, and double-layer vacuum EGATC

The results proved that double-layer vacuum EGATC was better than HP ETC in terms of outlet temperature differences. Meanwhile, double-layer non-vacuum

EGATC was the worst among those three. The existence of a vacuum pocket in between of outer glass tube and the inner glass tube with thin film selective surface coating serves as an insulation layer for efficient heat loss prevention. The sunlight penetrates through the transparent outer glass tube and is absorbed by the inner glass tube with thin film selective surface coating. The heat energy harnessed from the sunlight was trapped within the collector and subsequently transmitted to the thermal absorber at an optimum level.

4.8 EFFECT OF EVACUATED TUBE COLLECTOR PROPERTIES: DOUBLE LAYER VACUUM EGATC, SINGLE LAYER TRANSPARENT OUTER GLASS TUBE EGATC AND SINGLE LAYER THIN FILM SELECTIVE SURFACE COATING INNER GLASS TUBE EGATC

The outlet temperature differences between HP ETC, double-layer vacuum EGATC, and single layer transparent outer glass tube EGATC are shown in **Figure 4.10**. At 9:41 am, the solar radiation was 133.7 W/m^2, and the outlet temperature differences for HP ETC, double layer vacuum EGATC and single layer transparent outer glass tube EGATC were recorded at 29.6°C, 29.7°C, and 28.4°C respectively. During maximum solar radiation, 1074.9 W/m^2 at 12:05 am, the outlet temperature differences for HP ETC were recorded at 40.5°C, double layer vacuum EGATC was recorded at 42.2°C, and single layer transparent outer glass tube EGATC was recorded at 36.1°C. Lastly, at 3:50 pm, during the diffused solar radiation condition, 259.4 W/m^{2,} the reading of outlet temperature differences for HP ETC, double layer vacuum EGATC and single layer transparent outer glass tube EGATC were recorded at 45.3°C, 49.0°C and 41.2°C respectively.

From the analysis, the global solar radiation, Gt hour per day, was 4.90 hours, and air velocity, V, was 0.8 m/s. For HP ETC, double-layer vacuum EGATC and single-layer transparent outer glass tube EGATC, the total daily collected energy from global solar radiation, E($GtAc$), was 508.18 kJ. Total daily energy gain produced by solar thermal collector E ($Q\ Collector$) for HP ETC were 172.57 kJ, 206.37 kJ for

double layer vacuum EGATC and 148.37 kJ for single layer transparent outer glass tube EGATC. The efficiency of the collector obtained for HP ETC, double layer vacuum EGATC, and single layer transparent outer glass tube EGATC was 34.0%, 40.6%, and 29.2%, respectively. The daily stored energy by the thermal absorber, $QStore$ by HP ETC was 7.49 kJ, double layer vacuum EGATC was 10.90 kJ, and on the other hand, for single layer transparent outer glass tube EGATC was 3.73 kJ. For HP ETC, double-layer vacuum EGATC and single layer transparent outer glass tube EGATC, the collector's efficiency with storage ability obtained was 35.4%, 42.8%, and 29.9 %, respectively.

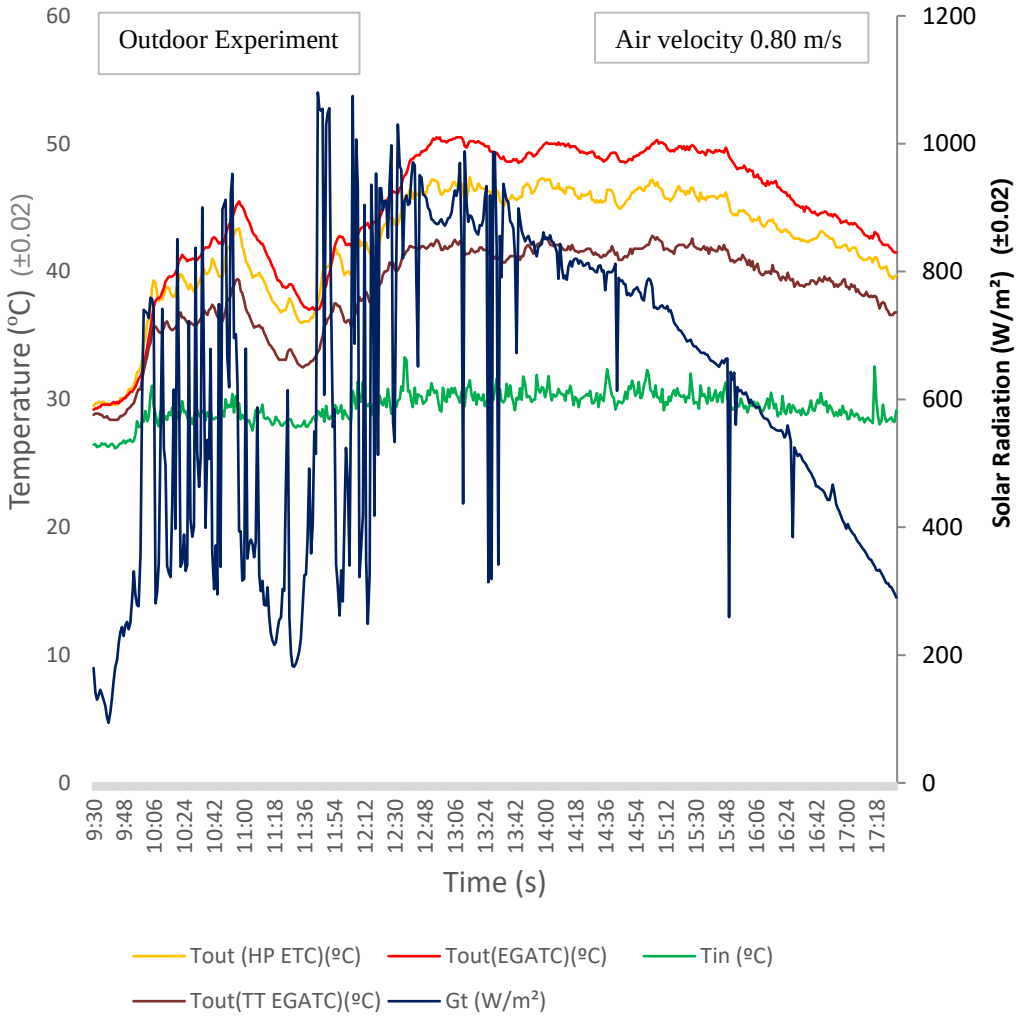

Figure 4.10: The outlet temperature differences between HP ETC, double-layer vacuum EGATC and single layer transparent outer glass tube EGATC

The results showed that double-layer vacuum EGATC was better than HP ETC in terms of outlet temperature differences. In the meantime, single-layer transparent outer glass tube EGATC was the worst among those three. The presence of a double layer between the outer glass tube and the inner glass tube minimizes thermal losses by conduction and convection.

Figure 4.11 shows the outlet temperature differences between HP ETC, double-layer vacuum EGATC, and single layer thin film selective surface coating inner glass tube EGATC. At 9:46 am, where the solar radiation was 265.6 W/m^2, the outlet temperature differences for HP ETC, double layer vacuum EGATC and single layer thin film selective surface coating inner glass tube EGATC were recorded at 33.1°C, 34.7°C, and 31.2°C respectively.

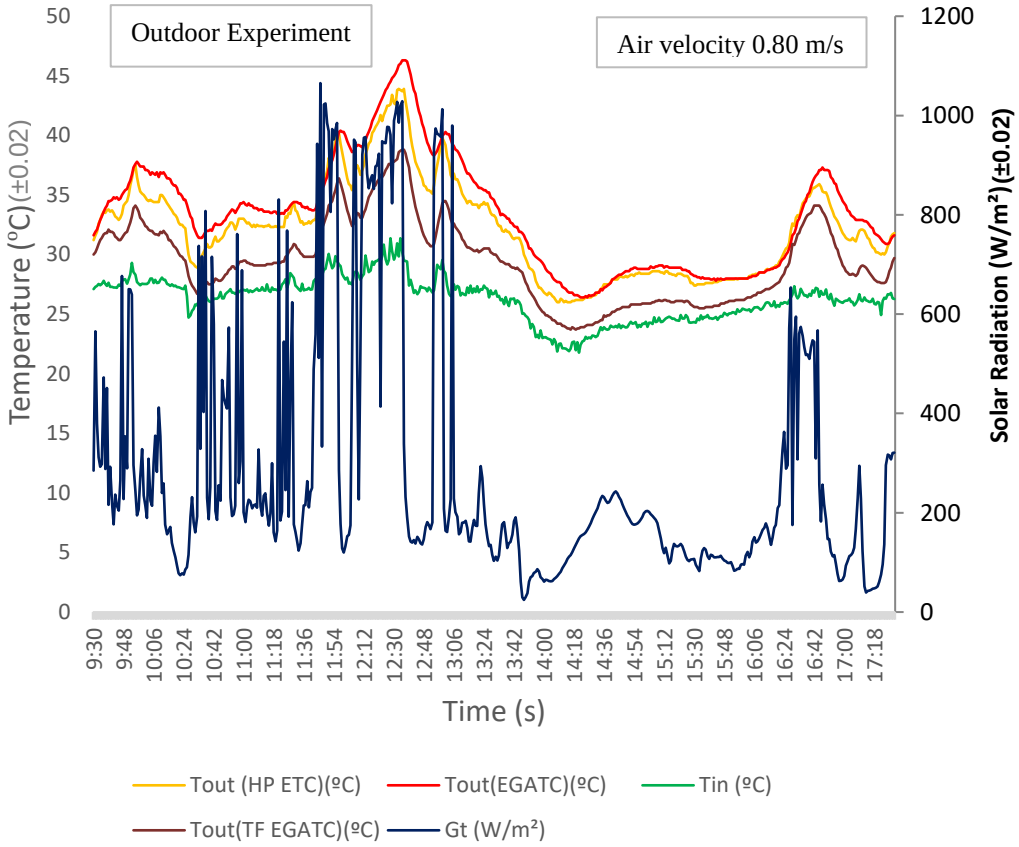

Figure 4.11: The outlet temperature differences between HP ETC, double-layer vacuum EGATC and single layer thin film selective surface coating inner glass tube EGATC

During high solar radiation, 1028.7 W/m^2 at 12:35 am, the outlet temperature differences for HP ETC were recorded at 43.7°C, double layer vacuum EGATC was recorded at 46.3°C and single layer thin film selective surface coating inner glass tube EGATC was recorded at 38.8°C. Lastly, at 16:59 pm, during the diffused solar radiation condition, 65.8 W/m^{2,} the reading of outlet temperature differences for HP ETC, double layer vacuum EGATC and single layer thin film selective surface coating inner glass tube EGATC were recorded at 31.8°C, 34.5°C and 29.1°C respectively.

From the analysis, the global solar radiation, Gt hour per day, was 2.25 hours, and air velocity, V, was 0.8 m/s. For HP ETC, double-layer vacuum EGATC and single-layer thin film selective surface coating inner glass tube EGATC, the total daily collected energy from global solar radiation, E($GtAc$), was 232.86 kJ. The total daily energy gain produced by solar thermal collector E ($Q\,Collector$) for HP ETC was 72.82 kJ, 90.57 kJ for double layer vacuum EGATC and 65.02 kJ for single layer thin film selective surface coating inner glass tube EGATC. The efficiency of the collector obtained for HP ETC, double layer vacuum EGATC and single layer thin film selective surface coating inner glass tube EGATC was 31.3%, 38.9%, and 27.9%, respectively. The daily stored energy by the thermal absorber, $QStore$ by HP ETC was 3.67 kJ, double layer vacuum EGATC was 4.46 kJ, and on the other hand, for single layer thin film selective surface coating inner glass tube EGATC was 2.39 kJ. For HP ETC, double-layer vacuum EGATC and single layer thin film selective surface coating inner glass tube EGATC, the efficiency of the collector with storage ability obtained were 32.9%, 40.8%, and 29.0 %, respectively.

The results proved that double-layer vacuum EGATC was better than HP ETC in terms of outlet temperature differences. Meanwhile, the single-layer thin film selective surface coating inner glass tube EGATC was the worst among those three. Although the thin film selective surface coating features 3 tiers of coating material (ALN-SS/Cu) with low emission and high absorption properties, it does not work well without the vacuum pocket's existence. It cannot minimize thermal losses by conduction and convection.

4.9 PERFORMANCE EXPERIMENTAL RESULT

The results showed the inlet and outlet temperature profile for both HP ETC and EGATC air heaters during the whole duration of the experiment on Day 1 (Tuesday, November 2019). From **Figure 4.12**, the inconsistent solar radiation profile during the day of experimental work was cloudy, with the radiation value fluctuating between 35.6 – 798.9 W/m^2. However, the performance was quite notable, where the difference between the outlet temperature for both collectors and ambiance during the initial stage of an experiment was 8.2 ^{o}C and 10.7 ^{o}C for HP ETC and EGATC, respectively.

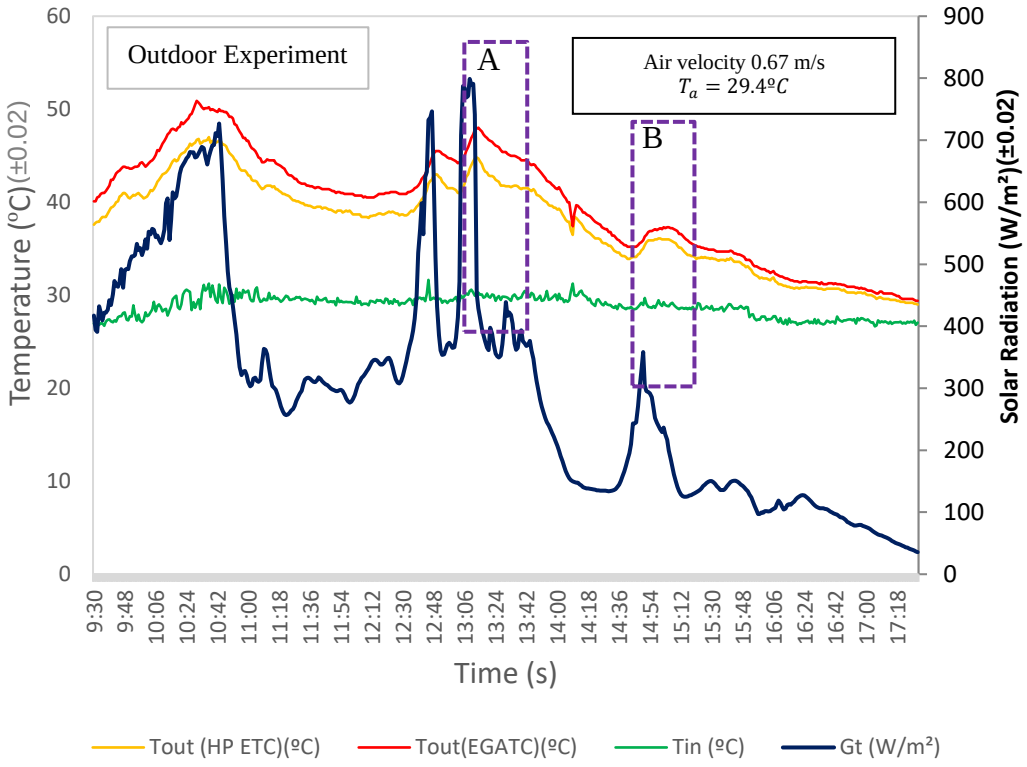

Figure 4.12: Outlet temperature differences between HP ETC air heater and EGATC air heater on Day 1

As the experiment continues, the solar radiation's heavy fluctuation affects the performance of both collectors. The maximum outlet temperature of the day was attained at 10.22 a.m. with solar radiation of 673.2 W/m2. The outlet temperature rises

to 46.7 ºC for HP ETC and 50.9 ºC for EGATC. However, due to the thermal buffer effect, direct heat conversion characteristics via EGATC influences the outlet temperature profile to be more consistent compared to the one with HP ETC. This can be seen by the discharge rate of each air heater outlet temperature profile as labeled by Area A and Area B. As per Area A, the temperature discharge rate of HP ETC and EGATC were -0.0012 ºC/s and -0.0011 ºC/s, respectively, with solar radiation dropping from 798.9 W/m^2 to 393.2 W/m^2. Meanwhile, as for Area B, at 227.7 W/m^{2,} radiation drop produced a temperature discharge rate of -0.0005 ºC/s and -0.0003 ºC/s for HP ETC and EGATC, respectively.

The results of the inlet and outlet temperature profile for both HP ETC and EGATC on Day 2 (Wednesday, November 2019) are shown in **Figure 4.13**. The inconsistent solar radiation profile during the day of experimental work was rainy and cloudy, with the radiation value fluctuating between 74.4 – 824.9 W/m^2.

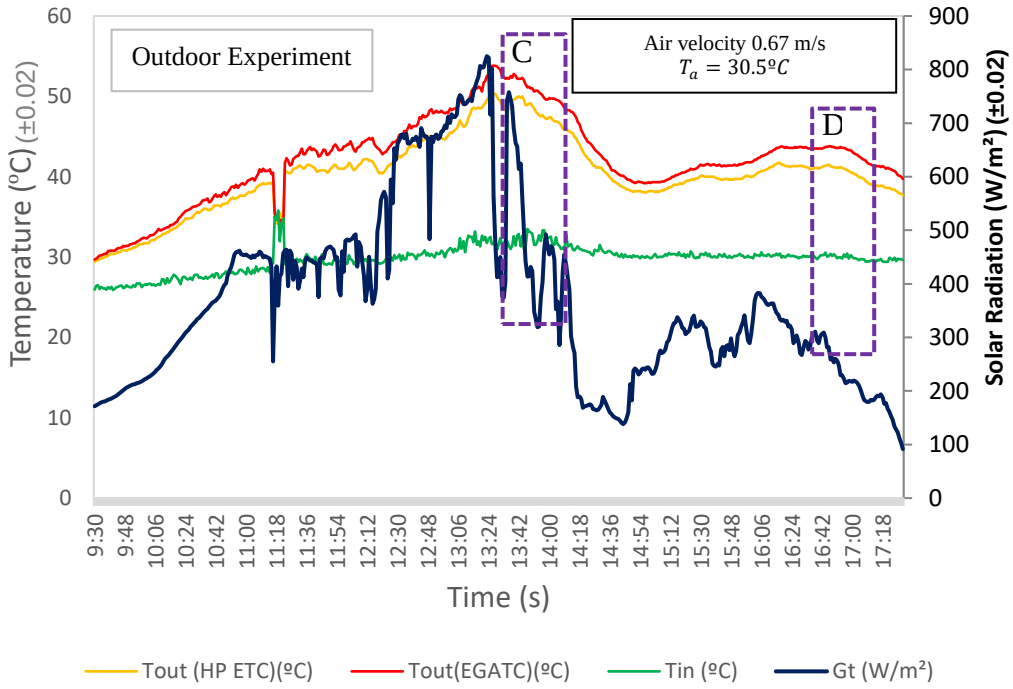

Figure 4.13: Outlet temperature differences between HP ETC air heater and EGATC air heater on Day 2

However, the performance of both collectors was quite notable, where the difference between the outlet temperature and ambiance during the initial stage of an experiment were -1.1 ^{o}C and -0.8 ^{o}C for HP ETC and EGATC, respectively. The maximum outlet temperature of the day was attained at 13.28 p.m. with solar radiation of 469.3 W/m^2. The outlet temperatures were maximum at 50.3 ^{o}C for HP ETC and 53.8 ^{o}C for EGATC.

As the experiment continues, the solar radiation's heavy fluctuation affects the performance of both collectors. However, direct heat conversion characteristics via EGATC influence the outlet temperature profile to be more consistent as compared to the one with HP ETC due to the thermal buffer effect. This can be seen by the temperature discharge rate of each air dryer's outlet temperature profile as labeled by Area C and Area D. As per Area C, the discharge rate of HP ETC and EGATC were -0.0037 ^{o}C/s and -0.0010 ^{o}C/s, respectively with solar radiation drop 505.8 W/m^2, from 825.0 W/m^2 to 319.2 W/m^2. Meanwhile, as for Area D, at 78.5 W/m^{2,} radiation drop with solar radiation from 293.0 W/m^2 to 214.5 W/m^2 producing temperature discharge rate of -0.0002 ^{o}C/s and -0.0001 ^{o}C/s for HP ETC and EGATC, respectively.

Based on **Figure 4.14,** the results show the inlet and outlet temperature profile for both HP ETC and EGATC on Day 3 (Thursday, November 2019). The radiation value was inconsistent and fluctuated between 0 – 969.3 W/m^2 due to rainy day. The difference between the outlet temperature for both collectors and ambiance during the initial stage of an experiment was 3.2 ^{o}C and 3.9 ^{o}C for HP ETC and EGATC, respectively. The maximum outlet temperature for the day was attained at 11.29 a.m. with solar radiation 420.6 W/m^2. The maximum outlet temperatures were 46.9 ^{o}C for HP ETC and 49.2 ^{o}C for EGATC. After a while, the diffusing solar radiation for a long duration affects both collectors' performance.

However, EGATC influenced the outlet temperature profile more consistently through its direct heat conversion characteristic compared with HP ETC. The thermal buffer effect can be seen by the discharge rate of each air dryer's outlet temperature

profile as labeled by Area E and Area F. As per Area E, the temperature discharge rates of HP ETC and EGATC were -0.0146 ^{o}C/s and -0.0084 ^{o}C/s, respectively, with a solar radiation drop of 561.9 W/m^2. Meanwhile, for Area F, solar radiation dropped from 147.1 W/m^2 to 14.9 W/m^{2,} producing temperature discharge rates of -0.0006 ^{o}C/s and -0.0005 ^{o}C/s for HP ETC and EGATC, respectively.

Therefore, EGATC provided a better energy buffer by increasing the thermal absorber wall thickness.

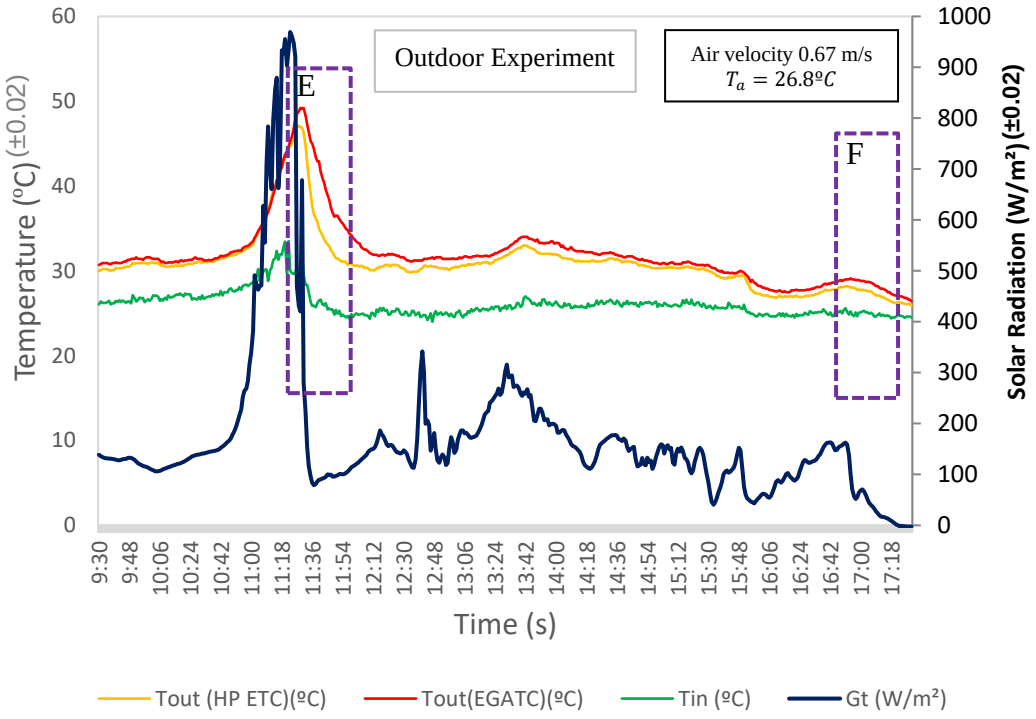

Figure 4.14: Outlet temperature differences between HP ETC air heater and EGATC air heater on Day 3

Based on the outlet temperature differences between the HP ETC air heater and the EGATC air heater each day, EGATC performance was better at the initial outlet temperature with a slightly higher temperature than the HP ETC. The initial outlet temperature was recorded early morning when the ambient humidity was high at low solar radiation. The low cumulative heat gains inside the evacuated glass were able to increase the temperature of the EGATC thermal absorber but failed to do the same for HP ETC. As HP ETC working principle, the working liquid inside the heat pipe must

be heated to a boiling temperature to allow it to function properly. The outlet temperature differences between the HP ETC air heater and EGATC air heater on each day are shown in **Table 4.8**.

Table 4.8: The outlet temperature differences between HP ETC air heater and EGATC air heater on each day

Day	Parameter	HP ETC	EGATC
1	Initial outlet temperature, ^{o}C (±0.02)	37.6	40.1
	Outlet temperature different, ^{o}C (to attain towards T_a = 29.4^{o}C) (±0.02)	8.2	10.7
	Solar radiation, W/m^2 (±0.02)	416.9	
2	Initial outlet temperature, ^{o}C (±0.02)	29.4	29.7
	Outlet temperature different, ^{o}C (to attain towards T_a = 30.5^{o}C) (±0.02)	-1.1	-0.8
	Solar radiation, W/m^2 (±0.02)	171.3	
3	Initial outlet temperature, ^{o}C (±0.02)	30.0	30.7
	Outlet temperature different, ^{o}C (to attain towards T_a = 26.8^{o}C) (±0.02)	3.2	3.9
	Solar radiation, W/m^2 (±0.02)	138.6	

While, for the maximum outlet temperature differences between the HP ETC air heater and EGATC air heater on each day, EGATC attained a slightly higher temperature compared to HP ETC at the medium range of solar radiation. The maximum outlet temperature produced by EGATC is also good enough to ensure the perfect drying of agricultural products. **Table 4.9** shows the maximum outlet temperature differences between the HP ETC air heater and the EGATC air heater on each experiment day.

Table 4.9: The maximum outlet temperature differences between HP ETC air heater and EGATC air heater on each day

Day	Parameter	HP ETC	EGATC
1	Maximum outlet temperature, ^{o}C (±0.02)	46.7	50.9
	Outlet temperature different, ^{o}C (±0.02)	4.2	
	Solar radiation, W/m^2 (±0.02)	673.2	
	Time	10.22 a.m.	
2	Maximum outlet temperature, ^{o}C (±0.02)	50.3	53.8
	Outlet temperature different, ^{o}C (±0.02)	3.5	

	Solar radiation, W/m^2 (±0.02)	469.3	
	Time	13.28 p.m.	
3	Maximum outlet temperature, ^{o}C (±0.02)	46.9	49.2
	Outlet temperature different, ^{o}C (±0.02)	2.3	
	Solar radiation, W/m^2 (±0.02)	420.6	
	Time	11.29 a.m.	

Table 4.10 shows the calculated values of the solar radiation range and temperature discharge rate obtained from the experimental run. Based on the results and observation, EGATC produces a small value of temperature discharge rate compared with HP ETC when the solar radiation drops. In other words, EGATC has been releasing a small amount of temperature in a second. The '-'ve sign of the temperature discharge rate represents the direction of the graph gradient.

Table 4.10: The calculated values of solar radiation range and temperature discharge rate obtained from the experimental runs

Area	Parameters	HP ETC	EGATC
A	Solar radiation range, W/m^2 (±0.02)	798.9 – 393.2	
	Solar radiation drops, W/m^2(±0.02)	405.7	
	Temperature discharge rate, ^{o}C/s (±0.00002)	-0.0012	-0.0011
B	Solar radiation range, W/m^2 (±0.02)	358.4 – 130.7	
	Solar radiation drops, W/m^2 (±0.02)	227.7	
	Temperature discharge rate, ^{o}C/s (±0.00002)	-0.0005	-0.0003
C	Solar radiation range, W/m^2 (±0.02)	825.0 – 319.2	
	Solar radiation drops, W/m^2 (±0.02)	505.8	
	Temperature discharge rate, ^{o}C/s (±0.00002)	-0.0037	-0.0010
D	Solar radiation range, W/m^2 (±0.02)	293.0 – 214.5	
	Solar radiation drops, W/m^2 (±0.02)	78.5	
	Temperature discharge rate, ^{o}C/s (±0.00002)	-0.0002	-0.0001
E	Solar radiation range, W/m^2 (±0.02)	677.9 – 116.0	
	Solar radiation drops, W/m^2 (±0.02)	561.9	
	Temperature discharge rate, ^{o}C/s (±0.00002)	-0.0146	-0.0084
F	Solar radiation range, W/m^2 (±0.02)	147.1 – 14.9	
	Solar radiation drops, W/m^2 (±0.02)	132.2	
	Temperature discharge rate, ^{o}C/s (±0.00002)	-0.0006	-0.0005

The thermal buffer effect is very useful for air heating applications in conditions with intermittent solar radiation and during the unavailability of solar radiation. **Figure 4.15** shows the daily performance between the HP ETC air heater and EGATC air heater. This outdoor experiment was conducted from 9.30 a.m. to 4.30 p.m. with an average wind speed of 0.28 m/s. In the beginning, the outlet temperature for both the HP ETC air heater and EGATC air heater was 33.6ºC and 34.6ºC, respectively, with solar radiation of 431.0 W/m^2. Then, the solar radiation fluctuated between 99.9 W/m2 to 838.9 W/m2 until 11.00 am before it continued decreasing until the afternoon. At 1.11 pm, those collectors were covered-up to create diffuse solar radiation conditions.

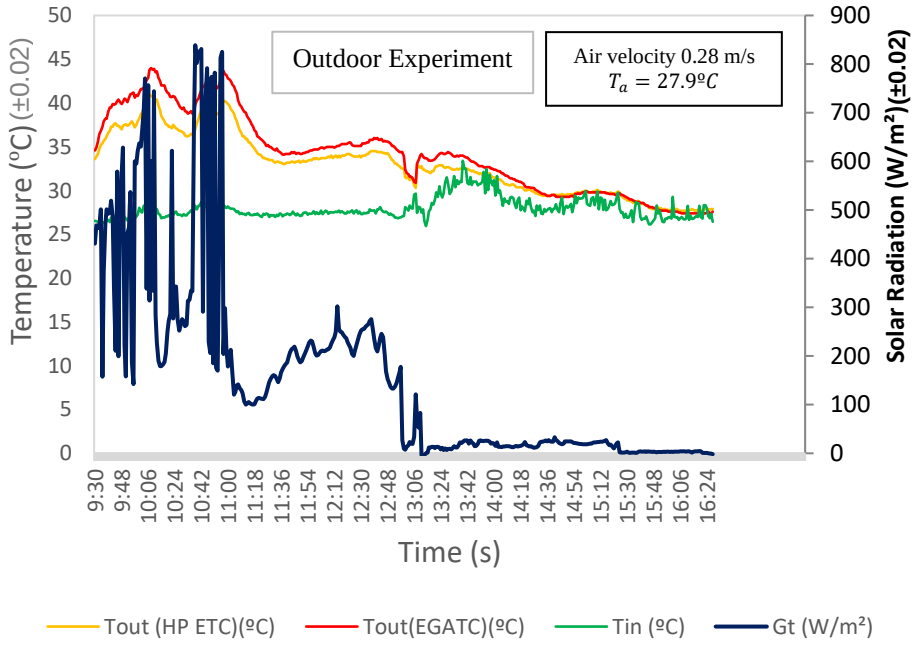

Figure 4.15: Daily performance with total energy storage between HP ETC air heater and EGATC air heater

During that time, the outlet temperature for both HP ETC and EGATC were 32.8ºC and 34.2ºC, respectively. After 30 minutes, the outlet temperature for both collectors decreased to 32.5ºC for HP ETC and 33.8ºC for EGATC. In order to attain ambient temperature, $T_a = 27.9ºC$, HP ETC outlet temperature needs 126 minutes while EGATC outlet temperature needs 129 minutes.

The thermal absorption response time between the HP ETC air heater and EGATC is shown in **Figure 4.16**. This outdoor experiment was done for a duration of 30 minutes. The first 15 minutes was the charging period with an average solar radiation of 570.9 W/$m^{2,}$ and for another 15 minutes, the solar radiation was removed to the null value to create the discharging period.

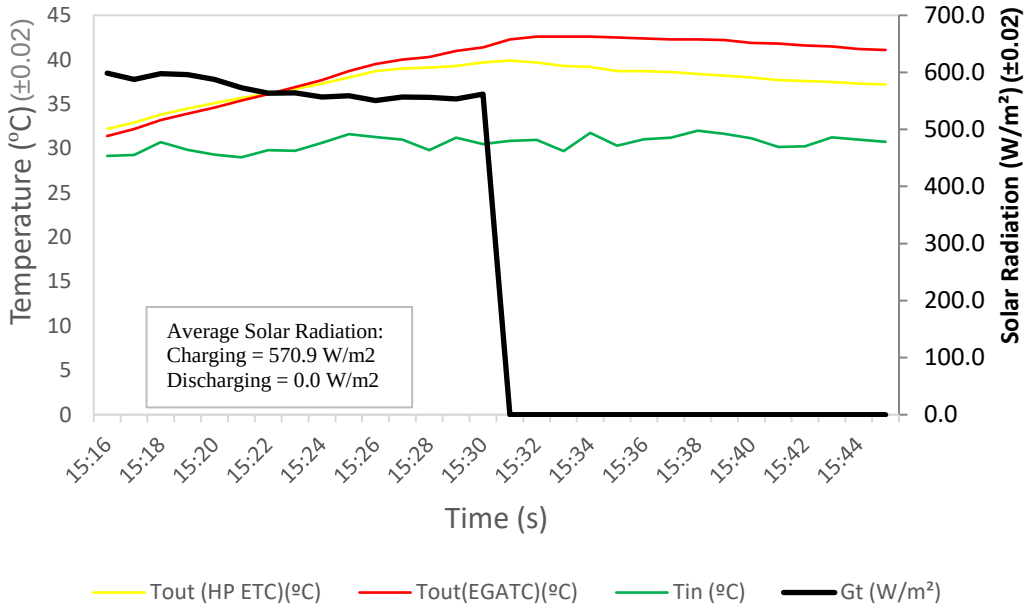

Figure 4.16: Thermal absorption response time for 15 minutes between HP ETC air heater and EGATC air heater while charging and discharging period

Since the initial outlet temperature was recorded in the evening, the ambient humidity was low, with an intermediate solar radiation range. The intermediate solar radiation created cumulative heat gain inside the evacuated glass and heated the working liquid inside the heat pipe. The working liquid experienced the phase change from liquid to superheated vapor, thus condensing to the heat pipe condenser located on the top of the heat pipe. The heat pipe condenser produced the high temperature (superheated temperature) and was attached to the plate as a heat transfer medium to the outlet air.

Therefore, HP ETC's initial outlet temperature (32.2ºC) was slightly higher than EGATC (31.4ºC) in the evening. As the experiment continued, after 8 minutes, the EGATC outlet temperature increased to 36.9 ºC compared to the HP ETC, 36.7ºC. At minute 16, the discharging condition was created by covering up both solar thermal collectors. EGATC outlet temperature remained slightly higher than HP ETC, which were 42.3ºC and 39.9ºC, respectively. The polar continued until the end of the experiment at minute 30. The outlet temperatures for both EGATC and HP ETC were 41.1ºC and 37.2ºC, respectively.

4.9.1 Performance and Efficiency

For assumption, the system in this study was considered a closed system and did not involve any velocity and elevation change. Hence, the heat transfer rate of the collector was expressed by Ahmad Fudholi et al. (2015) and Duffie & Beckman (2013):

$$\dot{Q}_{Collector} = \rho A v C_{p(air)}(T_o - T_i) \tag{4.3}$$

Equation 4.3 was used to convert energy from solar radiation into heat to increase the collector's outlet temperature by referring to the inlet temperature. While **Equation 4.4** was used to calculate energy from solar radiation that was converted into energy storage in the thermal absorber by referring to instantaneous energy accumulation for each second. The heat transfer rate of the thermal absorber storage was expressed by Ahmad Fudholi et al. (2015) and Duffie & Beckman (2013):

$$Q_{Store} = \frac{m_{ab} C_{p(ab)}(T_2 - T_1)}{t_2 - t_1} \tag{4.4}$$

Hence, the efficiency of the collector and storage was expressed as:

$$\eta_{Collector+Storage} = \frac{\dot{Q}_{Collector} + Q_{Store}}{G_t A_c} \times 100\% \quad (4.5)$$

By resolving **Equation 4.3** and **Equation 4.1** into **Equation 4.5**, the efficiency of the collector and storage was expressed as:

$$\eta_{Collector+Storage} = \frac{\rho A v C_{p(air)}(T_o - T_i) + \left(\frac{m_{ab} C_{p(ab)}(T_2 - T_1)}{t_2 - t_1}\right)}{G_t A_c} \times 100\% \quad (4.6)$$

Where

ρ = Density of air (kg/m^3)

A = Area of inlet duct (m^2)

v = Velocity of air at inlet duct (*m*/*s*)

$C_{p(air)}$ = Specific heat of air (kJ/kgK)

T_o = Air outlet temperature (K)

T_i = Air inlet temperature (K)

G_t = Global solar radiation ($Watt/m^2$)

A_c = area of collector (m^2)

m_{ab} = mass of thermal absorber (kg)

$C_{p(ab)}$ = Specific heat of thermal absorber (kJ/kgK)

T_2 = Temperature of thermal absorber after heat gain (K)

T_1 = Temperature of thermal absorber before heat gain (K)

t_2 = Time after heat gain (s)

t_1 = Time before heat gain (s)

As for reference, the total maximum heat storage capability obtained from **Equation 4.4** for EGATC was 38.22 kJ at solar radiation 1025.9 W/m^2. This outdoor experiment was done under real exposure to solar radiation with constant airflow from

09.30 a.m. to 5.30 p.m. Based on the efficiency evaluation analysis, EGATC is capable of storing larger heat compared to HP ETC, as shown in **Table 4.11**. The data for the analysis was obtained from the outdoor experiment on outlet temperature differences between the HP ETC air heater and the EGATC air heater. The total daily collected energy from global solar radiation (G_t) by the solar thermal collector, partially was converted into heat, which increases the outlet temperature, and at the same time, it was used as heat storage by the thermal absorber.

Table 4.11: The efficiency analysis obtained from the outdoor experiment

	DAY 1		**DAY 2**		**DAY3**	
	G_t hour/day = 2.39 hour (±0.002)		**G_t hour/day = 2.98 hour (±0.002)**		**G_t hour/day = 1.39 hour (±0.002)**	
	Avarage Airflow, V = 0.67 m/s (±0.002)		**Avarage Airflow, V = 0.67 m/s (±0.002)**		**Avarage Airflow, V = 0.67 m/s (±0.002)**	
	EGATC	**HP ETC**	**EGATC**	**HP ETC**	**EGATC**	**HP ETC**
E (**$G_t A_c$)** (kJ) (±0.002)	247.59	247.59	308.81	308.81	143.86	143.86
E ($\dot{Q}_{Collector}$) (kJ) (±0.002)	130.76	104.52	148.84	124.06	70.03	57.93
Efficiency (Collector) (%)(±0.02)	52.8	42.2	48.2	40.2	48.7	40.3
Q_{Store} (Daily) (kJ) (±0.002)	2.06	1.29	7.35	4.39	1.60	1.13
Efficiency (Collector + Storage) (%)(±0.02)	53.6	42.7	50.6	41.6	49.8	41.1

As Day 1 with global solar radiation, G_t hour per day was 2.39 hours with average airflow, V was 0.67 m/s, and total daily collected energy from global solar radiation (G_t) for an area of the collector (A_c) = 0.0288m^2, E($G_t A_c$) were 247.59 kJ for both EGATC and HP ETC collectors. Total daily energy gain produced by solar thermal collector E ($\dot{Q}_{Collector}$) for EGATC were 130.76 kJ and 104.52 kJ for HP ETC. By implementing **Equation 4.5**, the collector efficiency was 52.8% and 42.2% for EGATC and HP ETC, respectively. In addition, daily energy stored by the thermal absorber, Q_{Store} by EGATC was 2.06 kJ whilst by HP ETC was 1.29 kJ. From **Equation 4.6**, the collector's efficiency with storage ability was 53.6% and 42.7% for both EGATC and HP ETC, respectively.

On Day 2, the global solar radiation, G_t hour per day was 2.98 hours, and the average air flow, V, was 0.67 m/s. For both EGATC and HP ETC, total daily collected energy from global solar radiation, E($G_t A_c$) was 308.81 kJ. Total daily energy gain produced by solar thermal collector E ($\dot{Q}_{Collector}$) for EGATC were 148.84 kJ and 124.06 kJ for HP ETC. The collector's efficiency obtained for EGATC, and HP ETC was 48.2% and 40.2%, respectively. The daily stored energy by the thermal absorber, Q_{Store} by EGATC was 7.35 kJ; on the other hand, by HP ETC was 4.39 kJ. For both EGATC and HP ETC, the efficiency of the collector with storage ability obtained was 50.6% and 41.6%, respectively.

As of Day 3, the total daily collected energy from global solar radiation, E($G_t A_c$) was 143.86 kJ for both EGATC and HP ETC collectors with global solar radiation, G_t hour per day was 1.39 hours, and the average airflow, V was 0.67 m/s. Total daily energy gain produced by solar thermal collector E ($\dot{Q}_{Collector}$) for EGATC were 70.03 kJ and 57.93 kJ for HP ETC. The obtained efficiency of the solar collector was 48.7% for EGATC and 40.3% for HP ETC. The daily stored energy by the thermal absorber, Q_{Store} by EGATC and HP ETC were 1.60 kJ and 1.123 kJ, respectively. The collector's efficiency with storage ability for both EGATC and HP ETC were 49.8% and 41.1%, respectively.

4.10 MATHEMATICAL MODEL VALIDATION WITH EXPERIMENTAL VALUE

The results of the energy conservation equation (3.6-3.13) obtained from Microsoft Excel® software are stated in **Table 4.12**. The total difference in the percentage of 4.7% shows the model at each node was valid.

Table 4.12: The results of energy conservation equation

Node	Sum of energy (Watt)		Different (Watt)	Percentage (%)
	In	Out		
Evacuated glass	590.69	564.23	26.46	4.5
Outer absorber	7009.19	7482.92	473.73	6.3
Inner absorber	2043.80	2073.98	30.18	1.5
Working fluid	0.0775	0.0799	0.0024	3.0
Total	9641.75	10121.20	479.45	4.7

From **Figure 4.17**, it can be visibly seen that the efficiency of the collector increases with temperature differences (T_{out}-T_{in}) along the experiment for those mathematical modeling and experimental model. The efficiencies of all types increased during the charging period with the same experimental arrangement, i.e., 1mm thickness of non-coated absorber, solar radiation = 700 W/m^2, wind speed = 0.9 m/s @ 4.6v for both 0 Fin EGATC and 3 Fins EGATC. The results obtained show that the collector and storage efficiency for 0 Fin EGATC and 3 Fins EGATC was 71.2% and 71.0%, respectively.

It can be clearly seen that the efficiency was dependent on the number of fins. The more fins affect the lower the collector and storage efficiency. The findings were similar to Razak et al. (2016). They proposed that longitudinal fins attached inside the respective double pass solar air collector design as the performance lowering factor, as higher heat loss has occurred at the fins.

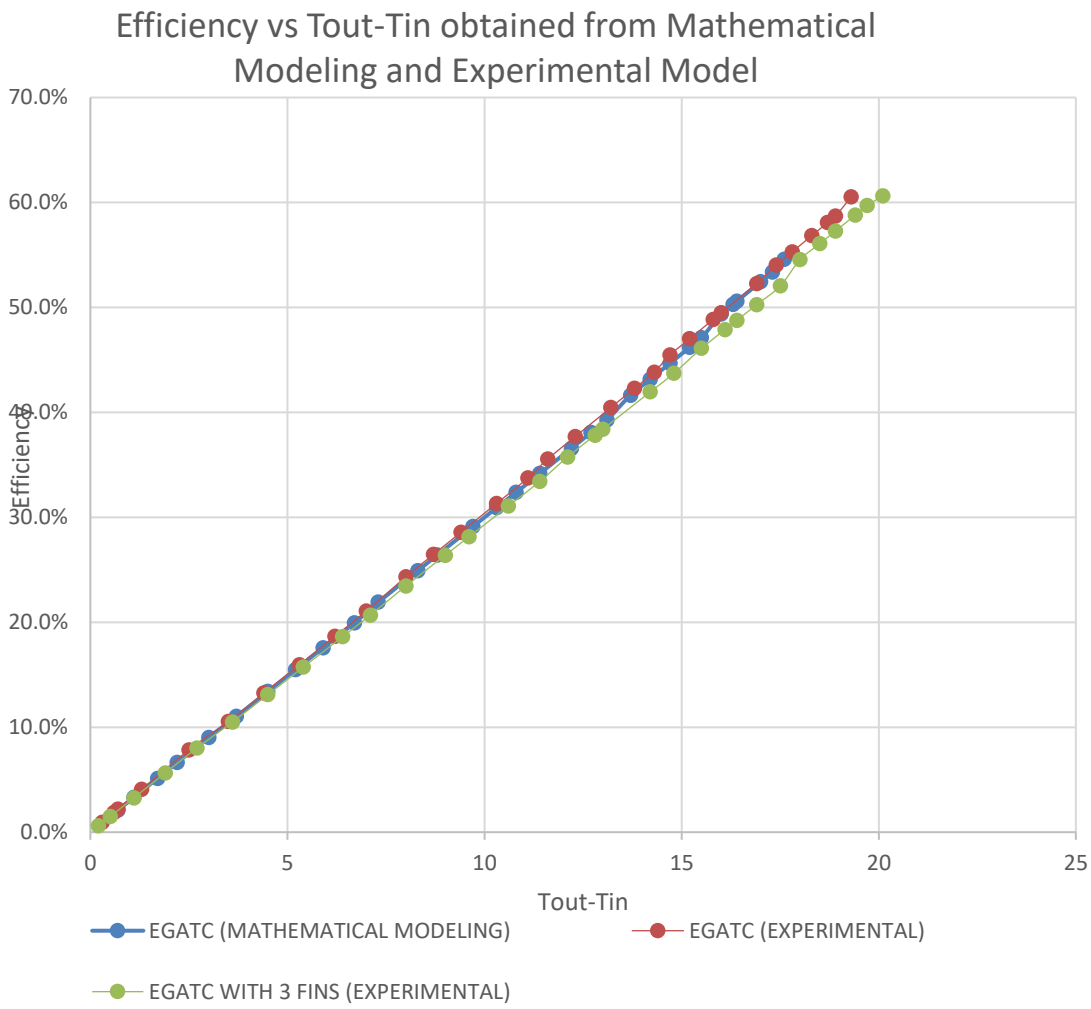

Figure 4.17: Efficiency vs Tout-Tin graph obtained from Mathematical Modeling and Experimental Model

On the other hand, **Table 4.13** shows the results obtained to validate the mathematical modeling with the experimental model. The collector efficiency for both mathematical modeling and experimental model were 30.5% and 33.1%, respectively. However, the collector with storage efficiency was 68.7% and 71.2% for those mathematical modeling and experimental model. Despite the fact that the error of collector efficiency and collector with storage efficiency between those mathematical modeling and EGATC experimental model were 7.9% and 3.5%, respectively. It was found that both theoretical and experimental results were in good agreement.

Table 4.13: The results obtained from algorithm through Microsoft Excel® software

Description	EGATC (MATHEMATICAL MODELING)	EGATC (EXPERIMENTAL)	EGATC WITH 3 FINS (EXPERIMENTAL)
Experiment details	Heat Transfer Experiment at 01/04/2020; 10:12 (1mm NC absorber, 0 Fin EGATC, S_R = 700 W/m^2, Wind Speed = 0.9 m/s @ 4.6v)	Experiment No. 11 at 12/11/2020; 13:55 (1mm NC absorber, 0 Fin EGATC, S_R = 700 W/m^2, Wind Speed = 0.9 m/s @ 4.6v)	Experiment No. 15 at 16/11/2020 (1mm NC absorber, 3 Fin EGATC, SR = 700 W/m^2, Wind Speed = 0.9 m/s @ 4.6v)
G_t hour/day	0.33	0.32	0.33
E(G_tA_c) (kJ)	33882.62	33262.27	34536.96
E ($\dot{Q}_{collector}$) (kJ)	10337.88	11006.94	11416.19
Efficiency (Collector) (%)	30.5	33.1	33.1
Q store (Daily) (kJ)	12942.97	12671.36	13099.66
Efficiency (Collector + storage) (%)	68.7	71.2	71.0

4.11 TECHNOECONOMICS EVALUATION OF EVACUATED GLASS-THERMAL ABSORBER TUBE COLLECTOR (EGATC)

In economics evaluation, the design itself was the main factor affecting the cost. This is because introducing new inventions was difficult in this area of study due to the cost constraint among the particular part. Introducing new technology in solar thermal collectors needs to deal with economic evaluations as it presents advantages. In addition, the economic feasibility will determine whether the product will be successful in the marketplace.

However, it is worth considering that what the market considers economically unprofitable today may improve after a few years. These considerations form the basis

of research work in the past decade, which could have a positive impact on the development of flat thermal collectors and could become sophisticated in the coming years (Colangelo et al., 2016). Thermal collectors usually indicate more than half of the total cost in solar thermal application systems (A. Fudholi et al., 2011). Therefore, it is important to have collectors with good efficiency as well as cost-effective for long -term application. The economic evaluation for this work focused on the solar collectors and thermal absorbers only, as the other components used in the experiments were for experimental purposes.

4.11.1 EGATC Cost Projection

The cost of thermal absorber material for one set of EGATC was RM 57.50, and if the evacuated glass was included, the total cost would amount to RM 110.95. The labour cost varies depending on the complexity of the thermal absorber design and the types of materials used. Klein et al. (1976) introduced the concept of solar savings. The difference between the conventional system and solar system utilized cost can be summarized as:

$$Solar\ savings = costs\ of\ conventional\ energy - costs\ of\ solar\ energy \tag{4.7}$$

In terms of cost comparison between HP ETC and EGATC for air heating applications, estimated savings that can be realized from using the solar thermal collector starting from the first-year operation was estimated at RM 0.51. That was equivalent to approximately 99.97 % savings than the cost of using HP ETC, which was significant in long term operation. The cost was calculated with the assumption that the cost for a total of 8 hours of effective operation every day was calculated with the low voltage industrial electrical tariff at RM0.38/kWh (TNB, 2020). Low energy saving obtained from the solar system was contributed by the low electrical

consumption, low maintenance cost, and minimal initial cost, which can be seen from the projected cost in **Table 4.14**.

Table 4.14: Cost projection of HP ETC and EGATC for air heating application at the first year of installation and cost-saving by solar energy

Description	**HP ETC**	**EGATC**
Power consumption, W	9.57	9.57
Operating hours, h	8	8
Hourly power consumption, kWh	76.56	76.56
Electricity price, RM/kWh	0.38	0.38
Cost for 1 day, RM	0.029	0.029
Cost for 1 year, RM	10.62	10.62
Maintenance cost per year, RM/year	50	50
Initial cost, RM	121.46	120.95
Total cost (first-year), RM	182.08	181.57
Cost savings, RM	0.51	
Saving rate, %	99.71	

The initial investment for a solar-operated system that an evacuated glass was needed for procuring the collector was estimated at approximately RM53.45 for 0.5m x 0.058m collector top surface area. This includes the collector's fabrication work, delivery cost, and workmanship. The HP ETC produces dry air solely using an aluminium plate as a heat exchanger system; thus, this contributes to the high cost of total operating cost. Using heat exchanger systems also leads to higher maintenance costs, as each model has their specially designed system. The maintenance of the EGATC is minimal, where the maintenance works involved were cleaning the collector cover from dust and foreign particles and direct current fan replacements. A cost comparison in terms of thermal absorber cost was made between different types of thermal absorbers, namely EGATC and HP ETC. The price fractions for each thermal absorber are outlined in **Table 4.15,** where the cost estimated was from material procurement and fabrication cost. The cheapest thermal absorber cost was EGATC, which cost RM 120.95, while HP ETC was RM 121.46. The price difference was prominent depending on the amount of material used for the thermal absorber and

difficulties in the fabrication process which explains why HP ETC was more costly than EGATC.

Table 4.15: Cost comparison for both thermal absorber, EGATC and HP ETC

	Components	Thermal absorber	
		EGATC	**HP ETC**
1	Raw material	Evacuated glass, SS pipe, PVC saddle	Evacuated glass, Copper heat pipe, Aluminium sheet
2	Evacuated glass top surface area dimension	0.5m x 0.058m	
3	Surface area (m^2)	$0.029m^2$	
4	Power produce by evacuated glass	9.57 watt	
5	Evacuated glass, Ø =58mm, L=500mm	RM 53.45	
6	Outer absorber (SS 304), Ø =38.5mm, t=1.0mm, L=550mm	RM 20.00	NA
7	Inner absorber (SS 304), Ø =12.7mm, t=1.0mm, L=615mm	RM 10.00	NA
8	PVC Saddle	RM 1.50	NA
9	D.C Ventilation Fan	RM3.00	NA
10	Insulation	RM1.00	NA
11	SS 304 Square Hollow, L = 50.8mm, W = 50.8mm, H = 63.5mm, t = 1mm	RM12.00	NA
12	SS 304 Plate, L = 60mm, W = 60mm, t = 1mm	RM6.00	NA
13	Monocrystalline Solar Panel, 10 watts, 12-volt	RM4.00	NA
14	Copper heat pipe	NA	RM 12.63
15	Cap to fix heat pipe	NA	RM 1.82
16	Aluminium sheet absorber	NA	RM 7.17
17	Plastic tube holder	NA	RM 3.39
18	Aluminium Plate,	NA	RM13.00
19	Workmanship	RM 10.00	RM 30.00
	Total	RM 120.95	RM 121.46

In terms of workmanship cost, EGATC was the cheapest due to its simple design that requires less material. Both EGATC and HP ETC indicate the same collector surface area (evacuated glass). The value is determined as follows:

The standard measurement for solar panel performance and efficiency refers to 1000 watt/m^2 solar radiation.

$$1m^2 = 1000W$$

The evacuated glass top surface area (flat perpendicular to solar radiation) was determined in Figure 5.18.

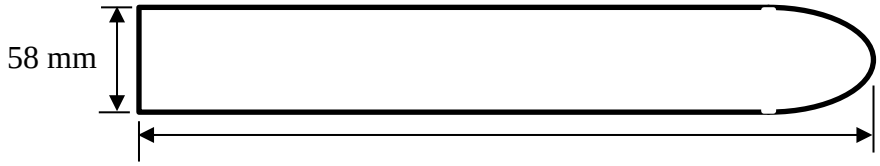

Figure 4.18: Evacuated glass measurement

$$A = P \times L \tag{4.8}$$
$$= 0.5m \times 0.058m$$
$$= 0.029\ m^2$$

Therefore, the power produced by the evacuated glass,

$$0.029m^2 = \frac{1000W}{1m^2} \times 0.029m^2$$
$$= 29W$$

The efficiency of EGATC was 51%, thus the power produced by the evacuated glass.

$$= 29W \times 51\%$$

$$= 14.79W$$

Hourly power consumption of 8 hours a day for a year,

$$= 14.79W \times 8\ hours$$
$$= 118.32\frac{Wh}{day}$$
$$= 0.11832\frac{kWh}{day}$$
$$= 0.11832\frac{kWh}{day} \times 365\ day$$
$$= 43.19\ kWh$$

Multiply by the electrical tariff for low voltage industrial by Tenaga Nasional Berhad (TNB), cost for 1 day;

$$= 0.11832\frac{kWh}{day} \times RM0.38\ kWh$$
$$= RM0.045/\text{ day}$$

Cost for 1 year;

$$= 43.19\ kWh \times RM0.38\ kWh$$
$$= RM16.41/\text{ year}$$

4.11.2 EGATC Cost Effectiveness

The costs involved in the fabrication of the EGATC are based on the cost of the thermal absorber materials and workmanship. **Table 4.15** shows the thermal absorber costs for both EGATC and HP ETC. The cost of EGATC is less cheap as it does not involve any complicated design like a heat exchanger plate. Meanwhile, the total materials cost

incurred without workmanship for the fabrication of the EGATC prototype is listed in **Appendix III: Table A3-3**.

The numerical cost-effectiveness calculations were implemented with the value for global solar radiation of 700 W/m^2 and average ambient temperature at 28 ºC. The solar thermal collector's effective operational time for a year was estimated at 300 days and 8 hours per day. The EGATC cost includes the cost of evacuated glass (RM53.45), the cost of thermal absorber materials (RM49.50), the cost of the ventilated chamber (RM15.00), the cost of insulation material (RM1.00), the cost of the solar panel (RM4.00), cost of electricity (RM 0.38 / kWh), cost of fabrication (RM10.00) and cost of maintenance was assumed at 40% of the initial cost. The interest rate was assumed at 10 % per year, and the collector's life duration was estimated at up to 10 years. **Table 4.16** show the details of the cost-effectiveness parameters.

Table 4.16: Cost-effectiveness parameters for EGATC

	Parameters	Value
1	Annual average radiation intensity	700 W/m^2
2	Operational time	Top = 300 days/ year, 8 hours/ day
3	Cost of evacuated glass	RM 53.45
4	Cost of thermal absorber materials	RM 49.50
5	Cost of ventilated chamber	RM15.00
6	Cost of insulation materials	RM1.00
7	Cost of solar Panel	RM4.00
8	Cost of electricity	RM0.38/ kWh
9	Cost of workmanship	RM10.00
10	Cost of maintenance	40% CI
11	Interest rate (i)	10%
12	Collector life time (n)	10 years

4.12 DISCUSSION

The investigation on thermal energy storage proved better thermal performance enhancement of EGATC for solar air heating applications by integrating several parameters. The analysis was carried out through an indoor experiment under artificial solar radiation. Based on the parameter experiment results and analysis, several discussions are presented, as follows:

i) Air velocity 0.9 m/s was identified as the ideal parameter since the wind speed was inversely proportional with the energy store, $Q_{Store,}$ in the meantime, it gained the highest outlet temperature at minutes 30. Solar intensity, the temperature of the working fluid, collector inclination, and tube aspect ratio affects the working fluid's natural circulation rate (Indra Budihardjo et al., 2007). A lower mass flow rate results in a high outlet temperature of the air (Vengadesan & Senthil, 2020). This is due to the lower mass flow rate, with the higher residential time of the flowing air around the surface of the thermal absorber increasing the heat transfer amount between them (Tyagi, Pandey, et al., 2012). On the other hand, at a higher mass flow rate, due to shorter residential time, a small amount of heat transfer between the flowing air and the thermal absorber led to a prolonged cooling time of the absorber, simultaneously increasing the thermal inertia of the thermal absorber.

ii) Zero (0) perforated fin was determined as the ideal parameter based on the better energy store, Q_{Store} value compared with seven (7) perforated fins. Seven (7) perforated fins produced turbulence air flow building up the outlet temperature (Raam Dheep & Sreekumar, 2020) at minute 30 but lowering the energy store, Q_{Store} value. Razak et al. (2016) proposed that longitudinal fins attached inside the respective double pass solar air collector design as the performance lowering factor, as higher heat loss has occurred at the fins. On the other side, zero (0) perforated fin with laminar air flow produced a slightly lower outlet temperature at minute 30 but gained a better energy

store, Q_{Store} value. The less differences in outlet temperature (0.3°C) showed no significant difference in the number of fins toward the shortened evacuated tube collector (ETC) design and in cases where the fins were placed inside an enclosed chamber with airflow.

iii) Non-coating outer absorber was recognized as the ideal parameter due to the better energy store, Q_{Store} value, and energy buffer compared with the Outer absorber's selective coating surface. The evacuated tube inner glass was coated by a one-sided refraction/reflection characteristic coating (thin film- selective surface coated material), allowing heat transfer via radiation and convection to the gap between the inner glass tube and the non-coating outer absorber. The reflection of the surface by a material of non-coating outer absorber itself, i.e., standard stainless steel finish, increases the reflection rate toward the inner glass of the evacuated tube hence increasing the energy store, Q_{Store} value, and energy buffer value (Arvind Kumar et al., 2020).

iv) 1mm outer absorber wall thickness was acknowledged as the ideal parameter on a high-temperature outlet compared to a 2mm outer absorber with a high energy store, $Q_{Store,}$ and energy buffer obtained. A thicker thermal absorber increases the mass, thus gaining high heat energy storage and energy buffer applications (X. Yang et al., 2020) but lowering the outlet temperature.

As per reporting of the evacuated tube parameter, it was discussed:

i) Double layer vacuum glass tube was promising as the best parameter compared with Double layer non-vacuum glass tube, Single layer transparent glass tube, and Single layer tin film glass tube showed better outlet temperature at minutes 30 and energy store, Q_{Store}. It was aligned with the theory that the vacuum pocket of evacuated glass eliminated the heat loss through convection and conduction between the absorber and ambiance; therefore, the collectors can operate at higher temperatures (Duffie & Beckman, 2013).

ii) The evacuated tube reacted much slower than the flat plate collector due to changes in intermittent solar radiation (Arvind Kumar et al., 2020). When the solar radiation value changed, the difference in response time was much smaller, affecting the thermal buffer and the outlet temperature.

The double pass flow experiment was conducted similarly with parameter experiment arrangement, device, and apparatus setup. Based on the experiment results, below are the discussions presented:

i) Zero (0) perforated fin with stainless-steel inner absorber EGATC showed better outlet temperature results than zero (0) fin with insulation material inner absorber. This stainless-steel inner absorber EGATC consists of conductive inner absorber material, which affected the mass of the total absorber and was set as a double pass arrangement. These were the main factors that initiated the initial heat convection inside the inner absorber before the airflow moved towards the outer absorber. According to Vengadesan & Senthil (2020), the metal matrix and packed bed porous thermal absorbers were recognized as an effective way to increase the air temperature distribution. It also acts as heat storage material as it stores maximum heat from the thermal absorber, and it can be efficiently transferred to the air due to the increased contact area between air and thermal absorber.

ii) The double pass airflow moved toward the outer absorber producing cumulative heat gained inside the outer absorber, thus doubling up the temperature at the outlet. At higher temperatures, the mass flow rate will be higher due to the higher density gradient (Ling et al., 2015). The types, mass, and arrangement of the conductive inner absorber material show that the double pass arrangement inside EGATC was significant. Vengadesan & Senthil (2020) concluded that implementing obstacles on the thermal absorber was the main factor in evolving the airflow path to increase the heat transfer area and time. An obstruction such as a perforated fin was

preferred over the plain as the airflow velocity increased over the holes. Hence, the secondary flow moved towards the main flow for complete fluid mixing.

Based on preliminary and performance experiments, the design proved to have better results compared to HP ETC on the outlet temperature and energy buffer storage. Both experiments were conducted as outdoor experiments by recording solar charging and discharging heat rates between EGATC and HP ETC as well as responding to weather changes such as diffused solar radiation during cloudy conditions. Based on both experimental works, the discussions are presented as follows:

i) EGATC had better performance in terms of air inlet and outlet temperature differences with high outlet temperature compared to HP ETC. The three (3) days of outdoor experimental results showed EGATC (Day 1: 50.9 ^{o}C, Day 2: 53.9 ^{o}C, Day 3: 49.2 ^{o}C) performed better with slightly higher temperatures at outlet temperature compared with HP ETC (Day 1: 46.7 ^{o}C, Day 2: 50.3 ^{o}C, Day 3: 46.9 ^{o}C). The outlet temperature results differed for each day between EGATC, and HP ETC was 4.2 ^{o}C, 3.6 ^{o}C, and 2.3 ^{o}C, respectively, with an average of 3.4 ^{o}C.

ii) EGATC had greater efficiency with better solar heat absorption to energy conversion response time and better thermal absorber heat storage, providing a consistent heat discharge rate compared to HP ETC. Based on the obtained results, EGATC (Day 1: 53.6%, Day 2: 50.6%, Day 3: 49.8%) had greater efficiency as compared to HP ETC (Day 1: 42.7%, Day 2: 41.6%, Day 3: 41.1%). The results of the efficiency difference for each day between EGATC and HP ETC were 10.9%, 9.0%, and 8.7%, respectively, with an average of 9.5%. Regarding energy buffer storage, EGATC had better energy storage compared to HP ETC at sudden weather changes such as cloudy. The outlet temperature of EGATC (42.3 ^{o}C) remained slightly higher compared to HP ETC (39.9 ^{o}C) at the beginning. The outlet temperature gradually dropped slower during discharging period until the end of the experiment after15 minutes, the outlet temperature was 41.1^{o}C

and 37.2ºC for both EGATC and HP ETC with temperature differences of 1.2ºC and 2.7ºC, respectively. EGATC demonstrated more design flexibility in terms of thickness and selected material of the thermal absorber. A thicker thermal absorber with high heat capacity material can be selected for higher heat energy storage applications.

iii) EGATC was designed to meet the requirement of Good Manufacturing Practice (GMP) for drying food, whereby a selective surface could be coated outside on a thermal absorber to avoid direct contact with drying material.

iv) The experiment was set up as a solar thermal collector in a flat orientation. The installation of EGATC does not require tilt angle and positioning of the northern and southern hemispheres compared to conventional HP ETC.

v) For air heating applications, EGATC provided directed heat conversion compared to HP ETC, which was the system that needed working liquid to be assembled with a water tank as an energy storage medium integrated with a heat exchanger to operate.

vi) EGATC had a broad surface area contact between the thermal absorber and air, which was the entire thermal absorber that could convert the heat directly, as compared to HP ETC, which relied on a heat pipe condenser with a small surface area. Heat transfer contact area and time duration were the significant factors in developing a higher temperature difference between the inlet and outlet (Vengadesan & Senthil, 2020).

4.13 CHAPTER SUMMARY

With the theoretical, experimental result and analysis support, it can be summarized that EGATC had greater efficiency in terms of heat storage capability, discharge rate, and thermal absorption response time as compared to HP ETC. Both HP ETC and EGATC use evacuated glass comprising outer glass and inner glass tubes. The outer glass tube (anti-reflection layer) with a vacuum pocket created the greenhouse effect, while the inner glass tube acted as a heat absorption material. The outer layer of the

inner glass tube (absorptance layer) was coated by the thin film-selective surface coating in order to absorb the heat from the vacuum pocket to the thermal absorber inside. The heat at the thermal absorber was then reflected by the inner layer of the inner glass tube (infrared-reflection layer), trapping and accumulating the heat inside. The heat is then transferred to the heat storage material, either aluminum fin for HP ETC or a thermal absorber for EGATC. The thermal absorber of EGATC also may act as a heat exchanger to transfer heat through convection towards the air.

EGATC can be introduced as the new design of solar thermal collectors to strengthen the conventional HP ETC. EGATC was positioned under the ETC section, which is in the same group as HP ETC, Direct-Flow ETC, and ETSC. EGATC was designed purposely for air heating applications while others, especially Direct-Flow ETC, were focusing on water heating, and HP ETC was targeting both water heating and air heating with the use of a heat exchanger. **Figure 4.19** shows the types of ETC and the location where EGATC is categorized.

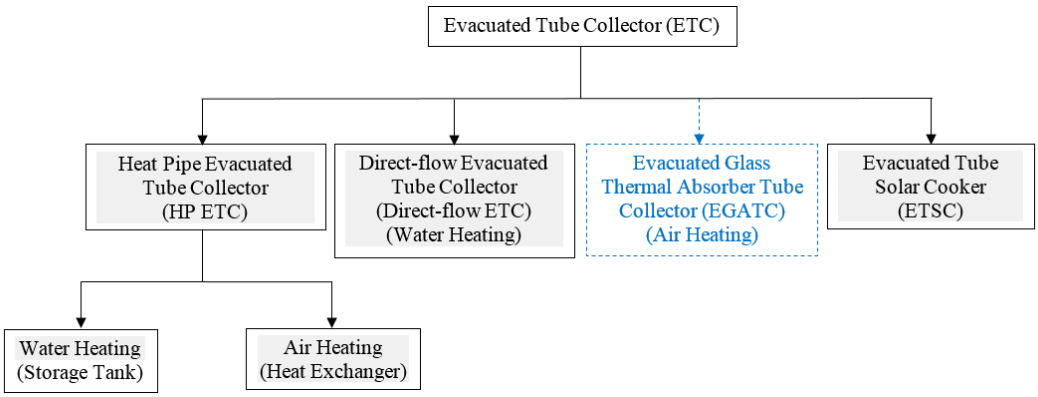

Figure 4.19: Types of Evacuated Tube Collector (ETC). Blue dotted box shows where EGATC was put in place

CHAPTER FIVE

CONCLUSION AND RECOMMENDATIONS

5.1 CONCLUSION

The existing design of the Heat-Pipe Evacuated Tube Collector (HP ETC) for water heating requires a storage tank, while an additional heat exchanger is required for air heating application which leads to extra spacing and cost. HP ETC also needs to be a tilt at the correct angle to optimize the system performance. Furthermore, the installation also needs to be positioned facing either south or north to ensure maximum energy absorption. These could lead to design limitations. The aim of this research was to design, develop and investigate the thermal performance of an Evacuated Glass-Thermal Absorber Tube Collector (EGATC) for air heating applications to overcome diffused radiation conditions. From this research, the following conclusions can be made:

i. The evacuated glass-thermal absorber tube collector (EGATC) was successfully designed and developed based on the processes involved, starting from the preliminary experiment, parameter experiment, and performance experiment. EGATC was developed from a conventional Evacuated Tube Collector (ETC), and the comparative results between HP ETC performance were evaluated. The three days of outdoor experiment results showed daily outlet temperature increased by 9.0%, 7.2%, and 4.9%, respectively, with an average of 7.0%. It was proven that EGATC had better performance in terms of the temperature difference and outlet temperature as compared to HP ETC. Meanwhile, the average efficiency for EGATC was 51.3% compared with HP ETC at 41.8%. In addition, the proper design of the EGATC inner absorber through the dryer chamber created a ventilated double pass flow, resulting in a

high cumulative outlet temperature. In order to minimize the thermal losses by convection and conduction, all the components involved were designed as a built-in system.

ii. The thermal absorber with double pass flow arrangement for EGATC was effectively improved based on the data obtained from the double pass flow experiment. The results show the outlet temperature of zero (0) perforated fin with stainless-steel inner absorber EGATC was 47.7°C compared with zero (0) fin with insulation material inner absorber 44.7°C after 30 minutes of charging with a difference of 6.3%. Regarding energy store, Q_{Store} , the stainless-steel inner absorber also had an advantage with 4.46kJ compared to the insulation material inner absorber of 4.40kJ with a 1.3% difference.

iii. The effect of parameters such as inner absorber surface area air contact (perforated fin), outer absorber selective coating surface, outer absorber wall thickness, double layer non-vacuum glass tube, single layer transparent outer glass tube, and single layer thin film inner glass tube on the performance of the EGATC was systematically investigated by parameter experiment. It has been conducted as per indoor setup under artificial solar radiation to measure the outlet temperature and energy storage rates. It was proven that the temperature outlet, energy store, and energy buffer could be enhanced with the combination of wind speed 0.9 m/s, zero (0) perforated fin, non-coating outer absorber, and 1mm outer absorber wall thickness. It was also reported that double-layer vacuum glass tubes promise better thermal performance enhancement compared with double-layer non vacuum glass tubes, single-layer transparent outer glass tubes, and single-layer thin film inner glass tubes.

iv. The mathematical equation related to each component of EGATC was analytically formulated based on the first law of thermodynamics. The combination of the developed equation forms a solar thermal collector model for the system. The total difference in the percentage of 4.7% shows the model

at each node was valid. The performance curves of the Evacuated Glass-Thermal Absorber Tube Collector (EGATC) for those 0 fins (mathematical modeling), 0 fin (experimental), and 3 fins (experimental) were obtained. The results show that the efficiency (collector + storage) is affected by the number of fins. The efficiency (collector + storage) was 68.7%, 71.2%, and 71.0%, respectively.

Hence, EGATC was designed purposely for air-heating applications used for drying in the food industry, while HP ETC was designed for more effective water-heating applications.

5.2 RECOMMENDATIONS

There are several more ideas that can be incorporated into this research and can be used in future work. The following are the future recommendations for this project:

1. The EGATC could be studied on the series and parallel design arrangement. The outer absorber could be designed in parallel, while the inner absorber could be designed in a series arrangement, resulting in series-parallel air flow.

2. The design of the EGATC system could be considered without a ventilation fan. The orientation must be in a slanting position to create natural convection. Thus, the performance could lead to an increase in thermal energy storage.

3. The thermal absorber, i.e., outer absorber and inner absorber, could be replaced with other related materials such as aluminium, copper, glass, or any combination of those materials such as aluminium and stainless-steel. Besides increasing performance and efficiency, indirectly will improve on its weight.

4. The outer absorber wall thickness design could be attached with fins to enhance the area of heat absorption.

5. The inner surface of the inner glass tube could be coated with selective surface coating. The coating may increase the performance of the absorption characteristic at the inner glass tube and simultaneously increase the internal thermal absorption of the thermal absorber.

6. Heat losses due to the dryer chamber top, bottom, and sidewall should be the main consideration while fabricating EGATC. The insulation should be properly designed with several layers to minimize heat losses.

7. The results obtained from the analysis also can be further verified by using statistical tools to help verify the data. Statistical analysis such as variance-one way (ANOVA) can be conducted to confirm that the data obtained was stable and the differences were not significant as far as the statistical method is concerned.

8. Although EGATC was designed purposely for air heating applications, the design also can be considered for solar cooker applications.

REFERENCES

Johnston A., Global Energy Review (2020). The impacts of the Covid-19 crisis on global energy demand and CO2 emissions. *International Energy Agency*.

Kocer, A., Atmaca, I., & Ertekin, C. (2015). A comparison of flat plate and evacuated tube solar collectors with f-chart method. *Journal of Thermal Science and Technology*, *35*(1), 77-86.

Abdul Majid, Z. A. (2011). Kajian Prestasi Sistem Pengering Pam Haba Terbantu Suria Dengan Pengumpul Suria Multifungsi. In *Universiti Kebangsaan Malaysia*.

Abdulmalek, S. H., Assadi, M. K., Al-Kayiem, H. H., & Gitan, A. A. (2018). Effect of Tube Diameter on the Design of Heat Exchanger in Solar Drying system. *IOP Conference Series: Materials Science and Engineering*. 328, 012028

Abhishek Kumar, Shreeram Barkhane. (2019). Selection of Material for Improving Heat Transfer Rate for Fins using CFD. *International Journal of Trend in Scientific Research and Development*.

Abo-Elfadl, S., Hassan, H., & El-Dosoky, M. F. (2020). Energy and exergy assessment of integrating reflectors on thermal energy storage of evacuated tube solar collector-heat pipe system. *Solar Energy*. 209, 470-484.

Abokersh, M. H., El-Morsi, M., Sharaf, O., & Abdelrahman, W. (2017). An experimental evaluation of direct flow evacuated tube solar collector integrated with phase change material. *Energy*. 139, 1111-1125

Abu-Hijleh, B. A. K. (2003a). Enhanced forced convection heat transfer from a cylinder using permeable fins. *Journal of Heat Transfer*. 125(5), 804.

Abu-Hijleh, B. A. K. (2003b). Natural convection heat transfer from a cylinder with high conductivity permeable fins. *Journal of Heat Transfer*. 125(5), 282.

Abuşka, M., Şevik, S., & Kayapunar, A. (2020). Experimental performance analysis of sensible heat storage in solar air collector with cherry pits/powder under the natural convection. *Solar Energy*. *200*, 2-9.

Ahmad, L., Khordehgah, N., Malinauskaite, J., & Jouhara, H. (2020). Recent advances and applications of solar photovoltaics and thermal technologies. *Energy*. 207, 118254.

Ahn, H. S., Lee, S. W., & Lau, S. C. (2007). Heat transfer enhancement for turbulent flow through blockages with round and elongated holes in a rectangular channel. *Journal of Heat Transfer*. 129(11), 1611.

Akanmu, W. P., & Bajere, P. A. (2015). Investigation of Temperature and Flow Distribution in a Serially Connected Thermosyphon Solar Water Heating Collector System. *Journal of Energy Technologies and Policy*, *5*(2), 56–68.

Alam, T., & Kim, M. H. (2017). Performance improvement of double-pass solar air heater – A state of art of review. In *Renewable and Sustainable Energy Reviews*. 79, 779-793.

AlEssa, A. H., & Al-Widyan, M. I. (2008). Enhancement of natural convection heat transfer from a fin by triangular perforation of bases parallel and toward its tip. *Applied Mathematics and Mechanics (English Edition)*. 29(8), 1033-1044.

Alghoul, M. A., Sulaiman, M. Y., Azmi, B. Z., & Wahab, M. abd. (2005). Review of materials for solar thermal collectors. In *Anti-Corrosion Methods and Materials*. 52(4), 199-206.

Andemeskel, A., Suriwong, T., & Wamae, W. (2017). Effects of Aluminum Fin Thickness Coated with a Solar Paint on the Thermal Performance of Evacuated Tube Collector. *Energy Procedia*. 138, 429-434.

Arora, S., Chitkara, S., Udayakumar, R., & Ali, M. (2011). Thermal analysis of evacuated solar tube collectors. *Journal of Petroleum and Gas Engineering*. *2*(4), 74-82.

ASHRAE. (2011). ASHRAE Handbook - HVAC Applications. In *www.ansi.org American Society of Heating, Refrigerating and Air-Conditioning Engineers, Inc.*

ASHRAE. (2019). 2019 ASHRAE Handbook - HVAC Applications, SI EDITION. In *ASHRAE*.

Awasarmol, U. V., & Pise, A. T. (2015). An experimental investigation of natural convection heat transfer enhancement from perforated rectangular fins array at different inclinations. *Experimental Thermal and Fluid Science*. 68, 145-154.

Ayompe, L. M., Duffy, A., Mc Keever, M., Conlon, M., & McCormack, S. J. (2011). Comparative field performance study of flat plate and heat pipe evacuated tube collectors (ETCs) for domestic water heating systems in a temperate climate. *Energy*. 36(5), 3370-3378.

Azhari, A. W., Alghoul, M. A., Zaidi, S. H., Ibrahim, A. H., Abdulateef, J. M., Zaharim, A., & Sopian, K. (2012). Development of Diffused Solar Radiation Maps using GIS Software for Malaysia. *Models and Methods in Applied Sciences*. 124-128

Babu, S., Abishraj, V. R., & Suthagar, S. (2017). Solar thermal energy storage on PCM based integrated saw tooth collector for institutions. *2016 1st International Conference on Sustainable Green Buildings and Communities, SGBC 2016*. pp. 1-6. IEEE.

Bahdad, A. A. S., Fadzil, S. F. S., & Taib, N. (2020). Optimization of daylight performance based on controllable light-shelf parameters using genetic algorithms in the tropical climate of Malaysia. *Journal of Daylighting*. *7*(1), 122-136.

Balbay, S., & Acıkgoz, C. (2020). Anti-Yellowing UV-Curable hybrid coatings prepared by the Sol–Gel method on polystyrene. *Progress in Organic Coatings*. 140, 105499.

Bamasag, A., Alqahtani, T., Sinha, S., & Phelan, P. (2019). Experimental investigation of a membrane distillation system using solar evacuated tubes. *ASME International Mechanical Engineering Congress and Exposition, Proceedings (IMECE)*. (Vol. 59438, p. V006T06A059). American Society of Mechanical Engineers.

Baradey, Y., Hawlader, M. N. A., Hrairi, M., & Ismail, A. F. (2018). Desalination Technologies : A Critical Review. *International Journal of Engineering Technology and Scientific Innovation*. pp.160-186

Baradey, Y., Hawlader, M. N. A., Ismail, A. F., & Hrairi, M. (2015). Waste Heat Recovery In Heat Pump Systems: Solution To Reduce Global Warming. *IIUM Engineering Journal*. *16*(2), 31-42.

Barriga, J., Ruiz-De-Gopegui, U., Goikoetxea, J., Coto, B., & Cachafeiro, H. (2014). Selective coatings for new concepts of parabolic trough collectors. *Energy Procedia*. 49, 30-39.

Bello, M., & Shanmugan, S. (2020). Achievements in mid and high-temperature selective absorber coatings by physical vapor deposition (PVD) for solar thermal Application-A review. In *Journal of Alloys and Compounds*. 155510.

Ben-Nakhi, A., Efterkhari, M. M., & Loveday, D. I. (2008). Natural convection heat transfer in a partially open square cavity with a thin fin attached to the hot wall. *Journal of Heat Transfer*. 130(5), 052502.

Bi, J., Yang, A., Liu, X., Wu, X., Chen, Q., Wang, Q., Lv, J., & Wang, X. (2015). Effects of pretreatments on explosion puffing drying kinetics of apple chips. *LWT*. 60(2), 1136-1142.

Borges, S. V., Mancini, M. C., Corrêa, J. L. G., & Leite, J. B. (2011). Drying kinetics of bananas by natural convection: Influence of temperature, shape, blanching and cultivar. *Ciência e Agrotecnologia*. 35(2), 368-376.

Bórquez, R., Melo, D., & Saavedra, C. (2015). Microwave–Vacuum Drying of Strawberries with Automatic Temperature Control. *Food and Bioprocess Technology*. 8(2), 266-276.

Boydağ, F. S. (1986). The optical properties of some steel surfaces with different surface preparations for high temperature use. *Solar Energy Materials*. 13(3), 185-195.

Budihardjo, I., & Morrison, G. L. (2009). Performance of water-in-glass evacuated tube solar water heaters. *Solar Energy*. 83(1), 49-56.

Budihardjo, Indra, Morrison, G. L., & Behnia, M. (2007). Natural circulation flow through water-in-glass evacuated tube solar collectors. *Solar Energy*. 81(12), 1460-1472.

Calín-Sánchez, Á., Figiel, A., Wojdyło, A., Szarycz, M., & Carbonell-Barrachina, Á. A. (2014). Drying of Garlic Slices Using Convective Pre-drying and Vacuum-Microwave Finishing Drying: Kinetics, Energy Consumption, and Quality Studies. *Food and Bioprocess Technology*. 7(2), 398-408.

Calise, F. (2012). High temperature solar heating and cooling systems for different Mediterranean climates: Dynamic simulation and economic assessment. *Applied Thermal Engineering*. 32, 108-124.

Carballo, J. A., Bonilla, J., Berenguel, M., Fernández-Reche, J., & García, G. (2019). New approach for solar tracking systems based on computer vision, low cost hardware and deep learning. *Renewable Energy*. *133*, 1158-1166.

Cengel, Y. A., & Boles, M. A. (2015). Thermodynamics: an Engineering Approach 8th Edition. In *McGraw-Hill*.

Chamoli, S., Chauhan, R., Thakur, N. S., & Saini, J. S. (2012). A review of the performance of double pass solar air heater. In *Renewable and Sustainable Energy Reviews*. 16(1), 481-492.

Chaudhary, K., Singh, G., Ramkumar, J., Anantha Ramakrishna, S., Srivastava, K. V., & Ramamurthy, P. C. (2020). Optically Transparent Protective Coating for ITO-Coated PET-Based Microwave Metamaterial Absorbers. *IEEE Transactions on Components, Packaging and Manufacturing Technology*. 1-1.

Chen, S., Li, H., Zhao, K., & Wu, D. (2020). Preparation of graphene films bridged with Ag nanowires and its application in heterojunction solar cells. *Solar Energy*. 198, 167-174.

Chi, F., Zeng, Y., Liu, C., Pan, N., Ding, C., & Yi, F. (2020). Highly stable self-cleaning antireflection coatings from fluoropolymer brush grafted silica nanoparticles. *Applied Surface Science*. 507, 144836.

Chopra, K., Pathak, A. K., Tyagi, V. V., Pandey, A. K., Anand, S., & Sari, A. (2020). Thermal performance of phase change material integrated heat pipe evacuated tube solar collector system: An experimental assessment. *Energy Conversion and*

Management. 203, 112205.

Chopra, K., Tyagi, V. V., & Pandey, A. K. (2020). Thermodynamic and techno-economic analysis of heat pipe ETC water heating system for Indian composite climate: An experimental approach. *Journal of Thermal Analysis and Calorimetry*. 139, 1395-1407.

Chopra, K., Tyagi, V. V., Pandey, A. K., & Sari, A. (2018). Global advancement on experimental and thermal analysis of evacuated tube collector with and without heat pipe systems and possible applications. In *Applied Energy*. 228, 351-389.

Choudhury, C., Chauhan, P. M., & Garg, H. P. (1995). Design curves for conventional solar air heaters. *Renewable Energy*. 6(7), 739-749.

Chow, S. P., Harding, G. L., Window, B., & Cathro, K. J. (1984). Effect of collector components on the collection efficiency of tubular evacuated collectors with diffuse reflectors. *Solar Energy*. 32(2), 251-262.

Chuah, D. G. S., & Lee, S. L. (1981). Solar radiation estimates in Malaysia. *Solar Energy*. 26(1), 33-40.

Colangelo, G., Favale, E., Miglietta, P., & De Risi, A. (2016). Innovation in flat solar thermal collectors: A review of the last ten years experimental results. In *Renewable and Sustainable Energy Reviews*. 57, 1141-1159.

Dabra, V. (2020). Optimization of Heat Losses of Concentric Coaxial Glass Tube Solar Air Collector. *Optimization in Engineering Research*.

Dabra, V., & Yadav, A. (2018). Effect of Pressure Drop and Air Mass Flow Rate on the Performance of Concentric Coaxial Glass Tube Solar Air Collector: A Theoretical Approach. *Arabian Journal for Science and Engineering*. 43(9), 4549-

4559.

Daliran, A., & Ajabshirchi, Y. (2018). Theoretical and experimental research on effect of fins attachment on operating parameters and thermal efficiency of solar air collector. *Information Processing in Agriculture*. 5(4), 411-421.

Department of Statistics Malaysia. (2022). Current Population Estimates, Malaysia, 2020. In *Department of Statistics Malaysia*.

Desa, W. N. Y. M., Fudholi, A., & Yaakob, Z. (2020). Energy-economic-environmental analysis of solar drying system: A review. In *International Journal of Power Electronics and Drive Systems*. 11(2), 1011.

Dey, T. (2020). UV-reflecting sintered nano-TiO2 thin film on glass for anti-bird strike application. *Surface Engineering*. 1-7.

Doymaz, I. (2012). Infrared drying of sweet potato (Ipomoea batatas L.) slices. *Journal of Food Science and Technology*. 49(6), 760-766.

Drosou, V. N., Tsekouras, P. D., Oikonomou, T. I., Kosmopoulos, P. I., & Karytsas, C. S. (2014). The HIGH-COMBI project: High solar fraction heating and cooling systems with combination of innovative components and methods. In *Renewable and Sustainable Energy Reviews*. 27, 463-472.

Du, M., Hao, L., Mi, J., Lv, F., Liu, X., Jiang, L., & Wang, S. (2011). Optimization design of Ti0.5Al0.5N/Ti 0.25Al0.75N/AlN coating used for solar selective applications. *Solar Energy Materials and Solar Cells*. 95(4), 1193-1196.

Duffie, J. A., & Beckman, W. A. (2013). Solar Engineering of Thermal Processes: Fourth Edition. In *Solar Engineering of Thermal Processes: Fourth Edition*. ISBN: 9780470873663,9781118671603.

Duffie, J. A., Beckman, W. A., & McGowan, J. (1985). Solar Engineering of Thermal Processes. *American Journal of Physics*. 53(4), 382.

Dutta, J., & Kundu, B. (2020). Thermal analysis on variable thickness absorber plate fin in flat-plate solar collectors using differential transform method. *Journal of Thermal Engineering*. 6(1), 157-169.

Eicker, U., Colmenar-Santos, A., Teran, L., Cotrado, M., & Borge-Diez, D. (2014). Economic evaluation of solar thermal and photovoltaic cooling systems through simulation in different climatic conditions: An analysis in three different cities in Europe. *Energy and Buildings*. 70, 207-223.

El-Sebaii, A. A., Aboul-Enein, S., Ramadan, M. R. I., Shalaby, S. M., & Moharram, B. M. (2011). Investigation of thermal performance of-double pass-flat and v-corrugated plate solar air heaters. *Energy*. 36(2), 1076-1086.

El-Sebaii, A. A., & Shalaby, S. M. (2012). Solar drying of agricultural products: A review. In *Renewable and Sustainable Energy Reviews*. 16(1), 37-43.

Elferink, M., & Schierhorn, F. (2016). Global demand for food is rising. Can we meet it? *Harvard Business Review*.

Elsheniti, M. B., Kotb, A., & Elsamni, O. (2019). Thermal performance of a heat-pipe evacuated-tube solar collector at high inlet temperatures. *Applied Thermal Engineering*. 154, 315-325.

Energy Saving Trust. (2010). *Solar PV panels will boost Shrewsbury homeowner's pension*. Energy Saving Trust.

Essa, M. A., Asal, M., Saleh, M. A., & Shaltout, R. E. (2021). A comparative study of the performance of a novel helical direct flow U-Tube evacuated tube collector.

Renewable Energy. 163, 2068-2080.

Fazlizan, A., Abdulmula, A., Amran, A. N., Lim, C. H., & Sopian, K. (2019). Performance evaluation of maximum light detection solar tracking system in the tropics. *Journal of Mechanical Science and Technology*. 33(3), 1391-1397.

Fiuk, J. J., & Dutkowski, K. (2019). Experimental investigations on thermal efficiency of a prototype passive solar air collector with wavelike baffles. *Solar Energy*. 188, 495-506.

Freeman, J., Hellgardt, K., & Markides, C. N. (2015a). An assessment of solar-powered organic Rankine cycle systems for combined heating and power in UK domestic applications. *Applied Energy*. 138, 605-620.

Freeman, J., Hellgardt, K., & Markides, C. N. (2015b). An Assessment of Solar-Thermal Collector Designs for Small-Scale Combined Heating and Power Applications in the United Kingdom. *Heat Transfer Engineering*. 36(14-15), 1332-1347.

Fudholi, A., Othman, M. Y., Ruslan, M. H., Yahya, M., Zaharim, A., & Sopian, K. (2011). Techno-economic analysis of solar drying system for seaweed in Malaysia. *Recent Researches in Energy, Environment and Landscape Architecture*. 11, 89-95.

Fudholi, A., Sopian, K., Ruslan, M. H., Alghoul, M. A., & Sulaiman, M. Y. (2010). Review of solar dryers for agricultural and marine products. In *Renewable and Sustainable Energy Reviews*. 14(1), 1-30.

Fudholi, Ahmad, & Sopian, K. (2019). A review of solar air flat plate collector for drying application. In *Renewable and Sustainable Energy Reviews*. 102, 333-345.

Fudholi, Ahmad, Sopian, K., Gabbasa, M., Bakhtyar, B., Yahya, M., Ruslan, M. H., & Mat, S. (2015). Techno-economic of solar drying systems with water based solar collectors in Malaysia: A review. In *Renewable and Sustainable Energy Reviews*. 51, 809-820.

Fudholi, Ahmad, Sopian, K., Ruslan, M. H., & Othman, M. Y. (2013). Performance and cost benefits analysis of double-pass solar collector with and without fins. *Energy Conversion and Management*. 76, 8-19.

Furbo, S. (2015). Using water for heat storage in thermal energy storage (TES) systems. In *Advances in Thermal Energy Storage Systems: Methods and Applications*. 31-47.

Furbo, S., & Jivan Shah, L. (2003). Thermal advantages for solar heating systems with a glass cover with antireflection surfaces. *Solar Energy*. 74(6), 513-523.

Gao, Z., Lin, G., Chen, Y., Zheng, Y., Sang, N., Li, Y., Chen, L., & Li, M. (2020). Moth-eye nanostructure PDMS films for reducing reflection and retaining flexibility in ultra-thin c-Si solar cells. *Solar Energy*. 205, 275-281.

Garba, U., Kaur, S., Gurumayum, S., & Rasane, P. (2015). Effect of hot water blanching time and drying temperature on the thin layer drying kinetics of and anthocyanin degradation in black carrot (Daucus carota L.) shreds. *Food Technology and Biotechnology*. 53.

George, M. A., Takamure, N., & McKenzie, D. R. (2020). Radiative heat transfer between coaxial cylinders in the evacuated tubular solar collector operating at high temperatures: The effect of infrared transparency of borosilicate glass. In *arXiv*.

Ghoneim, A. A., Shabana, H. M., Shaaban, M. S., & Mohammedein, A. M. (2016). Performance Analysis of Evacuated Tube Collector in Hot Climate. *European*

International Journal of Science and Technology. 5(3), 8-20.

Giri, S. K., & Prasad, S. (2007). Drying kinetics and rehydration characteristics of microwave-vacuum and convective hot-air dried mushrooms. *Journal of Food Engineering*. 78(2), 512-521.

Gong, J. hu, Jiang, Z., Luo, X. feng, Du, B., Wang, J., & Lund, P. D. (2020). Straight-through all-glass evacuated tube solar collector for low and medium temperature applications. *Solar Energy*. 201, 935-943.

Gorjian, S., Ebadi, H., Calise, F., Shukla, A., & Ingrao, C. (2020). A review on recent advancements in performance enhancement techniques for low-temperature solar collectors. In *Energy Conversion and Management*. 222, 113246.

Goswami, D. Y. (2015). Principles of Solar Engineering, Third Edition. In *PhD Proposal*.

Grandi, C., & D'ovidio, M. C. (2020). Balance between health risks and benefits for outdoor workers exposed to solar radiation: An overview on the role of near infrared radiation alone and in combination with other solar spectral bands. *International Journal of Environmental Research and Public Health*. 17(4), 1357.

Greco, A., Gundabattini, E., Gnanaraj, D. S., & Masselli, C. (2020). A comparative study on the performances of flat plate and evacuated tube collectors deployable in domestic solar water heating systems in different climate areas. *Climate*. 8(6), 78.

Hafez, A. Z., Soliman, A., El-Metwally, K. A., & Ismail, I. M. (2017). Tilt and azimuth angles in solar energy applications – A review. In *Renewable and Sustainable Energy Reviews*. 77, 147-168.

Hairat, M. K., & Ghosh, S. (2017). 100 GW solar power in India by 2022 – A critical review. In *Renewable and Sustainable Energy Reviews*. 73, 1041-1050.

Han, J., Lu, L., Yang, H., & Cheng, Y. (2019). Thermal regulation of PV façade integrated with thin-film solar cells through a naturally ventilated open air channel. *Energy Procedia*. 158, 1208-1214.

Herez, A., Ramadan, M., & Khaled, M. (2018). Review on solar cooker systems: Economic and environmental study for different Lebanese scenarios. In *Renewable and Sustainable Energy Reviews*. 81, 421-432.

Heydari, A., & Mesgarpour, M. (2018). Experimental analysis and numerical modeling of solar air heater with helical flow path. *Solar Energy*. 162, 278-288.

HKEX. (2021). *London Metal Exchange: Home*. London Metal Exchange.

Ho, C. D., Chang, H., Wang, R. C., & Lin, C. S. (2012). Performance improvement of a double-pass solar air heater with fins and baffles under recycling operation. *Applied Energy*. 100, 155-163.

Hollands, K. G. T., & Shewen, E. C. (1981). Optimization of flow passage geometry for air-heating, plate-type solar collectors. *Journal of Solar Energy Engineering, Transactions of the ASME*. 103(4), 323.

Hordeski, M. F. (2020). Megatrends for Energy Efficiency and Renewable Energy. In *Megatrends for Energy Efficiency and Renewable Energy*. CRC Press.

Hosseinzadeh, M., Faezian, A., Mirzababaee, S. M., & Zamani, H. (2020). Parametric analysis and optimization of a portable evacuated tube solar cooker. *Energy*. 116816.

Huang, X., Wang, Q., Yang, H., Zhong, S., Jiao, D., Zhang, K., Li, M., & Pei, G. (2019). Theoretical and experimental studies of impacts of heat shields on heat pipe evacuated tube solar collector. *Renewable Energy*. 138, 999-1009.

Ibrahim, M., Sopian, K., & Daud, W. R. W. (2009). Study of the drying kinetics of Lemon grass. *American Journal of Applied Sciences*. 6(6), 1070.

International Energy Agency. (2015). Technology Roadmap: Hydrogen and fuel cells. In *SpringerReference*.

International Energy Agency, The World Bank, Sarah, F., The World Bank, Rahut, D. B., Mottaleb, K. A., Ali, A., Aryal, J., Smith, B., Soares, P. M. M., Brito, M. C., Careto, J. A. M., Shahsavari, A., Akbari, M., Lee, J. T., Callaway, D. S., IRENA, Pirard, E., Hatem, T. M., … Essia, U. (2022). Global Solar Atlas. In *Renewable and Sustainable Energy Reviews*.

Inyang, U. E., Oboh, I. O., & Etuk, B. R. (2018). Kinetic Models for Drying Techniques—Food Materials. *Advances in Chemical Engineering and Science*. 8, 27-48.

Isac, L., Panait, R., Enesca, A., Bogatu, C., Perniu, D., & Duta, A. (2018). *Development of Black and Red Absorber Coatings for Solar Thermal Collectors*. 263-282.

Jabatan Meteorologi Malaysia. (2022). *Iklim Malaysia*. http://Www.Met.Gov.My/Home.

Jarimi, H., Lv, Q., Omar, R., Zhang, S., & Riffat, S. (2020). Design, mathematical modelling and experimental investigation of vacuum insulated semi-transparent thin-film photovoltaic (PV) glazing. *Journal of Building Engineering*. 101430.

Jarimi, H., Qu, K., Zhang, S., Lv, Q., Liao, J., Chen, B., Lv, H., Cheng, C., Li, J., Su, Y., Dong, S., & Riffat, S. (2020). Performance analysis of a hybrid thin film photovoltaic (PV) vacuum glazing. *Future Cities and Environment*. 6 (1).

Jung, E. S., Basit, M. A., Abbas, M. A., Ali, I., Kim, D. W., Park, Y. M., Bang, J. H., & Park, T. J. (2020). Improved CdS quantum dot distribution on a TiO2 photoanode by an atomic-layer-deposited ZnS passivation layer for quantum dot-sensitized solar cells. *Solar Energy Materials and Solar Cells*. 218, 110753.

Kaiser, E., Ouzounis, T., Giday, H., Schipper, R., Heuvelink, E., & Marcelis, L. F. M. (2019). Adding blue to red supplemental light increases biomass and yield of greenhouse-grown tomatoes, but only to an optimum. *Frontiers in Plant Science*. 9.

Kalogirou, S. A. (2016). Nontracking solar collection technologies for solar heating and cooling systems. In *Advances in Solar Heating and Cooling*. 63-80.

Kalogirou, S., Tripanagnostopoulos, Y., & Souliotis, M. (2005). Performance of solar systems employing collectors with colored absorber. *Energy and Buildings*. 37(8), 824-835.

Kalogirou, Soteris. (2003). The potential of solar industrial process heat applications. *Applied Energy*. 76(4), 337-361.

Kalogirou, Soteris A. (2004). Solar thermal collectors and applications. In *Progress in Energy and Combustion Science*. 30(3), 231-295.

Kalogirou, Soteris A. (2014). Solar Energy Engineering: Processes and Systems: Second Edition. In *Solar Energy Engineering: Processes and Systems: Second Edition*. Academic Press.

Kannan, C., Mohanraj, M., & Sathyabalan, P. (2021). Experimental investigations on jet impingement solar air collectors using pin-fin absorber. *Proceedings of the Institution of Mechanical Engineers, Part E: Journal of Process Mechanical Engineering*. *235*(1), 134-146.

Karmakar, A., Biswas, A., Philip, J. T., & Kuriachen, B. (2019). *Estimation of Heat Loss Factor with the Tilt Angle in a Solar Thermal Flat-Plate Collector*. 73-79.

Kazem, H. A., Chaichan, M. T., Al-Waeli, A. H. A., & Sopian, K. (2020). A review of dust accumulation and cleaning methods for solar photovoltaic systems. In *Journal of Cleaner Production*. 123187.

Khamlich, S., Nemraoui, O., Mongwaketsi, N., McCrindle, R., Cingo, N., & Maaza, M. (2012). Black Cr/α-Cr 2O 3 nanoparticles based solar absorbers. *Physica B: Condensed Matter*. 407(10), 1509-1512.

Khatib, T., Mohamed, A., Mahmoud, M., & Sopian, K. (2015). Optimization of the tilt angle of solar panels for Malaysia. *Energy Sources, Part A: Recovery, Utilization and Environmental Effects*. 37(6), 606-613.

Khatib, Tamer, Mohamed, A., Sopian, K., & Mahmoud, M. (2012). Solar energy prediction for Malaysia using artificial neural networks. *International Journal of Photoenergy*. 1-16.

Klein, S. A., Beckman, W. A., & Duffie, J. A. (1976). A design procedure for solar heating systems. *Solar Energy*. 18(2), 113-127.

Klein, S. A., Duffie, J. A., & Beckman, W. A. (1974). Transient considerations of flat-plate solar collectors. *Journal of Engineering for Gas Turbines and Power*. 96(2), 109.

Kotian, S., Jain, N., & Nikam, S. (2022). Numerical investigation of baffle orientation on recirculation zones in a shell and tube heat exchanger. *AIP Conference Proceedings* (Vol. 2421, No. 1, p. 060003). AIP Publishing LLC.

Kotian, S., Methekar, N., Jain, N., Vartak, P., Naik, P., & Bhusnoor, S. S. (2022). *Theoretical Investigation of Thermo-hydraulic characteristics of Shell and Tube Heat Exchanger*. In *Proceedings of the 26thNational and 4th International ISHMT-ASTFE Heat and Mass Transfer Conference December 17-20, 2021, IIT Madras, Chennai-600036, Tamil Nadu, India*. Begel House Inc.

Kouhila, M., Moussaoui, H., Lamsyehe, H., Tagnamas, Z., Bahammou, Y., Idlimam, A., & Lamharrar, A. (2020). Drying characteristics and kinetics solar drying of Mediterranean mussel (mytilus galloprovincilis) type under forced convection. *Renewable Energy*. 147, 833-844.

Krishnananth, S. S., & Kalidasa Murugavel, K. (2013). Experimental study on double pass solar air heater with thermal energy storage. *Journal of King Saud University - Engineering Sciences*. 25(2), 132-140.

Kumar, Amit, & Yadav, A. (2017). Experimental investigation of an air heating system using different types of heat exchangers incorporated with an evacuated tube solar collector. *Environmental Progress and Sustainable Energy*. 36(1), 232-247.

Kumar, Arvind, Said, Z., & Bellos, E. (2020). An up-to-date review on evacuated tube solar collectors. In *Journal of Thermal Analysis and Calorimetry*. 145, 2873-2889.

Kumar, L., Hasanuzzaman, M., & Rahim, N. A. (2019). Global advancement of solar thermal energy technologies for industrial process heat and its future prospects: A review. In *Energy Conversion and Management*. 195, 885-908.

Kumar, M., Sansaniwal, S. K., & Khatak, P. (2016). Progress in solar dryers for drying various commodities. In *Renewable and Sustainable Energy Reviews*. 55, 346-360.

Kumar, P. S., & Sagar, V. R. (2014). Drying characteristics of osmosed mango, guava and aonla. *Journal of Agricultural Engineering (New Delhi)*. 51(1), 31-36.

Kumar, R., & Chand, P. (2017). Performance enhancement of solar air heater using herringbone corrugated fins. *Energy*. 127, 271-279.

Kumar Singh, A., & Samsher. (2020). Analytical study of evacuated annulus tube collector assisted solar desaltification system: A review. In *Solar Energy*. 207, 1404-1426.

Kundu, B., Bhanja, D., & Lee, K. S. (2012). A model on the basis of analytics for computing maximum heat transfer in porous fins. *International Journal of Heat and Mass Transfer*. 55(25-26), 7611-7622.

Kwong, Q. J. (2020). Light level, visual comfort and lighting energy savings potential in a green-certified high-rise building. *Journal of Building Engineering*. 101198.

Lane GA. (1983). Solar Heat Storage: Latent Heat Materials. In *Boca Raton*.

Li, C., Huang, Q., & Wang, Y. (2020). Effect of Color Coating of Cover Plate on Thermal Behavior of Flat Plate Solar Collector. *Energies*. 13(24), 6696.

Li, Q., Gao, W., Lin, W., Liu, T., Zhang, Y., Ding, X., Huang, X., & Liu, W. (2020). Experiment and simulation study on convective heat transfer of all-glass evacuated tube solar collector. *Renewable Energy*. 152, 1129-1139.

Ling, D., Liu, G., Mo, G., Li, J., & Wang, X. (2015). Research on annual thermal performance of solar water heating balcony system. *Energy Procedia*. 70, 71-78.

Luo, B., Ye, D., & Wang, L. (2017). Recent Progress on Integrated Energy Conversion and Storage Systems. In *Advanced Science*. 4(9), 1700104.

M.Y.H., O., Sopian, K., Yatim, B., & Daud, W. R. W. (2000). Solar Drying Technology for Agricultural Produce. In *World Renewable Energy Congress VI*. 922-927.

Ma, G., Yin, Z., Liu, X., Qi, J., & Dai, Y. (2020). Developments of CPC solar evacuated glass tube collector with a novel selective coating. *Solar Energy*. 220, 1120-1129.

Mahdi, J. M., Lohrasbi, S., Ganji, D. D., & Nsofor, E. C. (2019). Simultaneous energy storage and recovery in the triplex-tube heat exchanger with PCM, copper fins and Al2O3 nanoparticles. *Energy Conversion and Management*. 180, 949-961.

Mahdjuri, F. (1979). Evacuated heat pipe solar collector. *Energy Conversion*. 19(2), 85-90.

Maisnam, D., Rasane, P., Dey, A., Kaur, S., & Sarma, C. (2016). Recent advances in conventional drying of foods. *Journal of Food Technology and Preservation*. 1(1)

Majid, Z. A. A., Othman, M. Y., Ruslan, M. H., Mat, S., Ali, B., Zaharim, A., & Sopian, K. (2009). Multifunctional solar thermal collector for heat pump application. *Proceedings of the 3rd WSEAS International Conference on Energy Planning, Energy Saving, Environmental Education, EPESE '09, Renewable Energy Sources, RES '09, Waste Management, WWAI '09*, pp. 342-346.

Malakar, S., Arora, V. K., & Nema, P. K. (2021). Design and performance evaluation of an evacuated tube solar dryer for drying garlic clove. *Renewable Energy*. 168, 568-580.

Mandalaki, M., & Tsoutsos, T. (2020). *Shading Systems: Their Relation to Thermal Conditions*. SpringerBriefs in Energy, 23-66.

Mao, C., Li, M., Li, N., Shan, M., & Yang, X. (2019). Mathematical model development and optimal design of the horizontal all-glass evacuated tube solar collectors integrated with bottom mirror reflectors for solar energy harvesting. *Applied Energy*. 238, 54-68.

Martinez, P. M., Pozdin, V. A., Papadimitratos, A., Holmes, W., Hassanipour, F., & Zakhidov, A. A. (2017). Dual use of carbon nanotube selective coatings in evacuated tube solar collectors. *Carbon*. 119, 133-141.

Mat Desa, W. N., Mohammad, M., & Fudholi, A. (2019). Review of drying technology of fig. In *Trends in Food Science and Technology*. 88, 93-103.

Matuska, T., & Sourek, B. (2017). Performance Analysis of Photovoltaic Water Heating System. *International Journal of Photoenergy*. 2017, 1-10.

McDonald, G. (1980). A preliminary study of a solar selective coating system using a black cobalt oxide for high temperature solar collectors. *Thin Solid Films*. 72(1), 83-88.

Mekhilef, S., Saidur, R., & Safari, A. (2011). A review on solar energy use in industries. In *Renewable and Sustainable Energy Reviews*. 15(4), 1777-1790.

Memon, S., & Eames, P. C. (2020). Design and development of lead-free glass-metallic vacuum materials for the construction and thermal performance of smart fusion edge-sealed vacuum glazing. *Energy and Buildings*. 227, 110430.

Memon, S., Katsura, T., Radwan, A., Zhang, S., Serageldin, A. A., Abo-Zahhad, E. M., Sergey, S., Memon, A. R., Khan, S. W., Yang, S., Haji Jama, H., Hoseinzadeh, S.,

Sara, I. D., Fang, Y., Danilevski, L., Isaev, R., & Kiani, A. (2020). Modern Eminence and Concise Critique of Solar Thermal Energy and Vacuum Insulation Technologies for Sustainable Low-Carbon Infrastructure. *International Journal of Solar Thermal Vacuum Engineering*. 1(1), 52-71,

Messaouda, A., Hamdi, M., Hazami, M., & Guizani, A. A. (2020). Analysis of an integrated collector storage system with vacuum glazing and compound parabolic concentrator. *Applied Thermal Engineering*. 169, 114958.

Messaouda, A., Hazami, M., Mehdaoui, F., Hamdi, M., Noro, M., Lazzarin, R., & Guizani, A. A. (2020). Thermal performance study of a vacuum integrated solar storage collector (ISSC) with compound parabolic concentrator (CPC). *International Journal of Energy Research*. 1-15.

Mills, A. F. (2017). Heat and mass transfer: Mass transfer. In *CRC Handbook of Thermal Engineering, Second Edition*.

Ministry of Energy Green Technology and Water. (2017). National Green Technology Master Plan 2017-2030. *Policy*.

Mitin, D. M., Bolshakov, A. D., Neplokh, V., Mozharov, A. M., Raudik, S. A., Fedorov, V. V., Shugurov, K. Y., Mikhailovskii, V. Y., Rajanna, P. M., Fedorov, F. S., Nasibulin, A. G., & Mukhin, I. S. (2020). Novel design strategy for GaAs-based solar cell by application of single-walled carbon nanotubes topmost layer. *Energy Science and Engineering*. 1-8.

Mohamad, A. A. (1997). High efficiency solar air heater. *Solar Energy*. 60(2), 71-76.

Mohd Chachuli, F. S., Mat, S., Ludin, N. A., & Sopian, K. (2021). Performance evaluation of renewable energy R&D activities in Malaysia. *Renewable Energy*. 163, 544-560.

Mohd Yusof Hj Othman, K. S. (2002). Teknologi Tenaga Suria. In *Universiti Kebangsaan Malaysia*.

Morrison, G. L., Budihardjo, I., & Behnia, M. (2004). Water-in-glass evacuated tube solar water heaters. *Solar Energy*. 76 (1-3), 135-140.

Morrison, G. L., Budihardjo, I., & Behnia, M. (2005). Measurement and simulation of flow rate in a water-in-glass evacuated tube solar water heater. *Solar Energy*. 78(2), 257-267.

Morrison, Graham L. (2013). Solar collectors. In *Solar Energy: The State of the Art*.

Moss, R. W., Shire, G. S. F., Henshall, P., Eames, P. C., Arya, F., & Hyde, T. (2018). Design and fabrication of a hydroformed absorber for an evacuated flat plate solar collector. *Applied Thermal Engineering*. 138, 456-464.

Motahayyer, M., Arabhosseini, A., & Samimi-Akhijahani, H. (2019). Numerical analysis of thermal performance of a solar dryer and validated with experimental and thermo-graphical data. *Solar Energy*. 193, 692-705.

Musembi, M. N., Kiptoo, K. S., & Yuichi, N. (2016). Design and Analysis of Solar Dryer for Mid-Latitude Region. *Energy Procedia*. 100, 98-110.

Mustapa, S. I., Peng, L. Y., & Hashim, A. H. (2010). Issues and challenges of renewable energy development: A Malaysian experience. *Proceedings of the International Conference on Energy and Sustainable Development: Issues and Strategies, ESD 2010*, pp. 1-6.

Nájera-Trejo, M., Martin-Domínguez, I. R., & Escobedo-Bretado, J. A. (2016). Economic Feasibility of Flat Plate vs Evacuated Tube Solar Collectors in a Combisystem. *Energy Procedia*. 91, 477-485.

Nauryzbekova, S., Nussupov, K., & Bakranova, D. (2021). Simulation of Antireflective coatings system based on Porous Si/DLC and SiO2/TiO2 for Si solar cells. *Materials Today: Proceedings*. 49, 2474-2477.

Ning, Y., Wang, J., Ou, C., Sun, C., Hao, Z., Xiong, B., Wang, L., Han, Y., Li, H., & Luo, Y. (2020). NiCr–MgF2 spectrally selective solar absorber with ultra-high solar absorptance and low thermal emittance. *Solar Energy Materials and Solar Cells*. 206, 110219.

Njomo, D., & Daguenet, M. (2006). Sensitivity analysis of thermal performances of flat plate solar air heaters. *Heat and Mass Transfer/Waerme- Und Stoffuebertragung*. 42(12), 1065-1081.

Nokhosteen, A., & Sobhansarbandi, S. (2020). Novel method of thermal behavior prediction of evacuated tube solar collector. *Solar Energy*.

Nowzari, R., Aldabbagh, L. B. Y., & Egelioglu, F. (2014). Single and double pass solar air heaters with partially perforated cover and packed mesh. *Energy*. 204, 761-768.

Nowzari, R., Mirzaei, N., & Aldabbagh, L. B. Y. (2015). Finding the best configuration for a solar air heater by design and analysis of experiment. *Energy Conversion and Management*. 100, 131-137.

Oh, T. H., Pang, S. Y., & Chua, S. C. (2010). Energy policy and alternative energy in Malaysia: Issues and challenges for sustainable growth. In *Renewable and Sustainable Energy Reviews*. 14(4), 1241-1252.

Olfian, H., Ajarostaghi, S. S. M., & Ebrahimnataj, M. (2020). Development on evacuated tube solar collectors: A review of the last decade results of using nanofluids. In *Solar Energy*. 211, 265-282.

Oliver, J. E. (2005). Climate classification. In *Encyclopedia of Earth Sciences Series*. 218-227.

Omojaro, A. P., & Aldabbagh, L. B. Y. (2010). Experimental performance of single and double pass solar air heater with fins and steel wire mesh as absorber. *Applied Energy*. 87(12), 3759-3765.

Ong, K. S. (1995). Thermal performance of solar air heaters: Mathematical model and solution procedure. *Solar Energy*. 55(2), 93-109.

Orel, Z. C., Gunde, M. K., & Hutchins, M. G. (2005). Spectrally selective solar absorbers in different non-black colours. *Solar Energy Materials and Solar Cells*. 85, 41-50.

Othman, M. Y. H., Sopian, K., Yatim, B., & Daud, W. R. W. (2006). Development of advanced solar assisted drying systems. *Renewable Energy*. 31(5), 703-709.

Outokumpu. (2021). Steel Grades , Properties and Global Standards. *Http://Www.Outokumpu.Com/SiteCollectionDocuments/Outokumpu-Steel-Grades-Properties-Global-Standards.Pdf*.

Papadimitratos, A., Sobhansarbandi, S., Pozdin, V., Zakhidov, A., & Hassanipour, F. (2016). Evacuated tube solar collectors integrated with phase change materials. *Solar Energy*. 129, 10-19.

Park, H., & Kim, D. (2021). Influence on the Haze Effect of Si Thin-Film Solar Cell on Multi-Surface Textures of Periodic Honeycomb Glass. *Transactions on Electrical and Electronic Materials*. 22(1), 80-90.

Parker, B. F., Colliver, D. G., & Walton, L. R. (1982). *Sensitivity Analysis Of Solar Air Heater Design Parameters.*

Pavan Kumar, E., Kumar Solanki, A., & Mohan Jagadeesh Kumar, M. (2021). Numerical investigation of heat transfer and pressure drop characteristics in the micro-fin helically coiled tubes. *Applied Thermal Engineering*. 182, 116093.

Perers, B. (1988). Comparison Of Thermal Performance For Flat Plate And Evacuated Tubular Collectors. In *Advances In Solar Energy Technology*, pp.615-619. Pergamon.

Pise, A. T., & Awasarmol, U. V. (2010). Investigation of Enhancement of Natural Convection Heat Transfer From Engine Cylinder With Permeable Fins. *International Journal of Mechanical Engineering and Technology (IJMET), 1(1), 238-247.*

Pluta, Z. (2011). Evacuated tubular or classical flat plate solar collectors. *Open Access Journal Journal of Power Technologies*. 91(3), 158.

Priyam, A., & Chand, P. (2018). Effect of wavelength and amplitude on the performance of wavy finned absorber solar air heater. *Renewable Energy*. 119, 690-702.

Raam Dheep, G., & Sreekumar, A. (2020). Experimental Studies on Energy and Exergy Analysis of a Single-Pass Parallel Flow Solar Air Heater. *Journal of Solar Energy Engineering, Transactions of the ASME*. Vol. 142, 1.

Radwan, A., Katsura, T., Memon, S., Serageldin, A. A., Nakamura, M., & Nagano, K. (2020). Thermal and electrical performances of semi-transparent photovoltaic glazing integrated with translucent vacuum insulation panel and vacuum glazing. *Energy Conversion and Management*. 215, 112920.

Ramanujam, J., Bishop, D. M., Todorov, T. K., Gunawan, O., Rath, J., Nekovei, R., Artegiani, E., & Romeo, A. (2020). Flexible CIGS, CdTe and a-Si:H based thin

film solar cells: A review. In *Progress in Materials Science*. 100619.

Ramos, A., Chatzopoulou, M. A., Guarracino, I., Freeman, J., & Markides, C. N. (2017). Hybrid photovoltaic-thermal solar systems for combined heating, cooling and power provision in the urban environment. *Energy Conversion and Management*. 150, 838-850.

Rassamakin, B., Khairnasov, S., Zaripov, V., Rassamakin, A., & Alforova, O. (2013). Aluminum heat pipes applied in solar collectors. *Solar Energy*. 94, 145-154.

Raza, S. A., Ahmad, S. S., Ratlamwala, T. A. H., Hussain, G., & Alkahtani, M. (2020). Techno-Economic Analysis of Glazed, Unglazed and Evacuated Tube Solar Water Heaters. *Energies*. 13, 6261.

Razak, A. A., Majid, Z. A. A., Azmi, W. H., Ruslan, M. H., Choobchian, S., Najafi, G., & Sopian, K. (2016). Review on matrix thermal absorber designs for solar air collector. In *Renewable and Sustainable Energy Reviews*. 64, 682-693.

Razak, A. A., Majid, Z. A. A., Basrawi, F., Sharol, A. F., Ruslan, M. H., & Sopian, K. (2019). A performance and technoeconomic study of different geometrical designs of compact single-pass cross-matrix solar air collector with square-tube absorbers. *Solar Energy*. 178, 314-330.

Razali, A. H., Abdullah, M. P., Hassan, M. Y., & Hussin, F. (2019). Comparison of New and Previous Net Energy Metering (NEM) Scheme in Malaysia. *ELEKTRIKA- Journal of Electrical Engineering*. 18(1), 36-42.

Rehman, T. ur, & Ali, H. M. (2020). Experimental study on the thermal behavior of RT-35HC paraffin within copper and Iron-Nickel open cell foams: Energy storage for thermal management of electronics. *International Journal of Heat and Mass Transfer*. 146, 118852.

Ridouane, E. H., & Campo, A. (2008). Heat transfer enhancement of air flowing across grooved channels: Joint effects of channel height and groove depth. *Journal of Heat Transfer*. 130(2), 021901.

Sabiha, M. A., Saidur, R., Mekhilef, S., & Mahian, O. (2015). Progress and latest developments of evacuated tube solar collectors. In *Renewable and Sustainable Energy Reviews*. 51, 1038-1054.

Sadeghi, G., Pisello, A. L., Safarzadeh, H., Poorhossein, M., & Jowzi, M. (2020). On the effect of storage tank type on the performance of evacuated tube solar collectors: Solar radiation prediction analysis and case study. *Energy*. 198, 117331.

Sajawal, M., Rehman, T. U., Ali, H. M., Sajjad, U., Raza, A., & Bhatti, M. S. (2019). Experimental thermal performance analysis of finned tube-phase change material based double pass solar air heater. *Case Studies in Thermal Engineering*. 15, 100543.

Sakhaei, S. A., & Valipour, M. S. (2019). Performance enhancement analysis of The flat plate collectors: A comprehensive review. In *Renewable and Sustainable Energy Reviews*. 102, 186-204.

Salih, M. M. M., Alomar, O. R., Ali, F. A., & Abd, H. M. (2019). An experimental investigation of a double pass solar air heater performance: A comparison between natural and forced air circulation processes. *Solar Energy*. 193, 184-194.

Sarbu, I., Sebarchievici, C., Sarbu, I., & Sebarchievici, C. (2017). Chapter 3 – Solar Collectors. In *Solar Heating and Cooling Systems*.

Sarkın, A. S., Ekren, N., & Sağlam, Ş. (2020). A review of anti-reflection and self-cleaning coatings on photovoltaic panels. In *Solar Energy*. 199, 63-73.

Satcunanathan, S., & Deonarine, S. (1973). A two-pass solar air heater. *Solar Energy*. 15(1), 41-49.

Saxena, Abhishek, Varun, & El-Sebaii, A. A. (2015). A thermodynamic review of solar air heaters. In *Renewable and Sustainable Energy Reviews*. 43, 863-890.

Saxena, Alok, Maity, T., Raju, P. S., & Bawa, A. S. (2012). Degradation Kinetics of Colour and Total Carotenoids in Jackfruit (Artocarpus heterophyllus) Bulb Slices During Hot Air Drying. *Food and Bioprocess Technology*. 5(2), 672-679.

Saxena, G., & Gaur, M. K. (2018). Exergy analysis of evacuated tube solar collectors: A review. In *International Journal of Exergy*. 25(1), 54.

Seidlitz, H. K., Thiel, S., Krins, A., & Mayer, H. (2001). Chapter 36 Solar radiation at the Earth's surface. In *Comprehensive Series in Photosciences*. 705-738.

Sekhar, Y. R., Sharma, K. V., & Rao, M. B. (2009). Evaluation of heat loss coefficients in solar flat plate collectors. *Journal of Engineering and Applied Sciences*. 4(5), 15-19.

Selvakumar, N., & Barshilia, H. C. (2012). Review of physical vapor deposited (PVD) spectrally selective coatings for mid- and high-temperature solar thermal applications. In *Solar Energy Materials and Solar Cells*. 98, 1-23.

Shafieian, A., Khiadani, M., & Nosrati, A. (2019). Strategies to improve the thermal performance of heat pipe solar collectors in solar systems: A review. In *Energy Conversion and Management*. 183, 307-331.

Shah, L. J., & Furbo, S. (2007). Theoretical flow investigations of an all glass evacuated tubular collector. *Solar Energy*. 81(6), 822-828.

Shankar Subramanian, R. (2006). Heat transfer in Flow Through Conduits. *Department of Chemical and Biomolecular Engineering Clarkson University*.

Shanmugam, N., Pugazhendhi, R., Elavarasan, R. M., Kasiviswanathan, P., & Das, N. (2020). Anti-reflective coating materials: A holistic review from PV perspective. *Energies*. 13(10), 2631.

Shariah, A., Al-Akhras, M. A., & Al-Omari, I. A. (2002). Optimizing the tilt angle of solar collectors. *Renewable Energy*. 26(4), 587-598.

Sharma, A., Tyagi, V. V., Chen, C. R., & Buddhi, D. (2009). Review on thermal energy storage with phase change materials and applications. In *Renewable and Sustainable Energy Reviews*. 13(2), 318-345.

Sharma, N., & Diaz, G. (2011). Performance model of a novel evacuated-tube solar collector based on minichannels. *Solar Energy*. 85(5), 881-890.

Sharol, A. F., Razak, A. A., Majid, Z. A. A., Azmi, M. A. A., & Tarminzi, M. A. S. M. (2020). Evaluation on the performance of cross-matrix absorber double-pass solar air heater (CMA-DPSAH) with and without thermal energy storage material. *Journal of Advanced Research in Fluid Mechanics and Thermal Sciences*. 70(2), 37-49.

Singh, I., & Vardhan, S. (2021). Experimental investigation of an evacuated tube collector solar air heater with helical inserts. *Renewable Energy*. 14404.

Singh, Satyender. (2020). Experimental and numerical investigations of a single and double pass porous serpentine wavy wiremesh packed bed solar air heater. *Renewable Energy*. 145, 1361-1387.

Singh, Satyender, & Dhiman, P. (2016). Thermal performance of double pass packed bed solar air heaters - A comprehensive review. In *Renewable and Sustainable Energy Reviews*. 53, 1010-1031.

Singh, Satyender, Dhruw, L., & Chander, S. (2019). Experimental investigation of a double pass converging finned wire mesh packed bed solar air heater. *Journal of Energy Storage*. 21, 713-723.

Singh, Shailendra, Anand, A., Shukla, A., & Sharma, A. (2021). Environmental, technical and financial feasibility study of domestic solar water heating system in India. *Sustainable Energy Technologies and Assessments*. 43, 100965.

Siva Kumar, S., Kumar, K. M., & Kumar, S. R. S. (2017). Design of Evacuated Tube Solar Collector with Heat Pipe. *Materials Today: Proceedings*. 4(14), 12641-12646.

Sobhansarbandi, S., Martinez, P. M., Papadimitratos, A., Zakhidov, A., & Hassanipour, F. (2017). Evacuated tube solar collector with multifunctional absorber layers. *Solar Energy*. 146, 342-350.

Song, J. S., Park, Y. S., & Kim, N. H. (2021). Hydrophobic anti-reflective coating of plasma-enhanced chemical vapor deposited diamond-like carbon thin films with various thicknesses for dye-sensitized solar cells. *Applied Sciences (Switzerland)*. 11(1), 358.

Sopian, K., Othman, M. Y., & Zaidi, S. H. (2012). Advances in solar assisted drying systems for marine and agricultural products. *World Renewable Energy Forum, WREF 2012, Including World Renewable Energy Congress XII and Colorado Renewable Energy Society (CRES) Annual Conferen*. Journal of Mechanical Engineering, 42(1).

Speyer, E. (1965). Solar energy collection with evacuated tubes. *Journal of Engineering for Gas Turbines and Power*. 87(3), 270.

Sridharan, M., & Shenbagaraj, S. (2021). Application of Generalized Regression Neural Network in Predicting the Thermal Performance of Solar Flat Plate Collector Systems. *Journal of Thermal Science and Engineering Applications*. 13(2).

Suryawanshi, S. D., & Sane, N. K. (2009). Natural convection heat transfer from horizontal rectangular inverted notched fin arrays. *Journal of Heat Transfer*. 131(8), 082501.

Tamrin, T., Pratama, F., & Septian, B. (2017). The Physical Quality of Milled Rice as Affected by Moisture Content and Relative Humidity during Delayed Rough Rice Drying. *Turkish Journal of Agriculture - Food Science and Technology*. 5(11), 1261-1263.

Tao, C., & Zhang, L. (2020). Fabrication of multifunctional closed-surface SiO2-TiO2 antireflective thin films. *Colloids and Surfaces A: Physicochemical and Engineering Aspects*. 585, 124045.

Tchinda, R. (2009). A review of the mathematical models for predicting solar air heaters systems. In *Renewable and Sustainable Energy Reviews*. 13(8), 1734-1759.

Tekin, Z. H., Başlar, M., Karasu, S., & Kilicli, M. (2017). Dehydration of green beans using ultrasound-assisted vacuum drying as a novel technique: drying kinetics and quality parameters. *Journal of Food Processing and Preservation*. 41(6), 13227.

Teles, M. de P. R., Ismail, K. A. R., & Arabkoohsar, A. (2019). A new version of a low concentration evacuated tube solar collector: Optical and thermal investigation.

Solar Energy. 180, 324-339.

Tian, Z., Zhang, S., Deng, J., Fan, J., Huang, J., Kong, W., Perers, B., & Furbo, S. (2019). Large-scale solar district heating plants in Danish smart thermal grid: Developments and recent trends. In *Energy Conversion and Management*. 189, 67-80.

TNB. (2022). Tenaga Nasional Berhad Annual Report 2020. In *Annual Report 2022*.

Tripanagnostopoulos, Y., Souliotis, M., & Nousia, T. (2000). Solar collectors with colored absorbers. *Solar Energy*. 68(4), 343-356.

Tyagi, V. V., Kaushik, S. C., & Tyagi, S. K. (2012). Advancement in solar photovoltaic/thermal (PV/T) hybrid collector technology. In *Renewable and Sustainable Energy Reviews*. 16(3), 1383-1398.

Tyagi, V. V., Pandey, A. K., Kaushik, S. C., & Tyagi, S. K. (2012). Thermal performance evaluation of a solar air heater with and without thermal energy storage An experimental study. *Journal of Thermal Analysis and Calorimetry*. 107(3), 1345-1352.

Ullah, A., Imran, H., Maqsood, Z., & Butt, N. Z. (2019). Investigation of optimal tilt angles and effects of soiling on PV energy production in Pakistan. *Renewable Energy*. 139, 830-843.

Van de Loo, B. W. H., Macco, B., Schnabel, M., Stodolny, M. K., Mewe, A. A., Young, D. L., Nemeth, W., Stradins, P., & Kessels, W. M. M. (2020). On the hydrogenation of Poly-Si passivating contacts by Al2O3 and SiNx thin films. *Solar Energy Materials and Solar Cells*. 215, 110592.

Vengadesan, E., & Senthil, R. (2020). A review on recent developments in thermal

performance enhancement methods of flat plate solar air collector. In *Renewable and Sustainable Energy Reviews*. 134, 110315.

Venkatesan, N., & Arjunan, T. V. (2015). An experimental investigation and performance analysis of evacuated tube assisted solar air heater. *International Journal of Applied Engineering Research*.

Wang, J., Law, C. L., Nema, P. K., Zhao, J. H., Liu, Z. L., Deng, L. Z., Gao, Z. J., & Xiao, H. W. (2018). Pulsed vacuum drying enhances drying kinetics and quality of lemon slices. *Journal of Food Engineering*. 224, 129-138.

Wang, Z., Diao, Y., Zhao, Y., Wang, T., Liang, L., & Chi, Y. (2018). Experimental investigation of an integrated collector–storage solar air heater based on the lap joint-type flat micro-heat pipe arrays. *Energy*. 160, 924-939.

Wannagosit, C., Sakulchangsatjatai, P., Kammuang-Lue, N., & Terdtoon, P. (2018). Validated mathematical models of a solar water heater system with thermosyphon evacuated tube collectors. *Case Studies in Thermal Engineering*. 12, 528-536.

Water, M. of E. G. T. and. (2010). The National Green Technology Policy. *Office*.

Wazwaz, A., Salmi, J., Hallak, H., & Bes, R. (2002). Solar thermal performance of a nickel-pigmented aluminium oxide selective absorber. *Renewable Energy*. 27(2), 277-292.

Weiss, W., & Spörk-Dür, M. (2018). Solar Heat Worldwide 2018. Global Market Development and Trends in 2017. Detailed Market Figures 2016. *IEA Solar Heating and Cooling Programme*.

WHO. (2002). Global Solar UV Index A Practical Guide. *World Health*. ISBN: 9241590076

Xia, E. T., & Chen, F. (2020). Analyzing thermal properties of solar evacuated tube arrays coupled with mini-compound parabolic concentrator. *Renewable Energy*. 153, 155-167.

Xia, E. T., Xu, J. T., & Chen, F. (2021). Investigation on structural and optical characteristics for an improved compound parabolic concentrator based on cylindrical absorber. *Energy*. 219, 119683.

Xu, C., Li, Y., & Yu, H. (2014). Effect of far-infrared drying on the water state and glass transition temperature in carrots. *Journal of Food Engineering*. 136, 42-47.

Xu, K., Du, M., Hao, L., Mi, J., Yu, Q., & Li, S. (2020). A review of high-temperature selective absorbing coatings for solar thermal applications. In *Journal of Materiomics*. 6, 167-182.

Xu, Y., Zhang, J., Ai, L., Lou, X., Lin, S., Lu, Y., Fan, B., Jin, J., & Song, W. (2020). Fabrication of mesoporous double-layer antireflection coatings with near-neutral color and application in crystalline silicon solar modules. *Solar Energy*. 201, 149-156.

Yakar, G., & Karabacak, R. (2010). Effects of holes placed on perforated finned heat exchangers at different angles on the Nusselt and Reynolds numbers. *Scientific Research and Essays*.

Yan, Y., Xue, Z., Xu, F., Li, L., Shen, K., Li, J., Yang, Z., & He, Z. (2022). Numerical investigation on thermal-hydraulic characteristics of the micro heat sink with gradient distribution pin fin arrays and narrow slots. *Applied Thermal Engineering*. 202, 117836.

Yang, W., Fan, Q. H., & Li, W. (2020). A Fully Transparent, Flexible μeCoG Array Based on Highly Conductive and Anti-reflective PEDOT:PSS-ITO-Ag-ITO Thin

Films. *15th IEEE International Conference on Nano/Micro Engineered and Molecular System, NEMS 2020*. 124-129.

Yang, X., Yu, J., Xiao, T., Hu, Z., & He, Y. L. (2020). Design and operating evaluation of a finned shell-and-tube thermal energy storage unit filled with metal foam. *Applied Energy*. 261, 114385.

Yurddaş, A. (2020). Optimization and thermal performance of evacuated tube solar collector with various nanofluids. *International Journal of Heat and Mass Transfer*. 152, 119496.

Yusof, Y., & Kalirajan, K. (2020). Variations in economic growth across states in Malaysia: an exploratory analysis. *Journal of Economic Studies*. 48(3).

Zaaoumi, A., Asbik, M., Hafs, H., Bah, A., & Alaoui, M. (2021). Thermal performance simulation analysis of solar field for parabolic trough collectors assigned for ambient conditions in Morocco. *Renewable Energy*. Vol. 164, 1479-1494.

Zhang, X., You, S., Ge, H., Gao, Y., Xu, W., Wang, M., He, T., & Zheng, X. (2014). Thermal performance of direct-flow coaxial evacuated-tube solar collectors with and without a heat shield. *Energy Conversion and Management*. 84, 80-87.

Zhang, Y. Y., Shin, S. H., Kang, H. J., Jeon, S., Hwang, S. H., Zhou, W., Jeong, J. H., Li, X., & Kim, M. (2021). Anti-reflective porous Ge by open-circuit and lithography-free metal-assisted chemical etching. *Applied Surface Science*. 546, 149083.

Zhao, B., Ao, X., Chen, N., Xuan, Q., Hu, M., & Pei, G. (2020). A spectrally selective surface structure for combined photothermic conversion and radiative sky cooling. *Frontiers in Energy*. 14(4), 882-888.

Zhnegguo, Z., Tao, X., & Xiaoming, F. (2004). Experimental study on heat transfer enhancement of a helically baffled heat exchanger combined with three-dimensional finned tubes. *Applied Thermal Engineering*. 24(14-15), 2293-2300.

Zhong, M., Chai, L., & Wang, Y. (2019). Core-shell structure of ZnO@TiO 2 nanorod arrays as electron transport layer for perovskite solar cell with enhanced efficiency and stability. *Applied Surface Science*. 464, 301-310.

Zubriski, S. E., & Dick, K. J. (2012). Measurement of the efficiency of evacuated tube solar collectors under various operating conditions. *Journal of Green Building*. 7(3), 114-130.

APPENDIX I

LIST OF PUBLICATIONS

Journals

1. Zakaria, Z. A., Majid, Z. A. A., Harun, M. A., Ismail, A. F., Ihsan, S. I., Sopian, K., Abdul Razak, A., & Sharol, A. F. (2021). Investigation on The Thermal Performance of Evacuated Glass-Thermal Absorber Tube Collector (EGATC) for Air Heating Application. *Journal of Advanced Research in Fluid Mechanics and Thermal Sciences*, *79*(2), 48–64. https://doi.org/10.37934/arfmts.79.2.4864.

2. Zairul Azrul Zakaria, Zafri Azran Abdul Majid, Muhammad Amin Harun, Ahmad Faris Ismail, Sany Izan Ihsan, Kamaruzzaman Sopian, Amir Abdul Razak, & Ahmad Fadzil Sharol. (2022). Experimental Investigation of Integrated Energy Storage on Thermal Performance Enhancement of Evacuated Glass-Thermal Absorber Tube Collector (EGATC) for Air Heating Application. *Journal of Advanced Research in Fluid Mechanics and Thermal Sciences*, *96*(1), 137–152. https://doi.org/10.37934/arfmts.96.1.137152

3. Zairul Azrul Zakaria, Zafri Azran Abdul Majid, Muhammad Amin Harun, Ahmad Faris Ismail, Sany Izan Ihsan, Kamaruzzaman Sopian, Amir Abdul Razak, Ahmad Fadzil Sharol, Mohd Syahriman Mohd Azmi. (2023) Mathematical Model Development of Evacuated Glass-Thermal Absorber Tube Collector (EGATC) for Air Heating Application. Journal of Science and Mathematics Letters, JSML, Volume 11, Issue 1, 73-82, ISSN 2462-2052, https://doi.org/10.37134/jsml.vol11.1.11.2023

4. Zairul Azrul Zakaria, Zafri Azran Abdul Majid, Muhammad Amin Harun, Ahmad Faris Ismail, Sany Izan Ihsan, Kamaruzzaman Sopian, Amir Abdul Razak, Ahmad Fadzil Sharol, Mohd Syahriman Mohd Azmi. (2023). Experimental Investigation of Pre-Heating Double Pass Flow Arrangement on Thermal Performance Enhancement of Evacuated Glass-Thermal Absorber Tube Collector (EGATC) for Air Heating Application. Engineering, Agricultural, Science and Technology Journal (EAST-J). (Manuscript draft: Accepted for publication)

5. Harun, M. A., Abdul Majid, Z. A., Zakaria, Z. A., Ismail, A. F., Ihsan, S. I., Sopian, K., Sharol, A. F., & Abdul Razak, A. (2021). Study on Selection of a Suitable Material and The Parameters for Designing a Portable Flat Plate Base-Thermal Cell Absorber (FPBTCA). *Journal of Advanced Research in Fluid Mechanics and Thermal Sciences*, *85*(1), 71–92. https://doi.org/10.37934/arfmts.85.1.7192.

6. Muhammad Amin Harun, Zafri Azran Abdul Majid, Zairul Azrul Zakaria, Ahmad Faris Ismail, Sany Izan Ihsan, Kamaruzzaman Sopian, Amir Abdul Razak, & Ahmad Fadzil Sharol. (2022). Performance Analysis of Flat Plate Base-Thermal Cell Absorber (FPBTCA): Low Thickness Design. *Journal of Advanced Research in Fluid Mechanics and Thermal Sciences*, *96*(2), 122–133. https://doi.org/10.37934/arfmts.96.2.122133

7. A.F. Sharol, A.A. Razak, Z.A.A. Majid, M.A.A. Azmi, M.A.S.M. Tarminzi, Y.H. Ming, Z.A. Zakaria, M.A. Harun, A. Fazlizan, K. Sopian. (2022). Effect of thermal energy storage material on the performance of double-pass solar air heater with cross-matrix absorber. *Journal of Energy Storage*, Volume 51, 104494, ISSN 2352-152X, https://doi.org/10.1016/j.est.2022.104494.

Conferences

1. Zairul Azrul Zakaria, Zafri Azran Abdul Majid, Muhammad Amin Harun, Ahmad Faris Ismail, Sany Izan Ihsan, Kamaruzzaman Sopian, Amir Abdul Razak, Ahmad Fadzil Sharol. (2021). Experimental Investigation of Integrated Energy Storage on Thermal Performance Enhancement of Evacuated Glass-Thermal Absorber Tube Collector (EGATC) for Air Heating Application, 5th International Conference on Mechanical, Automotive and Aerospace Engineering 2021 (ICMAAE 2021), 22nd– 23rd of June 2021, International Islamic University Malaysia, Kuala Lumpur.

2. Muhammad Amin Harun, Zafri Azran Abdul Majid, Zairul Azrul Zakaria, Ahmad Faris Ismail, Sany Izan Ihsan, Kamaruzzaman Sopian, Amir Abdul Razak, Ahmad Fadzil Sharol. (2021). Performance analysis of Flat Plate Base-Thermal Cell Absorber (FPBTCA), 5th International Conference on Mechanical, Automotive and Aerospace Engineering 2021 (ICMAAE 2021), 22nd– 23rd June 2021, International Islamic University Malaysia, Kuala Lumpur.

3. Zairul Azrul Zakaria, Zafri Azran Abdul Majid, Muhammad Amin Harun, Ahmad Faris Ismail, Sany Izan Ihsan, Kamaruzzaman Sopian, Amir Abdul Razak, Ahmad Fadzil Sharol, Mohd Syahriman Mohd Azmi. Mathematical Model Development of Evacuated Glass-Thermal Absorber Tube Collector (EGATC) for Air Heating Application. International Conference on Science, Technology, Engineering & Mathematics (ICSTEM2022) in conjunction with 10^{th} International Postgraduate Conference on Science & Mathematics 2022 (IPCSM2022), 24 September 2022, Sultan Idris Education University, Muallim, Perak.

4. Zairul Azrul Zakaria, Zafri Azran Abdul Majid, Muhammad Amin Harun, Ahmad Faris Ismail, Sany Izan Ihsan, Kamaruzzaman Sopian, Amir Abdul Razak, Ahmad Fadzil Sharol, Mohd Syahriman Mohd Azmi. Experimental Investigation of Pre-Heating Double Pass Flow Arrangement on Thermal Performance Enhancement of Evacuated Glass-Thermal Absorber Tube Collector (EGATC) for Air Heating Application. 3rd International Conference on Innovative Technology & Science (IC.ITS'22), 6th - 7th December 2022, University College of Yayasan Pahang (UCYP), Kuantan, Pahang.

APPENDIX II

INTELECTUAL PROPERTY

INVOIS CUKAI DIPERMUDAHKAN

PERBADANAN HARTA INTELEK MALAYSIA
Unit 1-7 Aras Bawah Tower B
Menara UOA Bangsar
No 5 Jalan Bangsar Utama 1,
59000, Kuala Lumpur, Malaysia.
Tel: 603-2299 8400 Faks: 603-2299 8989
GST NO: 000869019648

MyIPO

RESIT RASMI

Diterima Daripada	**Butiran Resit Rasmi**		
ZAFRI AZRAN ABDUL MAJID REDTEC ENTERPRISE PERAMU BARU LOT 352, Kuantan 26060 (MY)	Nombor Resit	:	RST/PHG-000671-2019
	Tarikh	:	15/07/2019 12:39:28
	Jumlah	:	290.00

Rujukan			**Butiran Bayaran**			
Pusat Bayaran	:	PAHANG-	Cara Bayaran	No Doc	Tarikh Doc	Amaun (RM)
No. Invois	:	1889097	KAD DEBIT	000331000234	15/07/2019	290.00
Catatan	:					

Keterangan	No pendaftaran	Kuantiti	Kos Per Unit	GST	Jumlah
PM1	PI2019004063	1.00	290.00	0.00	290.00

Cetakan Berkomputer Tidak Perlu Tandatangan

*Resit ini akan dianggap batal sekiranya cek tidak dapat ditunaikan.
Pelepasan di bawah Seksyen 56(3)(b) Akta Cukai Barangan dan Perkhidmatan 2014

NURAIN BINTI OTHMAN
SALINAN PELANGGAN

Figure A2-1: Official receipt of PM1 Form for MyIPO Industrial Design Certification

PERBADANAN HARTA INTELEK MALAYSIA
INTELLECTUAL PROPERTY CORPORATION OF MALAYSIA
(Agensi di bawah KPDNHEP)
Unit 1-7 & Mezzanine, Aras 12-19
Tower B, Menara UOA Bangsar
No. 5, Jalan Bangsar Utama 1
59000 KUALA LUMPUR
MALAYSIA

Tel : +603 - 2299 8400
Faks (Fax) : +603 - 2299 8989
Laman Web (Web) : www.myipo.gov.my

CERTIFICATE OF FILING

APPLICANT	:	1) ZAFRI AZRAN ABDUL MAJID 2) ZAIRUL AZRUL BIN ZAKARIA 3) MUHAMMAD AMIN BIN HARUN 4) AHMAD FARIS ISMAIL 5) SANY IZAN IHSAN 6) KAMARUZZAMAN SOPIAN
APPLICATION NO	:	PI2019004063
REQUEST RECEIVED ON	:	15 JULY 2019
FILING DATE	:	15 JULY 2019
AGENT'S/APPLICANT'S FILE REF.	:	-

Please find attached, a copy of the Request Form relating to the above application, with the filing date and application number marked thereon in accordance with Regulation 25(1).

Date : 16 JULY 2020

(NOORHISHAM BIN OTHMAN)
for Registrar of Patents
noorhisham@myipo.gov.my
03-22998812

To : ZAFRI AZRAN ABDUL MAJID
REDTEC ENTERPRISE, PERAMU BARU, LOT 352
26060 KUANTAN
PAHANG DARUL MAKMUR
MALAYSIA

(Agensi di bawah Kementerian Perdagangan Dalam Negeri dan Hal Ehwal Pengguna)

Figure A2-2: Official letter of Certificate of Filling for MyIPO Industrial Design Certification

PERBADANAN HARTA INTELEK MALAYSIA
INTELLECTUAL PROPERTY CORPORATION OF MALAYSIA
(Agensi dibawah KPDNHEP)
Unit 1-7 & Mezzanine, Aras 12-19
Tower B, Menara UOA Bangsar
No. 5, Jalan Bangsar Utama 1
59000 KUALA LUMPUR
MALAYSIA

Tel : +603 – 2299 8400
Faks(Fax) : +603 – 2299 8989
Laman Web (Web) : www.myipo.gov.my

APPLICATION NO.	:	PI2019004063
APPLICANT	:	1. ZAFRI AZRAN ABDUL MAJID 2. ZAIRUL AZRUL BIN ZAKARIA 3. MUHAMMAD AMIN BIN HARUN 4. AHMAD FARIS ISMAIL 5. SANY IZAN IHSAN 6. KAMARUZZAMAN SOPIAN
FILING DATE	:	15 JULY 2019
APPLICANT'S OR AGENT'S REF.	:	-

PRELIMINARY EXAMINATION - CLEAR FORMALITIES REPORT

Please find attached a copy of the Examiner's clear report under Section 29 of the Patents Act.

A request for Substantive Examination should be made on Form 5 or a request for Modified Substantive Examination should be made on Form 5A, together with the appropriate prescribed fee, within 18 months from the filing date of the application, otherwise the application may be treated as withdrawn.

Date : 3 DECEMBER 2020

(Nor Hashila binti Mohamad Hassim)
for Registrar of Patents
hashila@myipo.gov.my
03 2299 8810

To : ZAFRI AZRAN ABDUL MAJID
REDTEC ENTERPRISE, PERAMU BARU, LOT 352
26060 KUANTAN PAHANG
MALAYSIA

(Agensi di bawah Kementerian Perdagangan Dalam Negeri Dan Hal Ehwal Pengguna)

Figure A2-3: Official letter of Preliminary Examination-Clear Formalities Report for MyIPO Industrial Design Certification

INVOIS CUKAI DIPERMUDAHKAN

PERBADANAN HARTA INTELEK MALAYSIA
Unit 1-7 Aras Bawah Tower B
Menara UOA Bangsar
No 5 Jalan Bangsar Utama 1,
59000, Kuala Lumpur, Malaysia.
Tel: 603-2299 8400 Faks: 603-2299 8989
GST NO: 000869019648

MyIPO

RESIT RASMI

Diterima Daripada	**Butiran Resit Rasmi**		
ZAFRI AZRAN BIN ABDUL MAJID RADTEC ENTERPRISE, PERAMU BARU LOT 352, 26060 KUANTAN, PAHANG DARUL MAKMUR.	Nombor Resit	:	RST/PHG-001289-2020
	Tarikh	:	15/12/2020 08:48:37
	Jumlah	:	1,100.00

Rujukan			**Butiran Bayaran**			
Pusat Bayaran	:	PAHANG-	Cara Bayaran	No Doc	Tarikh Doc	Amaun (RM)
No. Invois	:	-	KAD DEBIT	001081000706	15/12/2020	1,100.00
Catatan	:					

Keterangan	No pendaftaran	Kuantiti	Kos Per Unit	GST	Jumlah
PM5	PI 2019004063	1.00	1,100.00	0.00	1,100.00

Cetakan Berkomputer Tidak Perlu Tandatangan
*Resit ini akan dianggap batal sekiranya cek tidak dapat ditunaikan.
Pelepasan di bawah Seksyen 56(3)(b) Akta Cukai Barangan dan Perkhidmatan 2014

NUR SAIDATUN SHEILA BINTI TALIB
SALINAN PELANGGAN

Figure A2-4: Official receipt of PM5 Form for MyIPO Industrial Design Certification

PERBADANAN HARTA INTELEK MALAYSIA
INTELLECTUAL PROPERTY CORPORATION OF MALAYSIA
(Agensi di bawah KPDNHEP)
Unit 1-7 & Mezzanine, Aras 12–19
Tower B, Menara UOA Bangsar
No. 5, Jalan Bangsar Utama 1
59000 KUALA LUMPUR
MALAYSIA

Tel : +603 - 2299 8400
Faks (Fax) : +603 - 2299 8689
Laman Web (Web) : www.myipo.gov.my

APPLICATION NO : PI2019004063

APPLICANT : 1) ZAFRI AZRAN ABDUL MAJID
2) ZAIRUL AZRUL BIN ZAKARIA
3) MUHAMMAD AMIN BIN HARUN
4) AHMAD FARIS ISMAIL
5) SANY IZAN IHSAN
6) KAMARUZZAMAN SOPIAN

APPLICANT'S/AGENT'S REF. : -

DATE OF MAILING : 16 JULY 2020

PRELIMINARY EXAMINATION - ADVERSE FORMALITIES REPORT

Please find attached a copy of the Preliminary examination report under Section 29 of the Patents Act, relating to the following deficiencies :

☐ **ANNEX A**: Deficiencies as to Regulation 5 to 11,50 and 51

☒ **ANNEX D**: Deficiencies as to Regulation 18.

You are invited to correct the deficiencies. Corrections should be received at the above Office or Branch Offices in Sabah or Sarawak within 3 months of the above date of mailing, otherwise the application may be refused.

Date : 16 JULY 2020

(NOORHISHAM BIN OTHMAN)
for Registrar of Patents
✉ **noorhisham@myipo.gov.my**
☎ **03-22998812**

To : ZAFRI AZRAN ABDUL MAJID
REDTEC ENTERPRISE, PERAMU BARU, LOT 352
26060 KUANTAN
PAHANG DARUL MAKMUR
MALAYSIA

Figure A2-5: Official letter of Preliminary Examination-Adverse Formalities Report for MyIPO Industrial Design Certification

APPENDIX III

ADDITIONAL DATA

Table A3-1: Mass of each thermal absorber components involved in parameter experimental

Type	*Mass (kg)*
Heat pipe	0.053
Heat pipe with aluminium fin	0.111
Outer absorber (1mm wall thickness)	0.490
Outer absorber (2mm wall thickness)	0.932
Inner absorber (0 fin)	0.167
Inner absorber (1 fin)	0.171
Inner absorber (3 fin)	0.182
Inner absorber (5 fin)	0.191
Inner absorber (7 fin)	0.203

Table A3-2: Total Mass of EGATC and HP ETC prototype

Components	**EGATC** Mass (Kg)	**HP ETC** Mass (Kg)
Evacuated glass	0.551	0.551
Outer absorber (Stainless steel)	0.490	NA
Inner absorber (Stainless steel)	0.167	NA
Ventilated chamber	0.328	NA
PVC saddle	0.005	NA
Insulation	0.004	NA
Heat pipe (Copper)	NA	0.053
Absorber (Aluminium)	NA	0.058
Cap to fix heat pipe	NA	0.028
Plastic tube holder	NA	0.043
Plate (Aluminium)	NA	0.71
TOTAL	**1.545**	**1.443**

Table A3-3: Bill of materials (BOM) in regard to the prototypes of EGATC fabrication

Nos.	Specification/ Dimension	Type/ Material	Component	Nos. of Unit	Price (RM)
1	O. D = 58mm, I. D = 48mm t = 5mm, L = 500mm	High Borosilicate, Vacuum tightness = 5.0×10^{-3}Pa	MISOLIE Technology, Double Layer Glass- Evacuated Tube	1	53.45
2	O. D = 38.5mm, t= 1.0mm, L = 550mm	Stainless Steel 304	Pipe (Outer absorber)	1	20.00
3	O. D = 12.7mm, t = 1.0mm, L = 615mm	Stainless Steel 304	Pipe (Inner absorber)	1	10.00
4	O. D = 36.3mm, I.D = 12.9mm, t = 1.0mm	PVC	Saddle, Dia. 6 mm x 8 holes	3	1.50
5	V = 12V, P = 4.8watt	N/A	D.C Ventilation Fan	1	3.00
6	Thickness = 5mm, k value = 0.035W/ mK	High quality flexible elastomeric closed cell nitrile rubber insulation	Insulflex®, High quality Insulation – Class 1	1	1.00
7	L = 50.8mm, W = 50.8mm, H = 63.5mm, t = 1mm	Stainless Steel 304	Stainless Steel Square Hollow	1	12.00
8	L = 60mm, W = 60mm, t = 1mm	Stainless Steel 304	Stainless Steel Plate	2	6.00
9	L = 80mm, W = 40mm (10 watts, 12-volt)	Monocrystalline	Radtech, Solar Panel	1	4.00
				Total	**110.95**

APPENDIX IV

TYPES OF SOLAR THERMAL COLLECTOR INVOLVED IN THE STUDY

Figure A4-1: Top view of Evacuated Glass- Thermal Absorber Tube Collector (EGATC) prototype

Figure A4-2: Side view of Evacuated Glass- Thermal Absorber Tube Collector (EGATC) prototype

Figure A4-3: Evacuated Glass- Thermal Absorber Tube Collector (EGATC) prototype used for air heating application

Figure A4-4: Heat Pipe Evacuated Tube Collector (HP ETC) prototype used for air heating application